SVENSKA GEOFYSISKA FÖRENINGEN

VOLUME 6, NUMBER 1 **Tellus** FEBRUARY 1954

A QUARTESLY JOURNAL OF GEOPHYSICS

Photographic Investigation of the Projection of Droplets by Bubbles Bursting at a Water Surface[1]

By C. F. KIENTZLER, A. B. ARONS, D. C. BLANCHARD, A. H. WOODCOCK

Woods Hole Oceanographic Institution.

(Manuscript received February 4, 1954)

Abstract

Bubbles of air reaching the air-water interface burst and eject liquid droplets into the air to heights large compared to their diameter. Photographic evidence is introduced to prove the existence of a jet of liquid which upon breaking up produces these droplets. The jet is shown to be produced by the collapse of the bubble cavity.

The droplets are found to be of the order of one tenth of the bubble size, for the range investigated (0.2 to 1.8 mm diameter), each bubble producing about 5 droplets.

The droplet-producing mechanism is essentially the same for fresh and sea water or sea water with oleic acid surface film. The time required for the bubble to burst and the jet formation to take place is found to be proportional to the bubble size. The sea water droplets produced by this mechanism leave, upon evaporation of the water, salt nuclei having the size range observed by WOODCOCK (1952).

It is suggested that such bursting of bubbles plays an important role in the natural production of air-borne sea-salt nuclei at the sea surface.

1. Introduction

Among meteorologists it has long been recognized that airborne chloride particles may play an important role in fog, cloud and precipitation processes.

KINCH (1887) and many other workers at widely different geographical locations have found chloride in rain waters. KÖHLER (1936) and HOUGHTON and RADFORD (1938) measured chloride in cloud and fog waters, which they attributed to the presence in the air of sea-salt nuclei on which the cloud and fog droplets formed. OWENS (1926) measured the sizes of some of the larger salt particles found in clear air near the sea surface, and WOODCOCK (1952) extended the range of salt particle size measured and showed that these particles are also present in clear air at cloud levels. It is the purpose of the present study to show that the mechanism of the bursting of small bubbles at the sea surface can account for the initial introduction of sea-salt nuclei into the air.

All of the above authors recognized that the sea surface was the source of the chlorides measured. KÖHLER (1941) proposed that the formation of spray at wave crests by strong winds was responsible for airborne salt nuclei. FACY (1951) suggested that rupturing of bubble films produce the observed weights of nuclei. STUHLMAN (1932) had previously suggested that the bursting of bubbles in distilled water produced jets (similar to "Worthington's Splashes") which broke into small droplets. The present study proves that jets occur when

[1] Contribution No. 691. Woods Hole Oceanographic Institution. Work supported by the Office of Naval Research, under contract number Nonr-798 (00) (NR-082-124).

small bubbles burst at the surface of fresh water and sea water. It is shown that the jets formed in sea water can account for a large portion of the range of weight of the salt particles observed in the free air. The relative percentage of the naturally occurring salt nuclei which originate from the break-up of jets and from other mechanisms remains to be investigated. High speed photography has been the primary tool in carrying out the present study.

2. Photographic Observation of Bursting Bubbles

As previously pointed out, STUHLMAN (1932) has suggested that the formation of a jet on the bursting of a bubble is the principle mechanism by which droplets are ejected into the air. In this investigation bursting bubbles (diameter 0.2 to 1.8 mm) in fresh and sea water were photographed from above and below the surface, in an effort to examine in more detail the mechanism proposed by Stuhlman.

Figure 1 shows still photographs (less than 30 microseconds exposure time) of one millimeter bubbles bursting in fresh water. The sequence has been established by comparison with high speed motion pictures. These photographs were made in an unsuccessful attempt to observe the rupture of the bubble surface film. The exposure time was much too long to stop this exceedingly rapid phenomenon. It is significant, however, that no droplets of large enough size to be resolved by the film and optical system were observed from bubbles of this size until *after* the jet formation. This is thought to indicate that the larger droplets are not produced when the bubble film is broken.

The initial burst of the bubble is observed as a slight wave train starting outward. The mouth of the cavity widens until it is almost twice the initial size. The jet suddenly projects upward, continues to rise as a thin column, and then the unstable column breaks into droplets of varying size. In general the last droplet to leave the jet has very little vertical motion and rapidly returns to the surface. The jet finally collapses completely, and the surface where the jet action occurred becomes completely smooth, without further oscillation.

The horizontal views in Figures 2 and 3 show the collapse of the cavity prior to the formation of the jet. These sequences indicate how a jet forms from a conical depression which, in turn, is formed from the initial spherical cavity. In the time interval from the initial rupture of the film until the depression has assumed a conical shape, a disturbance (probably associated with the drawing back of the upper lip of the cavity by surface tension) is observed to propagate downward along the bubble surface. Figures 2 and 3 are photographs of different, but exactly similar, events. Since the exposures are of slightly different phase, a combination of two sequences gives a fairly detailed picture of the successive stages of bubble collapse and jet droplet formation. (The two or three motionless droplets, which appear in these photographs, are adhering to the inner surface of the glass wall and were produced by jets from other bubbles.)

Figures 2 and 3 strongly suggest that the dynamics of the jet, the size of projected droplets, and the height reached by the droplets are determined by the shape and hydrodynamics of collapse of the cavity itself. Very large mass velocities are probably associated with the converging flow at the vertex of the cone. The extremely rapid withdrawal of the lip of the cavity, considerably prior to formation of the jet, leaves little foundation for STUHLMAN's (1932) proposed mechanism of jet formation under a "sucking" influence of a vortex ring formed by the ejected bubble gases.

It can be observed, in the last two pictures of Figure 3 (arrow) and in other photographs, that a barely visible small droplet is projected between two larger ones. These microscopic droplets are doubtlessly formed in the break-up of the jet. Similar phenomena have been photographed by other investigators in the break-up of a falling jet of water and in the break-up of raindrops. In other photographs (not published) large droplets were observed to strike the water surface and rebound with a much reduced diameter. These two phenomena, associated with the bursting of relatively large bubbles, indicate that these bubbles also produce the smaller-sized air-borne sea salt nuclei.

Figures 1, 2 and 3 show jets formed at the surface of tap water. Do the bursting of bubbles and the formation of the jet change

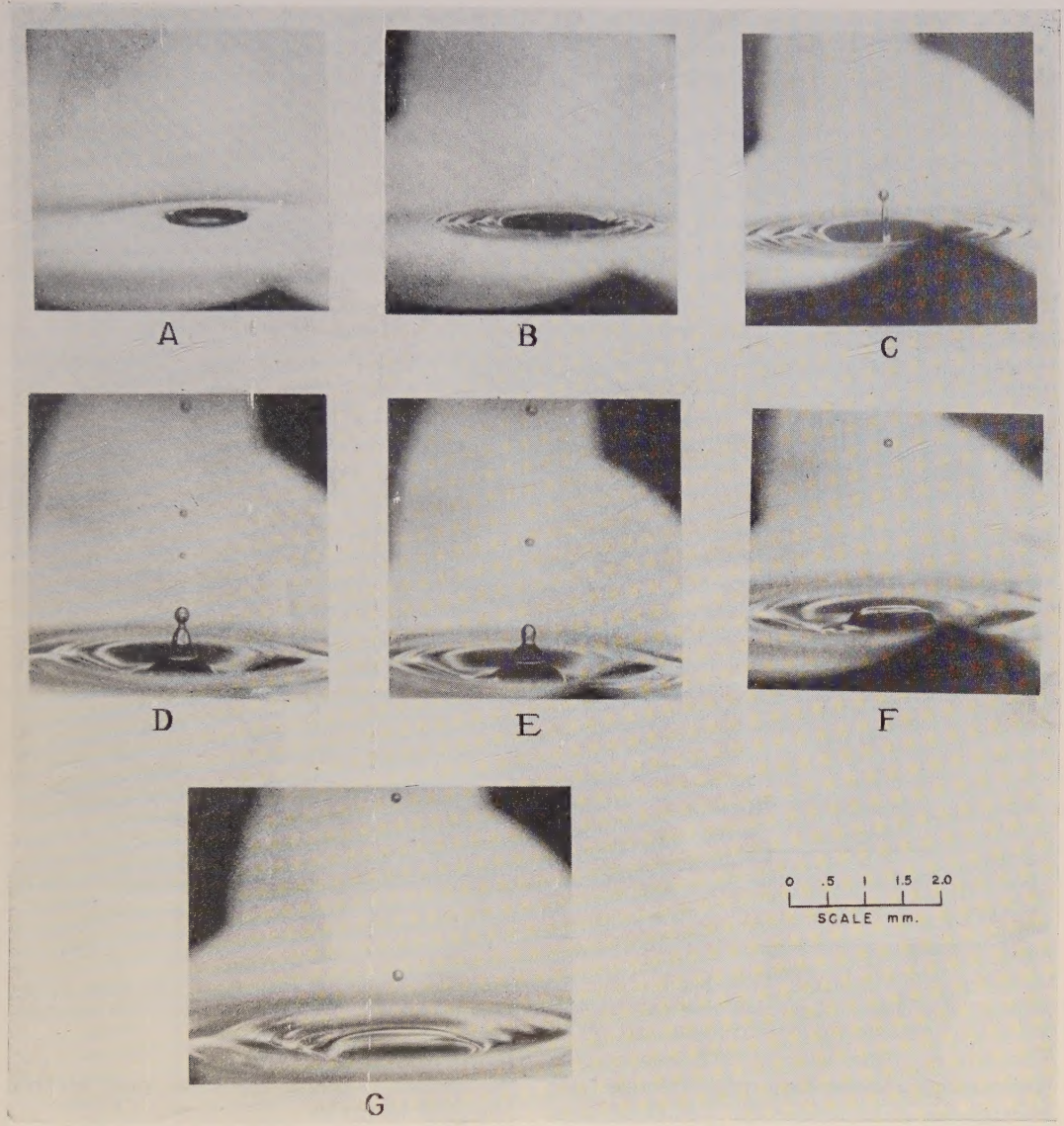

Fig. 1. Still photographs of 1.0 mm diameter bubbles bursting in fresh water. The sequence is based on comparison with high speed motion pictures. Angle of view about 10° below the horizontal. Exposure time ca. 30 μ sec. Time interval between pictures uncertain.

a. Bubble approaching surface.
b. Bubble just after rupture.
c. Initial rise of jet.
d, e, f, and g. Projection of droplets and decay of jet.

appreciably in salt water or in water with a contaminated surface? Similar photographs under various conditions indicate there is no significant change in the collapse of the cavity, or formation and break-up of the jet. In sea water the only marked difference was that a much longer period of time elapsed between the arrival at the surface and the bursting of the bubble. A second bubble from the source would arrive at the surface before the previous one had burst.

Compressed films of oleic acid on a sea

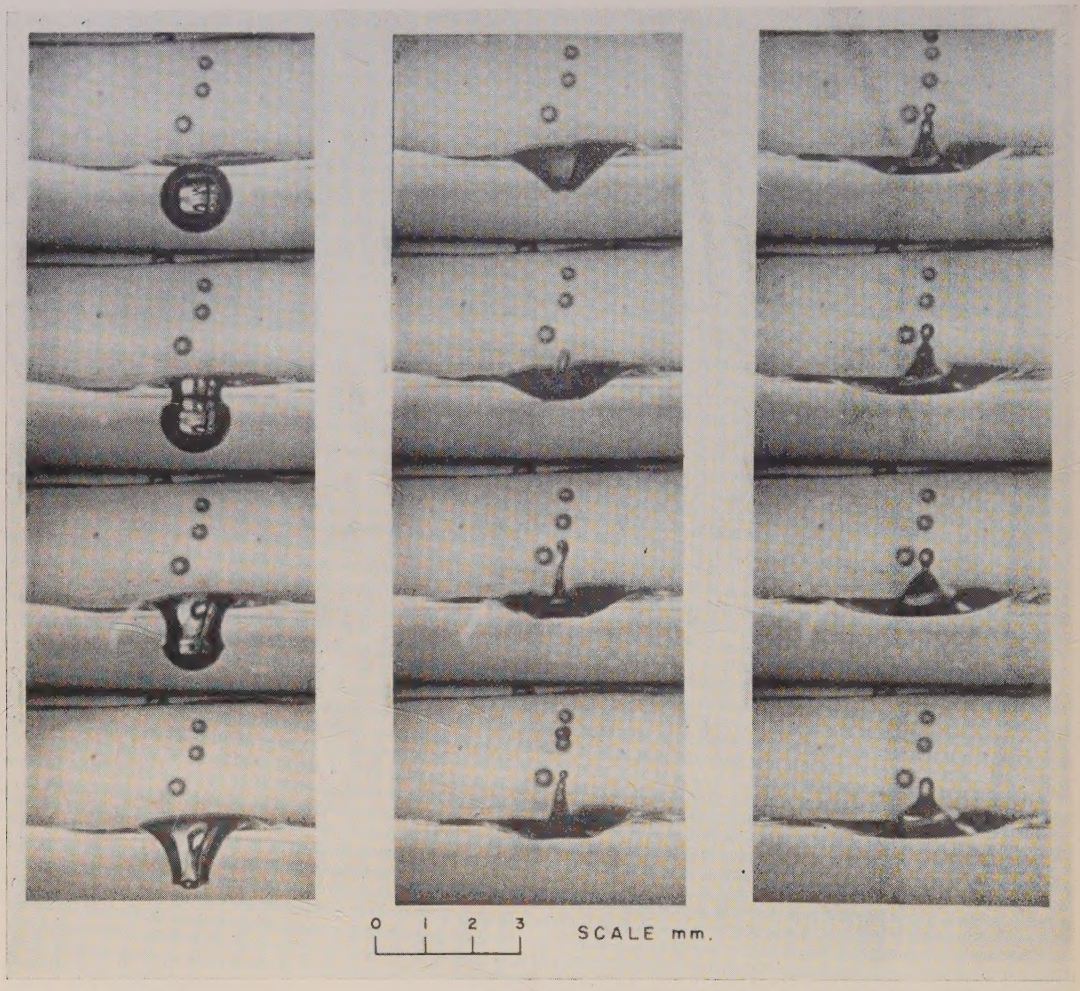

Fig. 2. High speed motion pictures of 1.5 mm diameter bubbles bursting in fresh water with clean surface. Angle of view horizontal through glass wall formed by glass microscope slide. Camera speed 3340 frames/sec.

water surface lower the surface tension and were observed to reduce the period of time spent by the bubble at the surface before bursting.

What is the effect of change in bubble size on the bursting mechanism? Observations of 0.4 mm bubbles in tap water, indicated that in general the picture was the same as that for the 1.7 mm bubbles. However, the time from initial burst to collapse of jet is considerably shorter than that of the larger bubbles. Measurements from photographs indicate that the total time is proportional to the bubble size. It was observed that the larger droplets sometimes bounce once or twice, when they hit the surface, whereas the small ones are not observed to do so.

In working with a still smaller bubble size (0.2 mm) in clean salt water, it was found that these small bubbles accumulate at the surface, forming a patch, the bursting occurring at random, and the jet formation and collapse taking place so rapidly as to be virtually incapable of resolution with the photographic techniques available to us. Oleic acid applied to the surface again produced the effect of shortening the time required for the rupture of the bubble.

Occasionally bubbles collide, forming a larger bubble by coalescence. This merging of

bubbles is sometimes observed to produce oscillations which bring about the formation of other much smaller bubbles.

Measurements of droplet sizes formed by all the different bubbles used in this investigation indicate that the average drop size is approximately one tenth the bubble size. Figure 1 D shows the usual range of droplet size variation found from individual jets. Each bubble jet produces about 5 droplets.

WOODCOCK (1952) gives a table of observed sea salt nuclei and the corresponding droplet diameters at sea-water concentrations. These data are reproduced on Table 1 together with a list of bubble diameters which would be expected to produce the corresponding droplets. The inference that may be drawn from Table I is that a bubble spectrum below 1.8 mm diameter could produce the observed spectrum of air-borne sea-salt nuclei. This result is consistant with STUHLMAN's (1932) observation that "for bubble diameter greater than 0.24 cm . . . . the ejection of the droplets was not of sufficient regularity to warrant quantitative interpretation".

Table 1. Diameter of bubbles which would produce sea-salt particles of sizes observed in the atmosphere.

Weight of sea-salt nucleus (micro-micro gms.)	Diameter of sea water droplet from which nucleus is derived (microns)	Approx. diameter of bubble which would produce corresp. droplet (microns)
1	3.8	40
10	8.1	80
10^2	17.4	170
10^3	37.6	380
10^4	91.0	910
10^5	174.0	1 700

3. Summary of Conclusions

1. The bursting of a bubble at the air-water interface in sea water or fresh water produces droplets that are ejected upward to heights large compared to the bubble size. The mechanism by which the droplets are formed and given an initial vertical velocity is found to be a result of the formation and break-up of a jet of liquid which evolves from the collapsing bubble. The energy associated with the jet formation and break-up is principally derived from the collapse of the bubble cavity some time after initial rupture of the surface film.

2. The essential mechanism of bubble bursting and jet formation and break-up is not changed with bubble diameter over the range investigated (0.2 – 1.8 mm). The total time required from rupture to decay of the jet was found to be proportional to the bubble size.

3. Bubbles bursting in sea water present essntially the same picture as those bursting in fresh water with the exception that a much longer period of time is required to rupture the bubble in sea water. Oleic acid on the surface has no observable effect other than to reduce the time between arrival of the bubble at the surface and the bursting of the bubble.

4. The droplets produced by bubbles up to 1.8 mm in diameter (the upper limit for optimum droplet production) are of the order of 1/10 the bubble size. This range of bubble size corresponds to a salt nucleus weight range observed in the atmosphere.

5. Occasionally, large bubbles are observed to produce much smaller droplets than those normally encountered. They appear simultaneously with the larger droplets. Also large droplets have been observed to reduce their mass upon rebound from the surface. These two methods suggest that large bubbles also are directly responsible for some of the lighter salt nuclei.

6. There is strong photographic evidence that the bursting of small bubbles plays an important role in the production of particles of the size range commonly encountered in the atmosphere. The jet mechanism is the only method of droplet production which has been considered here. The rupture of the film on these small bubbles may produce other much smaller particles. This question could not be investigated by our methods.

4. Experimental Techniques

Two types of photographic observation were made in this investigation (a) still photographs of very short exposure time (ca 30 microsec.), taken at random during the bursitng of a stream of bubbles, and (b) high speed motion pictures (ca 3,000 frames per sec.) of individual bubble bursts taken with an Eastman camera.

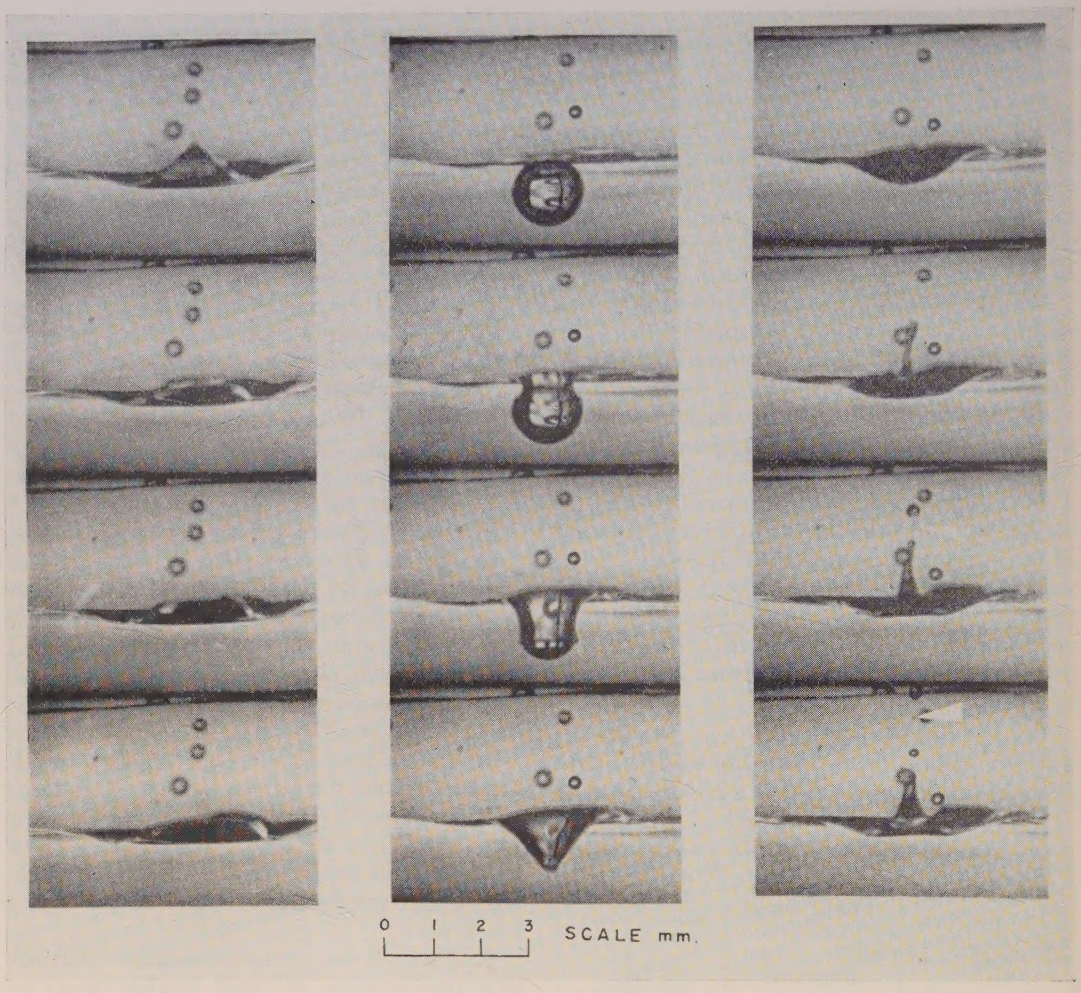

Fig. 3. First four frames at left show the final stages in the collapse of the jet shown in figure 2. The four frames in the middle and at the right were made with the camera speed 3 000 frames sec; other conditions being like those given for figure 2.
Note the barely resolvable droplet indicated by the marker at the lower right.

The photographic equipment for the still pictures consisted of an Argus C-3, 35 mm camera with a Cinter 50 mm lens on a 165 mm lens extension tube. The magnification of the lens system is 3.3 diameters. The light source was a General Radio Strobolux, Model 648-A. This model Strobolux is rated for a duration of flash of less than 30 microseconds with a flashing rate up to 100 flashes per second.

The high speed pictures were made with an Eastman Highspeed camera type III, which used 100 ft rolls of 16 mm film. The lens system for this camera was a Kodak Anastigmat f2.7, 63 mm lens and a 105 mm lens extension. The effective magnification was 1.7 diameters. A photospot (No. RSP2) lamp, at close range, was used as a light source. The Eastman High-speed has a frame exposure time of one fifth the picture cycle, and, since the average speed was near 3,000 frames per second, the average exposure was about 65 microseconds.

In both the stroboscopic and high speed photographs, back lighting was used. Light reflected by a mirror from the light source was directed through the bubble into the lens. It was found that this method produced enough

illumination to enable the use of a small aperture with both cameras.

The bubbles were formed at the end of a drawn out glass capillary placed 10—20 mm. below the liquid surface. The bubble size was varied by changing either the tip size or air pressure. The liquids used in this investigation were tap water, sea water and sea water with the surface modified with a compressed film of oleic acid. The fresh and sea water surfaces were flushed prior to photographing and free from known surface contamination. The bulk liquid temperature was in general at the ambient air temperature which varied from 21° C to 25° C.

The horizontal photographs of the bubbles bursting at the surface were taken through a glass microscope slide that had been placed in the glass jar that contained the bubble source. The inner surface had been previously coated with General Electric Dri-film to reduce the rise of the meniscus along the slide.

5. Acknowledgments

The authors wish to acknowledge the valuable comments and advice of C. H. Keith of the Woods Hole Oceanographic Institution and wish to thank Dr E. Swift, Jr, of the Naval Ordance Laboratory for the technical assistance which made this investigation possible.

REFERENCES

Facy, L., 1951: Éclatement des lames mincer et noyaux de condensation. *Journal Scientifique de la météorologie.* III-11: 86—98.

Houghton, H. G., and W. H. Radford, 1938: On the measurement of drop size and liquid water content in fogs and clouds. I. Microscopic measurement of the size of natural fog particles. *Pap. phys. Oceanogr. Meteorol.*, **6** (4): 1—18.

Kinch, E., 1887: The amount of chlorine in rain-water collected at Cirencester. *Jour. chem. Soc.* 51, 92—94.

Köhler, H., 1936: The nucleus in and the growth of hygroscopic droplets. *Trans Faraday Soc.*, 32: 1152—1161.

Köhler, H., 1941: An experimental investigation on sea water nuclei. *Nova Acta Reg. Soc. Sci. Upsaliensis,* ser. **4**, 12, No. 6, 55 pp.

Owens, J. S., 1926: Condensation of water from the air upon hygroscopic crystals. *Proc. Roy. Soc. Lond.*, (A) **110**: 738—752.

Stuhlman, Jr., O., 1932: The mechanics of effervescence. *Physics* (J. appl. Physics), **2** (6): 457—466.

Woodcock, A. H., 1952: Atmospheric salt particles and raindrops. *J. Meteor.*, **9**, 200—212.

Quasi-periodic Cyclogenesis in Relation to the General Circulation

By JEROME NAMIAS, U.S. Weather Bureau, Washington, D.C.

(Manuscript received Dec. 14, 1953)

Abstract

A striking case of recurring cyclogenesis at ten day intervals during February 1953 with a tendency to continue until mid-May has been studied against the background of the planetary circulation averaged over periods up to thirty days. The data suggest a periodicity-producing mechanism whose period may be defined by the underlying long period (e.g., 30-day) mid-tropospheric wave pattern.

In this particular case the patterns of waves observed on 5-day mean charts oscillated about certain more stable centers of action in a manner consistent with vorticity considerations. These oscillations recurrently deployed continental polar and maritime tropical air masses into juxtaposition and set the stage for cyclone growth. The movement and development of these cyclones strengthened the westerlies, thereby temporarily permitting increase of the planetary wave length. After the energy of thermal contrast was tapped and the cyclones moved off or filled, the regional westerlies declined leading to long wave retrogression and the initiation of the cycle anew.

The annoying "change in phase" which has beset workers in periodicity for years is shown to be associated with abrupt though logical rearrangements of the mean planetary circulation incident to change of season.

1. Introduction

The search for periodicity in meteorological elements has commanded the attention of many research workers during the past century. Because of the obvious application of such studies to extended forecasting many papers on the subject are listed in the Bibliography on General and Extended Forecasting published in the January 1951 issue of the American Meteorological Society's Meteorological Abstracts and Bibliography. While most of these papers appear to be empirical and the authors try to unravel the tangled skeins of nature's records, some attempts have been made to compute from theoretical considerations natural periods of oscillation in the atmosphere. In such oscillations the atomospheric envelope, once disturbed, presumably fluctuates about its normal in a rhytmic manner. SHAW (1936) has aptly termed this phenomenon "resilience".

In spite of the numerous researches on periodicity over the past century, the only periodic phenomena which are unqualifiedly accepted by meteorologists the world over, and which appear to be capable of physical explanation and detection year in and year out are the diurnal and annual cycles. Other so-called periods, while seemingly valid for limited time intervals, have a distressing way of failing when examined in the light of new samples of data. These failures are often attributed to "change of phase," a convenient phrase in any periodologist's vocabulary.

The tendency to recurrence of synoptic weather map patterns for differing time intervals led the Russian School (PAGAVA, 1940) to define a "natural periodicity". This "natural period" is not a fixed interval of time in the usual sense, – rather, it is an interval during

which the lines of synoptic activity (the tracks of cyclones and anticyclones, for instance) are much the same. The interval, or natural period, may last for five, six, seven or even up to sixteen days, after which another type of activity takes place and lasts about the same length of time as its predecessor. During one so-called "synoptic season", however, the interval of common synoptic activity tends to remain about the same, changing abruptly by two days or more with the onset of another "synoptic season". This is apparently another way of expressing the "change of phase", and presumably indicates that some new impulse or feature has been added to or subtracted from the circulation that formerly was not of importance.

Fresh interest in periodicities has been evoked by the striking weekly recurrences in rainfall pointed out by LANGMUIR (1950, 1953), who attributed them to periodic cloud seeding, and by subsequent work or BRIER, HALL (1950) and HAWKINS (1952), who revealed 7-day periodicities for intervals during which no comparable periodic cloud-seeding was performed. The lay public is occasionally aware of periodic weather phenomena before the forecaster, who may be overly preoccupied with the daily weather map.

The author's interest in periodicity stems largely from long experience in making 5- and 30-day forecasts of general circulation and weather, for in this work one cannot escape the fascination of recurring weather regimes (NAMIAS, 1953). Since 30-day mean maps of atmospheric circulation characterize quite effectively the average and prevailing weather of the month, it is possible that the length and character of atmospheric periodicity are closely associated with the patterns of the general circulation. In such a case the underlying planetary circulation depicted by a mean over a period of a month or so, may not only reflect or predetermine the paths and behavior of

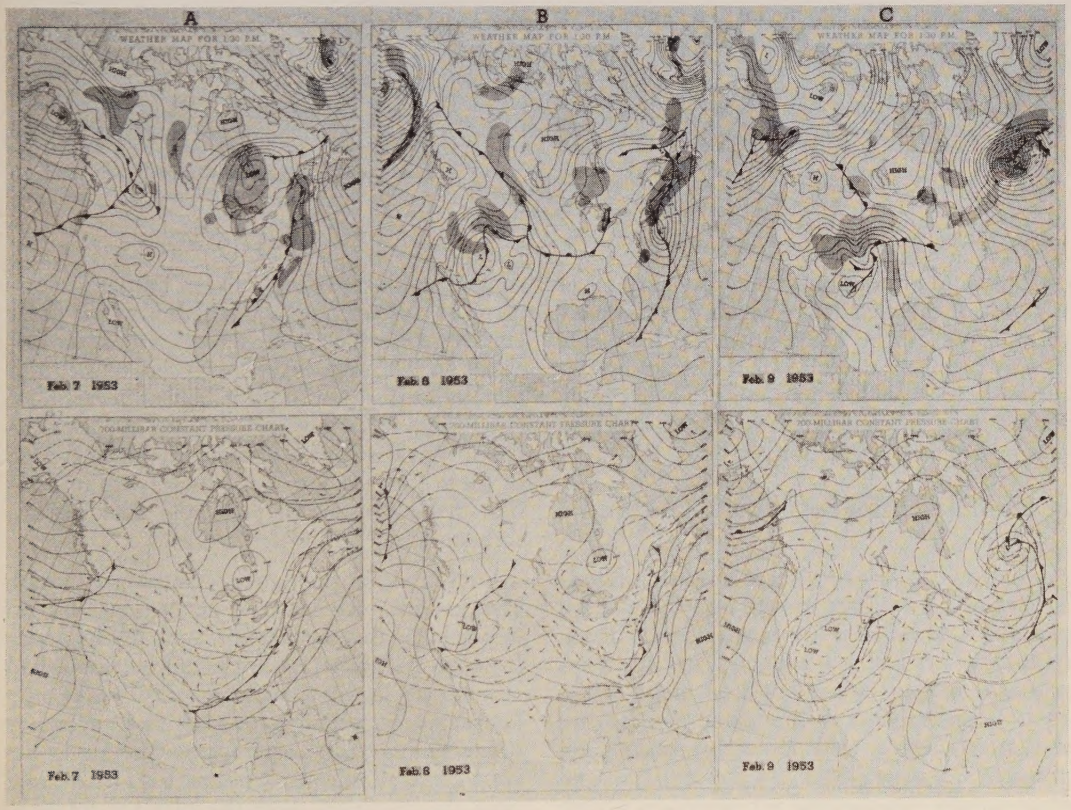

Fig. 1. Sea level (upper) and 700 mb (lower) charts for 1830 Z and 1500 Z respectively on 7, 8, and 9 February 1953.

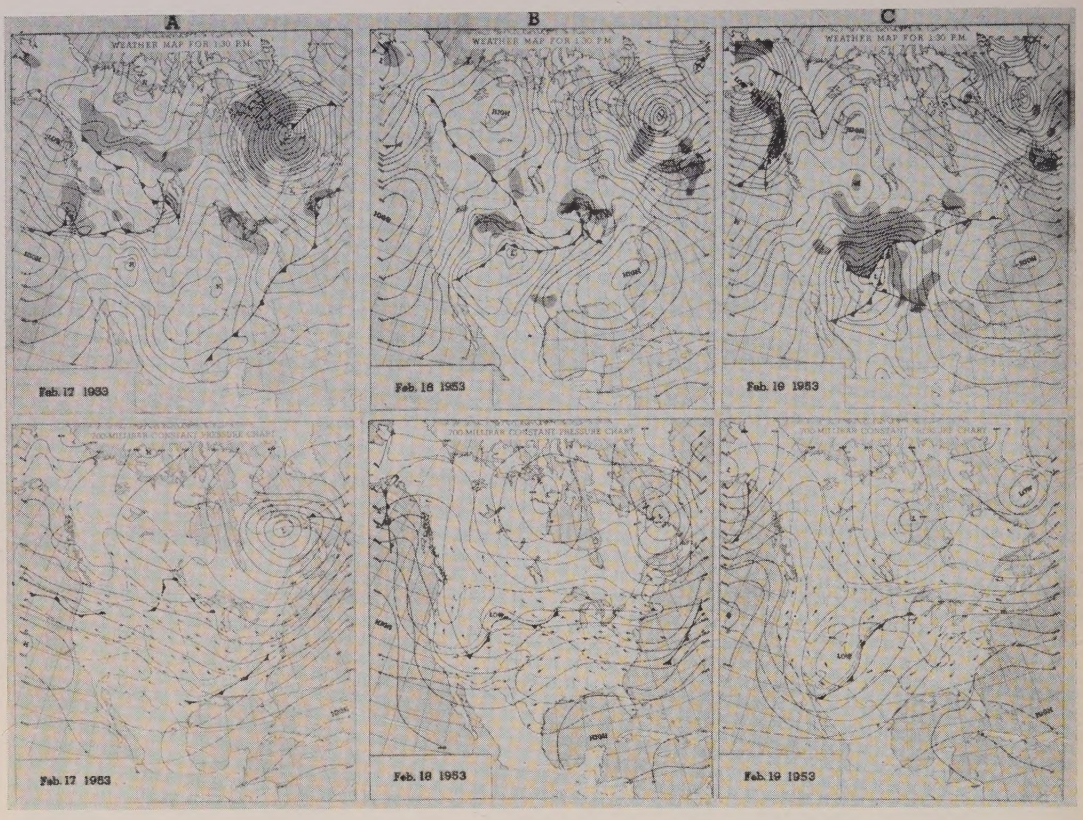

Fig. 2. Sea level (upper) and 700 mb (lower) charts for 1830 Z and 1500 Z respectively on 17, 18, and 19 February 1953.

cyclones and anticyclones, but also may serve as a sort of calendar from which predominant periodicities can be determined. In this paper an effort will be made to demonstrate how a chain of events leading to quasi-periodic cyclogenesis may be associated with the form of mean planetary circulation patterns.

2. Periodic cyclogenesis during February 1953

During February 1953 three unusually rapidly developing cyclones moved into the western plateau of the United States at intervals of ten days. The series of sea level and 700 mb maps reproduced from official printed maps of the U.S. Weather Bureau for these periods are shown in Figs 1 to 3. In each series a high pressure area at sea level (on the 7th, 17th and 27th) rapidly vanishes and is replaced by a deep cyclone within 24 to 48 hours. Similarly, ridge conditions aloft give way to the rapid development of closed cyclonic circulations. The great effect of these developments on regional weather shall not be discussed here, except to mention that these storms produced extensive areas of rain, sleet, and snow and affected much of the country in the course of their life history. One of them (the second of the three) was responsible for high winds, blizzards, dust storms, tornadoes and abnormal freezes.

Detection of the wave disturbance which plunged into the western plateau was by no means easy for the analyst, and in the series from 7 – 9 February only a minor ripple had been found in the polar front off Oregon on 7 February. Subsequent to this map pressures began falling with amazing rapidity along the west coast (4 mb per 3 hours at 2130 Z), and later the pressures over the plateau did likewise. Similar features attended the later two

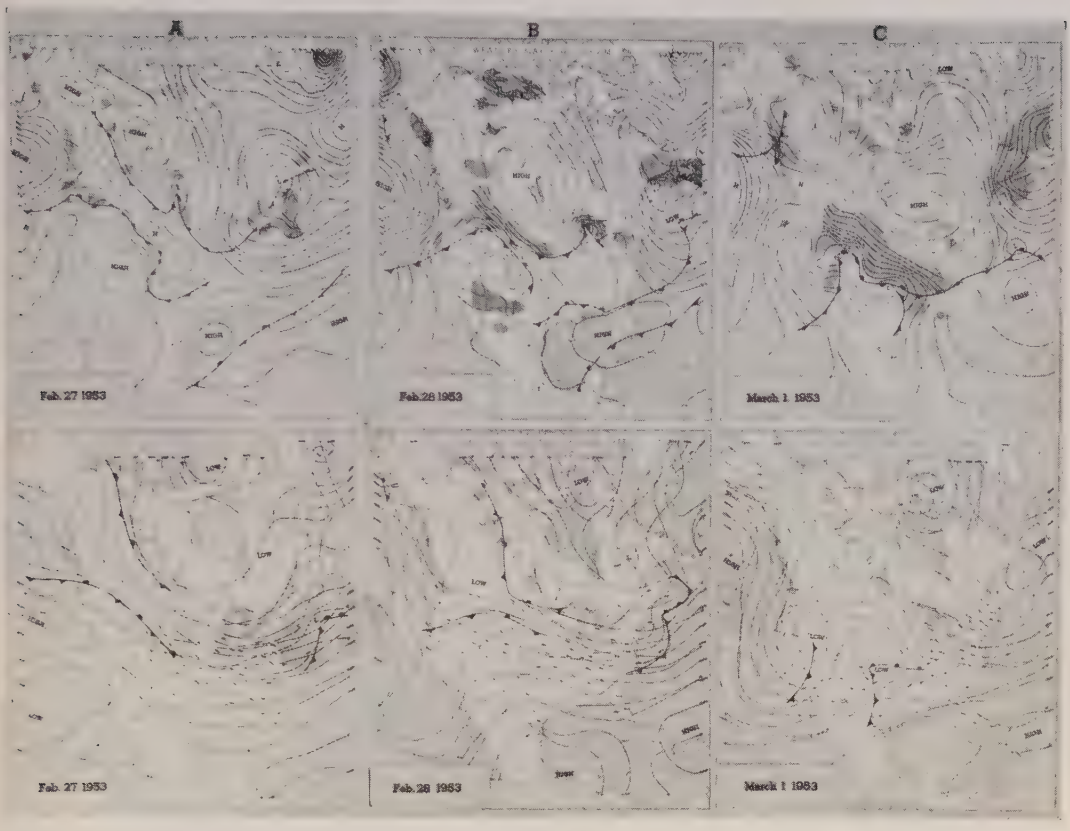

Fig. 3. Sea level (upper) and 700 mb (lower) charts for 1830 Z and 1500 Z respectively on 27 and 28 February, and 1 March 1953.

cases, when the analysts were apparently more alert to the possible existence of a nascent wave off the west coast. However, in all three cases the development was so spectacular that the official 30-hour and medium range prognostic charts appreciably underestimated the deepening.

The regularity, similarity and abruptness of these three storm developments is graphically illustrated by the plot of 700 mb height variations at 40°N, 110°W (near Salt Lake City) shown in Fig. 4 (top).

From this figure it will be noted that also in the period from March through the first half of May there was some suggestion of a continuation of sharp minima occurring about each ten days. This matter will be discussed at greater length later on. Meanwhile attention shall be focussed on other pertinent features of the February cyclogenesis.

Following the classical work of Rossby (1939), modern synoptic meteorology lays much stress on the planetary wave trains in the upper westerlies as governors of cyclonic activity at sea level. In fact, these concepts have for many years furnished the basis of preparing 5-day prognostic charts (Namias, 1947). The detection of the long planetary waves as opposed to the short cyclone waves has been effected by the use of time-averaged mean maps which usually filter out the short waves quite effectively. Five-day mean maps for the 700 mb level for periods just preceding the plateau cyclogenesis are shown in Fig. 5. In all three cases the wave lengths between the troughs over the western Pacific and United States (or western Atlantic on the 23rd to 27th) are uncommonly long in temperate latitudes. [Wave lengths are here measured between longitudes where the contours reach a mini-

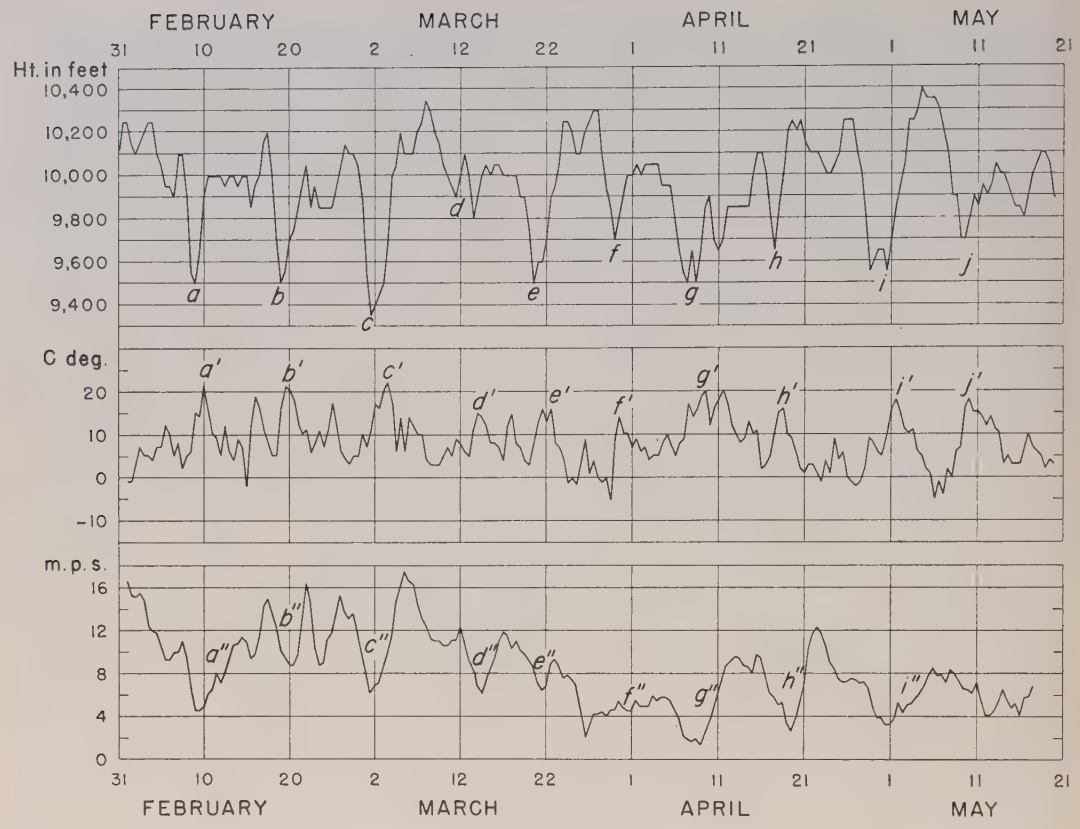

Fig. 4. Twice daily (0300 Z and 1500 Z) values of 700 mb height at 40° N 110° W (top), temperature difference at 700 mb between 30° N 100° W and 40° N 110° W (middle), and North American zonal index (bottom) (computed for latitude belt 35° N—55° N between 65° W and 125° W), all for the period February through early May 1953. Letters refer to quasi-periodic fluctuations usually associated with plateau cyclogenesis.

mum (troughs) or maximum (ridges) latitude.] At 40°N, for example, they are:

3— 7 February – 97 degrees of longitude
13—17 February – 138 " " "
23—27 February – 144 " " "

Since these waves are asymmetrical, the distance between the trough in the western Pacific and the ridge over western United States accounts for much of the great wave length. These values at 40°N for the three periods in chronological order are 65 degrees of longitude, 92 degrees and 59 degrees. Studies of 5-day mean charts over North America (NAMIAS and CLAPP, 1944) have indicated the average wave length during winter to be about 83 degrees of longitude at 45°N latitude and the stationary wave length 98°, although these statistics refer to twice the distance between trough and ridge over the United States. From this comparison as well as from forecasting experience it is concluded that the planetary wave in which the ensuing cyclone becomes embedded has become unusually extended — a condition well-known to favor retrogression of the eastern trough of the wave train or perhaps development of a new trough at a position in more harmony with wave length (vorticity) considerations. The subsequent adjustment of the planetary wave as observed from the 5-day mean maps just subsequent to those in Fig. 5 (that is for the periods 8—12 February, 18—22 February, and 28 February—4 March) is shown by the ridge and trough lines extracted from these maps. Here the "retrogression" of both ridge and trough are clearly indicated.

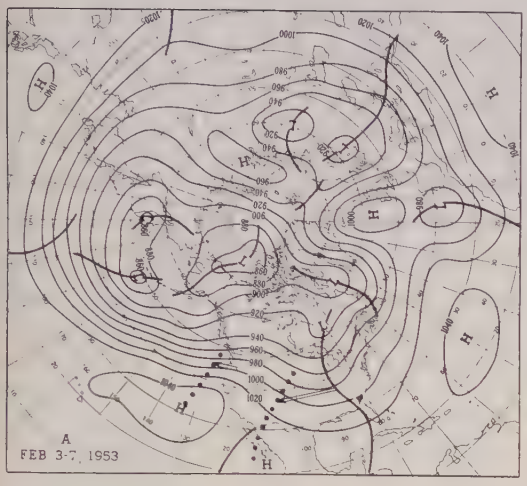

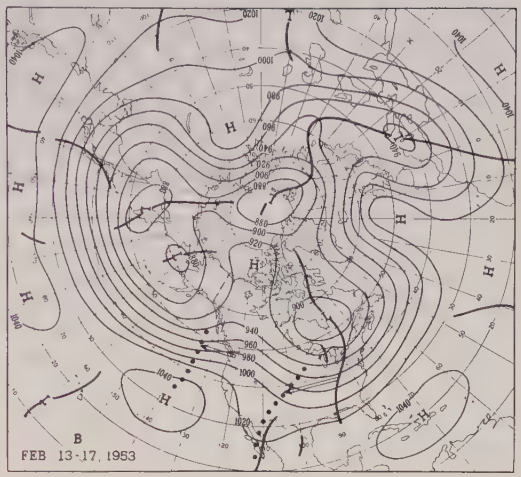

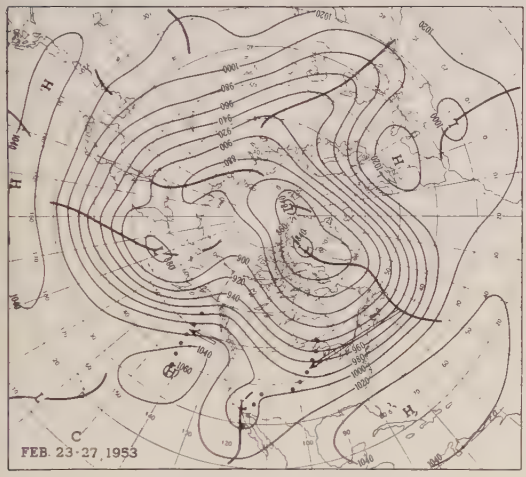

Fig. 5. 5-day mean charts of 700 mb contours (in tens of feet) for periods just preceding abrupt cyclogenesis over western plateau. (a) 3—7 February 1953 (b) 13—17 February 1953 (c) 23—27 February 1953. Trough lines (solid heavy) are drawn for minimum latitude of contours. Arrows denote displacements of major U.S. troughs and ridges to next 5-day mean where dotted lines indicate new positions.

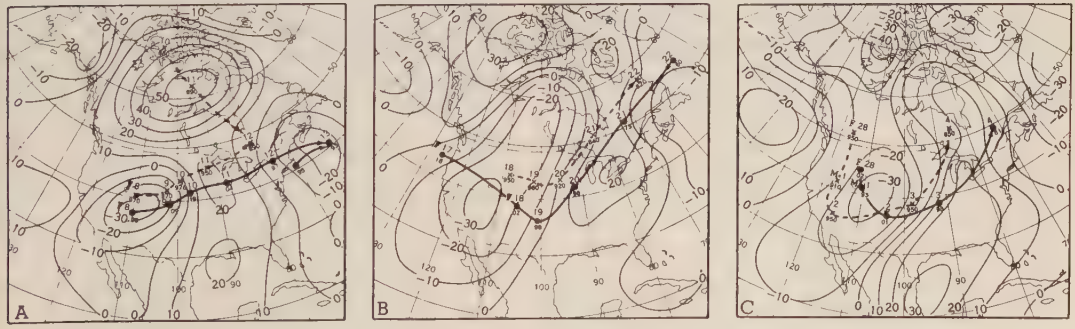

Fig. 6. Departure from normal of thickness (in tens of feet) between 1000 mb and 700 mb subsequent to cyclogenesis over western plateau (a) 1500 Z, 10 February 1953 (b) 1500 Z, 19 February 1953 and (c) 1500 Z, 3 March 1953. Heavy curved arrows connect points giving daily positions (by day of month) and intensities of primary cyclone centers at sea level (in mbs) and 700 mb (in tens of feet) which emanated from plateau cyclogenesis.

Thus the pronounced cyclogenesis over the western plateau appears to have originated in an over-extended planetary wave, which favored the development of the west coast perturbation in order to bring about the necessary shortening of the long waves. To what extent the cyclone developments were barotropic or how much contribution came from the baroclinicity in the vicinity is not possible to determine without laborious computations much easier done by electronic machines. However, inspection of the thermal fields preceding the development (lower charts in Figs 2a, 3a, and 4a) suggests that the barotropic contribution was the principal one,—at least in the initial stages of the first and third cases.

Coincident with each deepening cyclone and formation of the upper cold low, polar air masses were advected southward into the trough and tropical air masses northward ahead of it. This differential advection soon led to an abnormally large temperature difference between the western plateau and the central plains region. The departure from normal of the layer isotherms (thickness anomalies) between 700 and 1000 mb just subsequent to the western cyclogenesis are shown in Fig. 6.

The subsequent history of the principal perturbation which emanated from the plateau trough is also indicated in Fig. 6 by curves showing the 24 hr positions and intensities of cyclone centers at sea level and the corresponding center or short wave trough aloft. At the few times when the sea level continuity was not straightforward, a great deal of help was derived from the course of the 700 mb perturbations and the suggestion of steering afforded by the 5-day mean 700 mb pattern (not reproduced) in which they were embedded,—a procedure which might be used profitably where official storm track charts are published.

While the general trajectories of the cyclones in Fig. 6 seem to be governed chiefly by the concurrent 5-day mean steering patterns of their respective periods (not shown), the differences in deepening after leaving the plateau area are related to the pre-existing thermal fields. The cyclones of 19—21 February and 2—4 March underwent very strong deepening as they left the plateau area (998 mb from 20 March to 975 mb on 21 March, and 998 mb on 3 March to 981 mb on 4 March), while the cyclone from 9 February to 12 February was much weaker, reaching an intensity of only 997 mb on 12 February. These differences are apparently associated with the extent and orientation of the thermal anomalies. In the two cases of the strong cyclones (21 February and 4 March) the preceding anomalous temperature contrast extended in a general meridional direction for great distances, while in the case of the weak cyclone (11 February) the thermal contrast is limited to more southerly latitudes whereas warmer than normal air existed in Canada. Consequently, the cyclones moving away from the plateau area (generally northeastward) in the two later cases could continually draw upon the potential energy of mass distribution along much of their paths while in the first case the cyclone had access to a much more limited supply of thermal energy.

The initial temperature contrast associated with the plateau cyclogenesis occurs between Texas and the central plateau where warm maritime tropical and cold polar air masses are brought into juxtaposition. An index of this temperature contrast at 700 mb as a function of time has been plotted in Fig. 4 (middle). Here again the periodicity shows up; in this case as sharp peaks of maximum temperature contrast which lag the 700 mb height minima about a day.

As the cyclones proceed northward and increase in intensity a regional increase in zonal wind speed occurs over the United States, as shown by the zonal wind speeds in the latitude belt 35°N to 55°N observed between 65°W and 125°W and plotted in Fig. 4 (bottom). The increasing bursts of upper westerlies are shown as a″, b″ and c″ which follow on the heels of the plateau trough development (the height minima) and peaks of temperature contrast. The failure of sharp bursts of zonal wind speed to materialize from mid-March to early April resulted from a strong wave of blocking which effectively depressed the storm track (and westerlies) south of the latitude band (35°—55°) in which this index was measured. In fact, the peak speeds of the westerlies at 700 mbs prevailed between 35° and 40° during this period of blocking. It is probable that the periodicity in zonal wind speed would be more pronounced in an index which measured the peak speed independent of latitude.

3. The mechanism underlying the February periodic cyclogenesis

Thus far a description of some of the prominent synopic features attending the plateau cyclogenesis has been offered. In order to assist

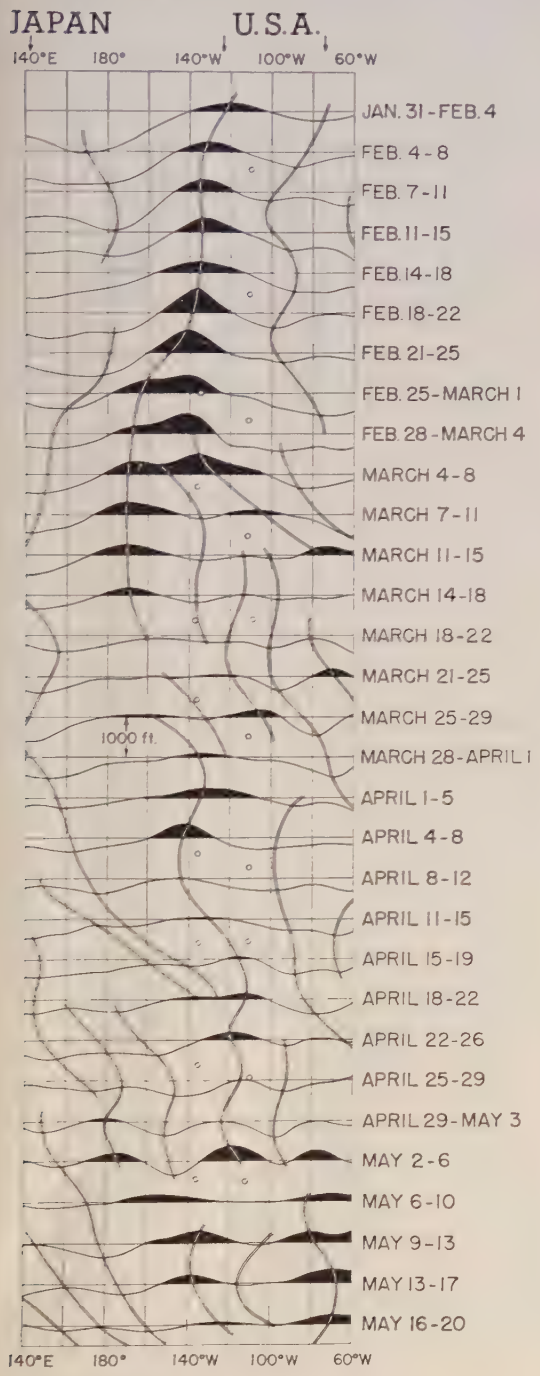
JAPAN
U.S.A.
140°E 180° 140°W 100°W 60°W
JAN. 31 - FEB. 4
FEB. 4 - 8
FEB. 7 - 11
FEB. 11 - 15
FEB. 14 - 18
FEB. 18 - 22
FEB. 21 - 25
FEB. 25 - MARCH 1
FEB. 28 - MARCH 4
MARCH 4 - 8
MARCH 7 - 11
MARCH 11 - 15
MARCH 14 - 18
MARCH 18 - 22
MARCH 21 - 25
MARCH 25 - 29
1000 ft.
MARCH 28 - APRIL 1
APRIL 1 - 5
APRIL 4 - 8
APRIL 8 - 12
APRIL 11 - 15
APRIL 15 - 19
APRIL 18 - 22
APRIL 22 - 26
APRIL 25 - 29
APRIL 29 - MAY 3
MAY 2 - 6
MAY 6 - 10
MAY 9 - 13
MAY 13 - 17
MAY 16 - 20
140°E 180° 140°W 100°W 60°W

Tellus VI (1954), 1

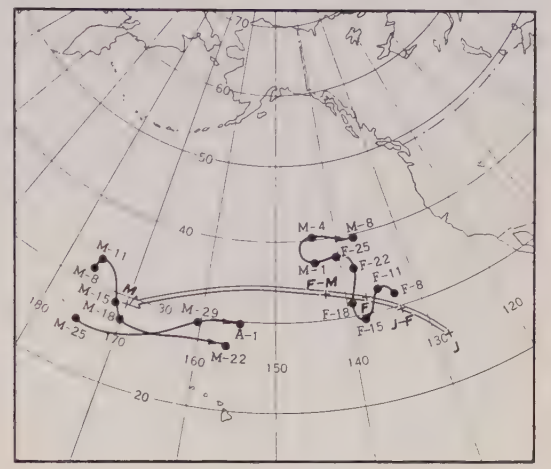

Fig. 8. 5-day (solid circles) and 30-day (crosses) mean positions of principal center of Pacific anticyclone at 700 mb level. Dates are indicated by monthly initials and numbers, e. g. F-11 means 5-day period ending 11 February, J-F means mid-January to mid-February, etc.

the reader in placing these into the perspective of longer timescale, Figs 7 and 8 have been constructed. The former gives 700 mb height profiles at 40°N extracted from routinely computed 5-day mean maps which are prepared twice a week from twice-daily analyses. Troughs and ridges are indicated by lines marking the lowest and highest contour heights (respectively) reached along the latitude. Areas of the curves are shaded where heights are above the base line of 10,000 feet. These base lines are exactly 1000 feet apart, thereby facilitating a quick visual estimate of height difference from 10,000 feet and of height changes from one period to the next. The ordinate of the graph is also an approximate time scale since the distance between successive base lines is about one half-week. In Fig. 8 are shown the mean positions of the eastern Pacific anticyclonic center at 700 mb for 5-day and 30-day periods.

Fig. 8 shows that from 8 February to 8 March the eastern Pacific upper level anticyclone was

Fig. 7. Profiles of the 700 mb surface at 40° N for 5-day means during the months February through early May 1953. Heavy vertically oriented curves give positions of principal troughs and ridges. Open circles indicate roughly the periods indicated by minima in Figs 4 and 11. Shaded portions of curves show areas where 700 mb height exceeds 10,000 feet. Base lines of curves are equally spaced as indicated in the dimensional marker in the middle.

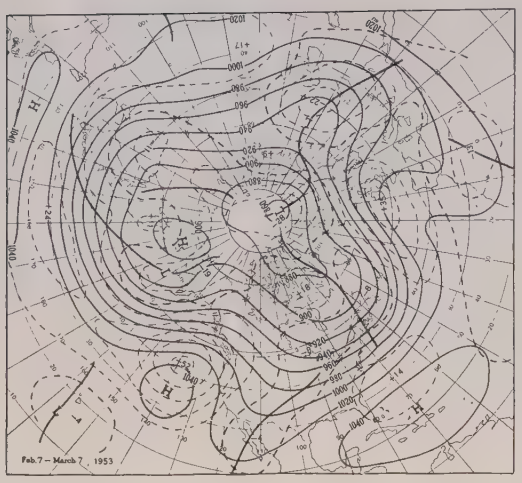

Fig. 9. 30-day mean 700 mb contour chart (in tens of feet) and its anomaly (broken lines) for the period of most pronounced 10-day periodicity, 7 February—7 March 1953.

a prominent and quasi-stationary feature of the planetary wave train. It is important to note, however, that although moving rather erratically it gyrated about a generally northwestward path. This mean component of motion is also indicated in the path of the 30-day mean center from January through mid-March. The main habitat, as well as the character of the fundamental mid-tropospheric center of action during the period of cyclogenesis, is perhaps best shown by the 30-day 700 mb chart for 7 February to 7 March, Fig. 9, on which the height anomalies are superimposed.

The quasi-stationary, though slowly retrogressive nature of the ridge during February and early March is also evident in the profiles of Fig. 7. Each burst of cyclogenesis over the western plateau was preceded by a long wave length between the quasi-stationary east Pacific ridge and the eastern U.S.A. trough, or also between the two troughs on either side of the ridges. During these periods of long wave length preceding cyclogenesis and retrogression of the major long wave troughs, the zonal flow over the half-hemisphere 0° long. westward to 180° was high, subsequently falling to lower values attending and following the cyclogenesis, as indicated in Table 1.

The above description of synoptic events makes it possible to suggest the mechanism producing periodic cyclogenesis.

Table 1. Zonal flow at 700 mb at 40°N (from 0° westward to 180° taken from wind speed profiles)

	Period	Geostrophic Wind Speed (mps)
preceding cyclogenesis	31 Jan.—4 Febr.	14.0
following »	7—11 February	12.0
preceding »	14—18 »	15.0
following »	18—22 »	13.0
preceding »	21—25 »	13.0
following »	28 Febr.—4 March	9.0

In February, the fundamental pattern (the 30-day mean shown in Fig. 9) indicates that the strongest anomaly (520 feet) lies in the area dominated by the eastern Pacific upper level anticyclone whose semi-permanence has already been mentioned (see Fig. 7). Other anomalies in the Pacific or over North America and the western Atlantic appear relatively weak so that the most anomalous component of the planetary wave train, the eastern Pacific ridge, seems to be the more stable feature of the general circulation, while other adjacent and more remote areas largely respond to its dictates. The manner of this response brings us back to the sequence of events associated with the cyclogenetic periodicity.

During periods of high zonal flow the long-wave trough over the United States is permitted to reside east of the 30-day mean position, although the eastern Pacific ridge remains essentially in the preferred position indicated by the longer period mean. This fact agrees with the wellknown barotropic wave-equation where the stationary wave length is directly proportional to the square root of the zonal wind speed. The periods of high index, particularly over North America, are those subsequent to the northeastward movement and deepening of the great cyclones which emanate from the western plateau and feed on the thermal contrast initially established by planetary wave retrogression.

In other words, there appears to have been an intertwined series of events: A quasi-stationary and abnormally strong eastern cell of the Pacific High developed early in February. This anticyclone regulated the downstream pattern in a manner depending upon the strength of the westerlies. During an initial period of weakening circulation and greater growth of the anticyclone the downstream trough was favored over the plateau, not far from the

ridge. The development of this trough proceeded as a small perturbation appeared on the Pacific coast and deepened with amazing speed. In so doing it induced strong flows of polar and tropical air on its west and east sides respectively (see Fig. 6) since the geographical location of this deepening storm lay fairly proximate to sources of both continental polar and tropical Gulf air. Having developed such a strong and extensive thermal contrast, further cyclogenesis of one or more cyclones along the Polar Front was favored, for these cyclones could feed upon the rich diet of thermal energy as they proceeded northeastward. The increased kinetic energy fed into the westerlies by the northward migration of the deepening cyclones created high index periods thereby permitting the planetary trough over the United States to occupy a position farther east of the quasi-permanent Pacific ridge than in the longer period mean. After the major source of energy for the cyclones, the thermal contrast, was used up in the cyclogenetic process and friction set in to decrease the westerlies after the cyclones left the area or filled, the stage was set for retrogression of the long wave trough into the plateau, when the chain of events once again repeated.

With our present meteorological knowledge it would be difficult if not impossible to compute the time involved in this cycle of interdependent events. Ten days, the observed time, appears long in view of the many claims for periods lasting from five to seven days. However, NAGAO (1952) maintained that a 10-day period in air pressure is often found in the neighborhood of the Kanto district of Japan, particularly from April to June and from September to October. In a study of natural periods in Russia during 1926—1935 PAGAVA (1940) gave the frequency of 10-day periods as occurring there only 7 % of the time while six to eight day periods occurred 65 % of the time.

Before leaving the February case, 10-day periodic cyclogenesis in another area shall be described. This occurred in the vicinity of the Hawaiian Islands where an easterly wave appears in the underlying pattern of the 30-day mean (Fig. 9). The 5-day mean maps or daily maps during this period show that this low latitude trough becomes active more or less in sympathy with the eastern Pacific upper level high and the southwestern plateau trough. It does this as the westerlies in the Pacific fluctuate in strength and position, so that the easterly wave periodically builds up into the westerlies, splitting the narrow zonally-oriented semipermanent ridge to its north (Fig. 9). The 10-day periodic nature of the activity of this trough and its association with the lower latitude portion of the western plateau trough are shown in Fig. 10. The slight lag in these curves suggests that there was some contribution to the enhancement of the Pacific High by the Hawaiian trough.

4. Termination of the February regime

While the general circulation during February oscillated about a fairly stable position, it was pointed out that there was a slow westward drift of the eastern Pacific anticyclone. This drift is evident in Figs 7 and 8 and is associated with a comparable retrogression of the central and western Pacific trough. The

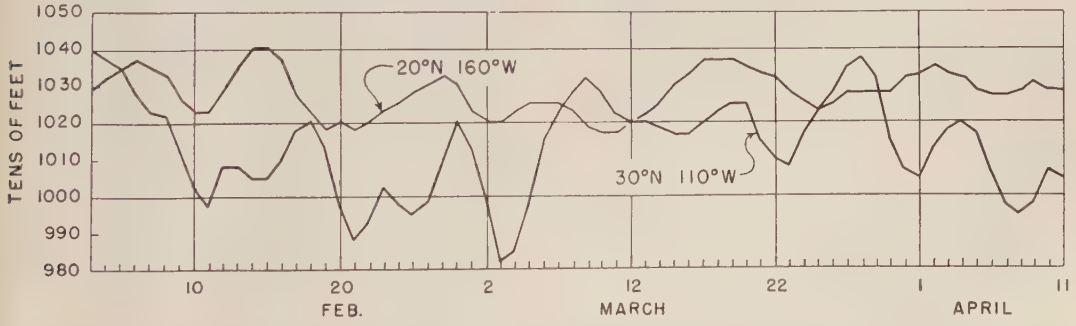

Fig. 10. Daily 700 mb heights (upper) at 20° N 160° W (near Kawai in the Hawaiian Islands) and (lower) at 30° N 110° W at the base of the western plateau trough. Note the periodicity and resonance during February which abruptly terminates in March.

major westward shift in this trough occurs between 18 February and 15 March during which period it gradully retrogrades from 180° to a position just west of Japan. Simultaneously, there is the marked increase in height between 160°W and 180°, the area which ultimately becomes the seat of the major ridge (after 8 March) while the ridge farther east progresses and declines. This is the usual manner in which retrogression operates. The downstream trough subsequent to the retrogression is now favored just off the west coast of the United States—a position in harmony with the new seat of the central Pacific ridge. Note that this new wave train is out of phase with the pattern which occupied the same area during most of February. The break in regime along the west coast occurred abruptly between the 5-day periods ending 8 March and 11 March, when, in spite of the overlapping character of the periods the 700 mb heights at 130°W fell more than 600 feet.

Before discussing the repercussions of this change in regime upon cyclogenetic periodicity an attempt will be made to explain its evolution, or at least to cite some factors which are apparently important in the development. In the "self-developmental" hypothesis advanced by the author (NAMIAS, 1953) to account for changes in long period mean patterns of atmospheric circulation, there was assumed to be some inertia in mean circulations. Because of this, changes in insolation incident to change in season can operate differentially upon the centers of action and their component planetary waves which have prevailed during a period of say two weeks to a month. These changes then introduce displacements and distortions in the centers of action which are amplified, suppressed or in some way brought into greater harmony through the great teleconnections operating between the various troughs and ridges (operating primarily through vorticity flux) of the general circulation.

In the present situation it appears that the initiation of the retrogression may be largely ascribed to the marked weakening of the Asiatic monsoon anticyclone which normally occurs from late winter to early spring and the consequent retrogression of the upper level Asiatic coastal trough which is also a climatological feature at this time. For example, normal monthly maps (U.S. Weather Bureau, 1952) show that the semipermanent Asiatic anticyclone at sea level falls away from about 1033 mb to 1028 mb at its center from February to March. Concurrently, the normal trough at the 700 mb level at 40°N recedes from 160°W to 150°W with a similar retrogression of the central Pacific ridge. In February and March of 1953 the changes were as follows:

	1953	Normal
Change in Intensity of Sea Level Asiatic High	− 15 mb	− 5 mb
Retrogression of Asiatic Coastal Trough	25° long.	10° long.

It is also interesting to compare in Table 2 the changes in 700 mb contour height at 40°N over the Pacific from February to March as normally observed with the changes in 1953.

Table 2. Changes in 700 mb height along 40° N from February to March

	140°E	150°	160°	170°E	180°
Normal change (tens of feet)...	+ 9	+12	+19	+22	+19
1953 Change	+16	+22	+37	+52	+67
	170°W	160°	150°	140°W	
Normal changa (tens of feet)	+18	+15	+11	+ 6	
1953 Change	+68	+44	+ 8	−19	

It appears that during 1953 the changes in circulation from February to March over Siberia and the Pacific followed the general course of normal seasonal change *but with much greater intensity*. In other words, in 1953 an amplification of the normal change occurred: —the Siberian High fell away faster, the coastal trough retrograded more and the Pacific ridge increased more than normal. These amplifications of the normal change appear even more striking when one notes from Fig. 7 that a large portion of this change took place between the periods 21—25 February and 25 February —1 March. Precisely why and how this amplification came about is presently impossible to answer. However, if one assumes some form of carry over (inertia) of the anomaly of the eastern Pacific ridge as the retrogression takes place, the large rises in the central Pacific may be accounted for. The greater reduction in the strength of the Asiatic high than normally occurs is associated with the increase in

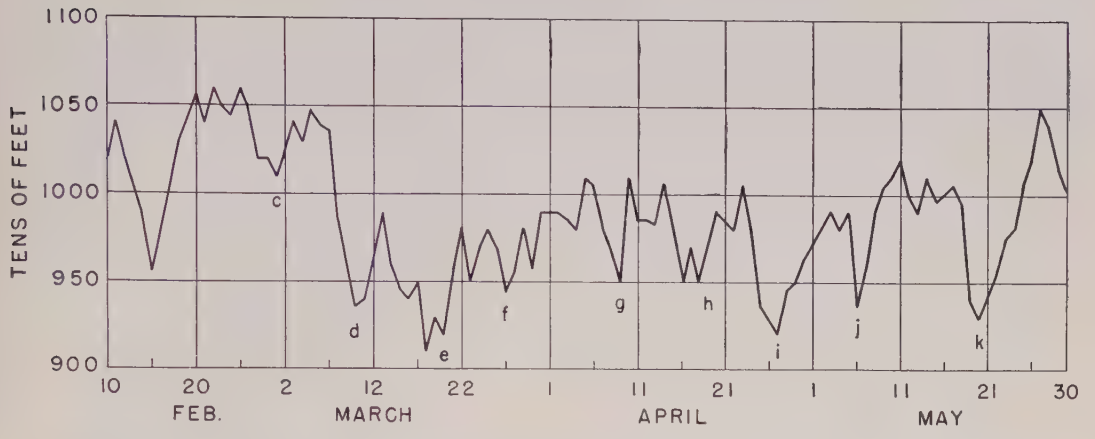

Fig. 11. Daily (1500 Z) height of 700 mb surface at 45° N 135° W showing the establishment of 10-day cyclogenetic periodicity off the west coast during March and April.

westerlies over it in March compared to February. This increase, in turn, is associated with the strong northeast-southwest tilt of the trough over western Russia.

(a) *Effect of the change in regime on periodicity*

With the sudden appearance of a trough off the west coast of the United States in place of a ridge, the clear-cut nature of the periodicity observed in February vanishes, as indicated in Fig. 4 (top). However, one can still find a suggestion of the re-establishment of ten-day periodicity, especially beginning with the abrupt drop around 20 March and continuing with successive deep minima through 9 May. These reasonably periodic minima are believed to be secondary phenomena induced by emanations from the primary trough off the west coast which was a quasi-permanent feature of the March and April circulations. The primary storms leading to a 10-day periodicity appear to have developed in advance of the upper level ridge of the mean underlying pattern in a manner somewhat similar to the storms over the plateau in February. Thus a 10-day cyclogenetic periodicity can be detected in the site of the trough (e.g. at 45°N, 135°W) in March and April as indicated in Fig. 11. Note that this periodicity did not appear until the west coast trough became established (after the first week in March) although a weak forerunner appeared around 1 March. This forerunner was not due to a separate cyclogenesis off the west coast, but to strong deepening of the plateau cyclone, which, responding to the long-period retrogression of the planetary wave, could for the first time influence this area (45°N—135°W). Thus it would seem that the nature of the periodicity is linked primarily to the fundamental pattern of the general circulation and not to the orography.

The disturbances which plunge into the planetary mean trough off the west coast in Spring are seldom stationary but travel embedded in a generally westerly flow aloft onward to the western plateau. They usually undergo redevelopment just east of the Continental Divide, perhaps in response to the creation of a trough to the lee of the Divide under selected wind conditions. This redevelopment often results in a very short wave length between troughs on either side of the plateau. The recurrence of such troughs during March was so prominent that they show up in the 30-day mean (Fig. 12).

The break in regime beginning after the first week in March is much more effective in destroying the periodicity observed in the vicinity of the Hawaiian Islands (see Fig. 10) than over the western plateau. The reason for this and also for the abrupt cessation of resonance between the Hawaiian trough and the southern portion of the plateau trough seen in Fig. 10 is due to the retrogression of the strong Pacific ridge. As may be seen from the mean flow pattern for March (Fig. 12) this retrogression relegates the Hawaiian trough entirely to the role of an easterly wave, with no opportunity to enter into the circulation

of the westerlies as it could in February when the neck of ridge to its north was very tenuous (Fig. 9). In other words, the strong anticyclone north of the Hawaiian area in March shielded the area from quasi-periodic variations associated with the westerly wave train to the north. Here is an excellent example of how changes in phase in periodicity at a point can be brought about by very large scale features of the general circulation.

5. The mean circulation after April and the termination of the 10-day periodicity during May

The mean flow pattern initiated after the first week in March prevailed more or less until the end of the month, particularly with respect to the recurrence of trough activity off the west coast. However, strong seasonal effects accompanying the transition to Spring produced later modifications in the 5-day mean wave patterns. For example, as the zonal index at 700 mb fell from an average of 9.4 mps in March to 7.3 mps in April (a somewhat greater drop than normal) an increase in wave number was favored leading to another quasi-permanent trough in the central and eastern Pacific. In general, as may be seen from Fig. 7, the 5-day mean flow patterns were in a state of transition during most of April and did not become stably organized until late in the month after which time there were only minor fluctuations through the first week of May. In spite of the April transition the 10-day character of the periodicity in 700 mb height continued as shown in Figs 4 and 11. When considered against the background of the longer period (30-day) mean, the continuation of the periodicity is perhaps not so surprising since April's pattern (not shown) resembled February's (Fig. 9) (when the periodicity was most pronounced) in the general nature of the westerlies and positions of troughs and ridges over the Pacific and North America.

Another sharp break in pattern occurred after 2—6 May with the new stable pattern (9—13 May) quite out of phase with the original. Here the abrupt transition was due to the insertion of a new trough, formerly existing only at high latitudes, into the temperate latitude westerlies over east Asia. The effect of this abrupt change in planetary circulation

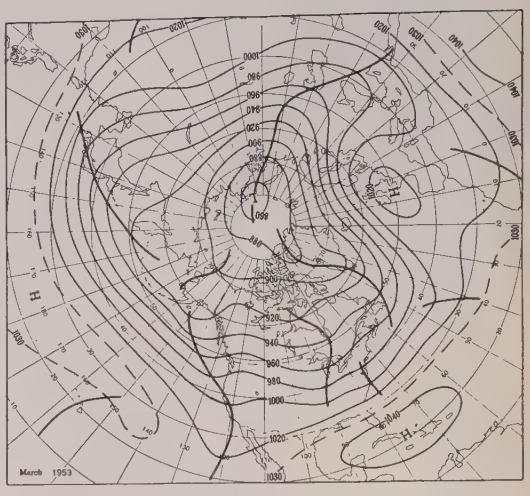

Fig. 12. Mean contours of the 700 mb surface (in tens of feet) for March 1953.

upon the periodicity is quite evident in Figs 4 (top) and 11 where the 10-day characteristic vanishes, and more complex fluctuations set in. Perhaps the variations in Fig. 11 are assuming a longer period.

6. Other periodicities in relation to the general circulation

In some recent articles dealing with periodicity it has been customary to devote considerable time and effort to statistical analysis in order to buttress the reality of the periodicity suggested. Extensive work of this character has not been performed in connection with the present work because the author feels that the periodicity of the minima in Figs 4 and 11 is sufficiently clear from inspection, and besides, no claim is made that the periodicity is exact. It is a "quasi-periodic" cyclogenesis. Neverthless, a few of the more common statistics have been computed for those to whom numbers have a stronger appeal than graphs and maps.

A 10-day sine-wave was fitted to the height values at 40°N 110°W shown in Fig. 4 (top) for the period 4 February to 14 May. This embraced 100 days and 10 waves. The correlation of the observed data with the fitted sine-curve turned out to be 0.52 with an amplitude of 154 feet. A similar analysis of the data in Fig. 11 from 4 March to 10 May (70 days and 7 waves) gave a correlation of 0.42 and ampli-

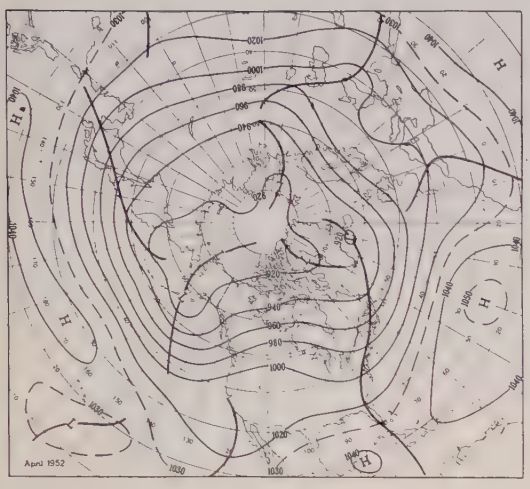

Fig. 13. Mean contours of the 700 mb surface (in tens of feet) for April 1952.

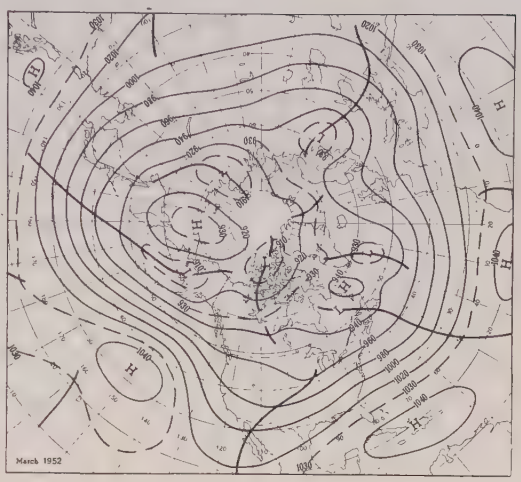

Figure 14. Mean contours of the 700 mb surface (in tens of feet) for March 1952.

tude 182 feet. While these values are not overwhelming they are perhaps comparable to those obtained for 7-day periods (LANGMUIR, 1950) computed for similar lengths of time. It is noteworthy from Fig. 4 (top) that a sine-curve is not the most appropriate description of the variation. Rather, the 700 mb values appear to fluctuate in a minor way about a constant value for several days before plunging precipitously to low values as the cyclogenesis sets in. In other words, if one wished to obtain a higher correlation he could fit some other type of curve to the data.

In order to see how frequently 10-day periodicities in the height of the 700 mb surface over the western plateau occur during late winter and spring, daily values at 40°N 110°W were plotted for the twenty years beginning 1933. From these graphs it was concluded (by an independent worker) that:

1. The 10-day wave is not common at this place and season, and none could be found as striking as the one investigated.
2. The period during which the plots most resembled those investigated (i.e. had a 10-day periodicity of good amplitude) was from 25 February to 15 May 1952.

The 30-day mean 700 mb maps associated with this latter period are reproduced in Figs 13 and 14. The similarity of the April 1952 pattern over the Pacific to March 1953 (Fig. 12) is apparent. The similarity of March 1952 (Fig. 14) with February 1953 (Fig. 9) is even more striking. However, a fairly rapid transition to the April regime took place in late March of 1952, and this did not permit the 10-day periodicity to be as striking as in February 1953.

Once again the suggestion arises that the length and character of the periodicity may be inherent in the long-period (e.g. 30-day) mean circulation pattern. It is unlikely that the relatively uncommon 10-day periodicity would appear in maps bearing similar patterns (and similar anomalies) unless such a connection existed.

Another indication that there may be an intimate relationship between periodicity and the long period mean planetary wave pattern is afforded by a chart published by HALL (1950), showing amplitudes and phases of the clear-cut 7-day periodicities which occurred in April 1950 and were first brought to light by LANGMUIR (1950). Hall's chart is reproduced in Fig. 15, along with the 700 mb 30-day mean for the same period (Fig. 16). Comparing these two figures it seems clear that where the amplitude of the 7-day cycle reaches a maximum the curvature of the 700 mb contours is greatest (in ridges or troughs). The phases on Hall's chart also suggest that the 7-day periodic components may have similar phase in the troughs of the planetary wave train (e.g. off Japan, the west coast of United States and the east coast). The tendency to resonance of this

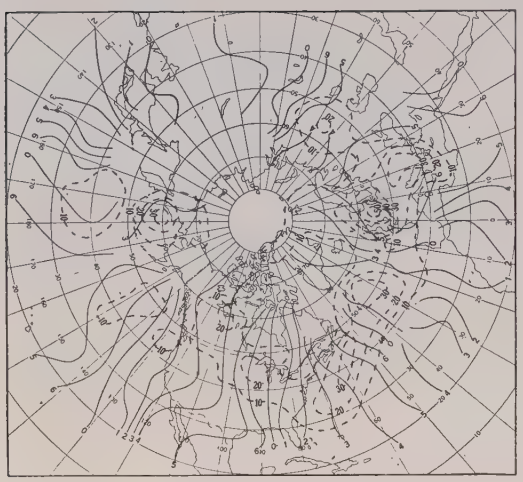

Fig. 15. Amplitude (dashed lines, in tens of feet) and phase (day of maximum height [solid lines] where 0 is for Sunday, 1 for Monday, etc.) of 7-day periodic component during 2—29 April 1950 [reproduced from Hall (1950)].

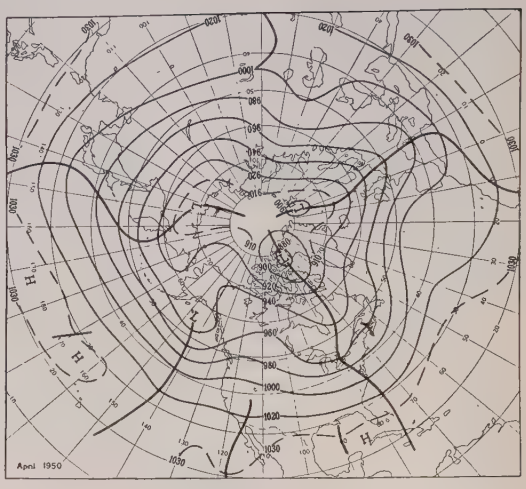

Fig. 16. Mean contours of the 700 mb surface (in tens of feet) for April 1950.

type was mentioned in connection with the Hawaiian and southern plateau troughs in the 1953 case. These suggestive connections between amplitude, phase and long period mean pattern will require further research.

The tentative conclusions which may be drawn from the above few paragraphs are that the character of periodicities in mid-tropospheric pressure (which, of course, are also associated with periodicities in other elements, including weather) may be inherent in long period mean flow patterns. These patterns reflect the underlying positions and intensities of the centers of action, which in turn may condition the life history of storms and anticyclones, setting the stage for their birth, growth and movement. Insofar as the mean long period (e.g. 30-day) flow pattern remains unchanged with time, the evolution of day to day storms may proceed similarly and periodically. However, owing to seasonal changes, and perhaps other phenomena, the long period mean patterns are themselves gradually changing form, thereby leading to changes in periodicity. When the mean patterns abruptly change, signaling great changes in the weather regime, the periodicity is also apt to change phase and length abruptly.

To the extent that correct 30-day prognoses of mean planetary flow patterns can be made (NAMIAS, 1953) these conclusions suggest the possibility of predicting the spells of weather within a month as well as its average characteristics.

REFERENCES

HALL, F., 1950: *Trans. of the N. Y. Acad. of Sciences*, **14**, Ser. II, p. 45.

HAWKINS, H. F., Jr. 1952: *Mon. Wea. Rev.*, **80**, p. 82.

LANGMUIR, I., 1950: *Bull. Amer. Met. Soc.*, **31** p. 386.

— 1953: Final Report No. RL-785, Project Cirrus, Schenectady, N. Y.

NAGAO, T., 1952: *Met. Soc. of Japan*, XXX, p. 65.

NAMIAS, J., 1947: Extended Forecasting by Mean Circulation Methods, Washington, D.C. (*U.S. Weather Bureau*).

— 1952: *Bull. Amer. Met. Soc.*, **32**, p. 279.

— 1953: Met. Monographs, II, No. 6, *Amer. Met. Soc.*

NAIMAS, J., and CLAPP, P. F., 1944: *J. Met.*, **1**, p. 57.

PAGAVA, S. T., and others, 1940: Basic Principles of the Synoptic Method of Long-Range Weather Forecasting, Leningrad, U.S.S.R. (*Hydrometeorological Publ. House*) (Translation prepared by Weather Information Service, Headquarters, Army Air Forces.)

ROSSBY, C.-G., and Collaborators, 1939: *J. Mar. Res.*, **2**, p. 38

SHAW, SIR NAPIER, 1936: Manual of Meteorology, II, 2nd ed., Comparative Meteorology, Chapter VII, *Chambridge* (*University Press*).

U.S. Weather Bureau, 1952: *U.S. Wea. Bur. Tech. Paper* No. 21, 73 pp.

The Use of Normals in Numerical Forecasting

by R. S. SCORER

Imperial College, London

(Manuscript received July 18, 1953)

Abstract

If there exists, in the spectrum of fluctuations of weather, a period of relatively low amplitude, and if a set of normal values of the right kind can be defined, then dynamical equations for the behaviour of the atmosphere can be used for the numerical prediction of charts meaned over the period of low amplitude.

1. Introduction

The complete equations of motion for the atmosphere are too complicated to solve by existing methods and the data are not available for making even a rough estimate of many of the terms, such as those involving friction, convection by clouds, and so on. The question posed, therefore, is whether normal values can be used as substitutes for any of these. The belief that they can be of value is based on the ability of forecasters to use their experience in forecasting: that experience is condensed and classified in the forecaster's memory as it takes place, and there is some hope that if the classification could be made available to a machine it might improve upon numerical forecasts which are based on equations which are known to omit many important influences.

This discussion is in very general terms because it is believed that the principle stated may find application on many scales. It was suggested by the work of CLAPP (1953) who used normal values in the barotropic vorticity equation applied to 5-day mean charts, and it seemed worthwhile to state a general principle of which Clapp had discussed a particular example.

2. The definition of a normal

The idea of a normal value is based on the supposition that the atmosphere behaves habitually in a particular way. If there were in no sense a repitition of its behaviour no normals could be defined. If there is some sort of repitition a normal can be defined as the average of a specified large number of occasions. We can speak of "annual rainfall" because, although it varies from year to year, rainfall amounts are repeated within not very wide limits in many parts of the world from year to year. We can speak of the normal temperature for a time of year in places where the annual variation exceeds considerably the short period fluctuations. The concept of normal temperature is not generally useful except as a reference value because the diurnal variations and variations due to the passage of weather systems are large enough to render

the normal useless as a forecast for a particular time in the future. But if these short period fluctuations are sufficiently short we can take a mean value for a period long enough to contain several such fluctuations and yet short enough to represent a time of year, and we may say with some confidence that the mean value for such a period in the future will aproximate closely to the average over many years.

Unfortunately instances are easily found in the records of fluctuations of almost any period we care to name. Exceptional seasons are frequently experienced, but if one could evolve a forecasting method that could be applied at times that are not so exceptional it would be of great value. Clapp chose the period of 5 days. One could argue that this is short enough for seasonal variations to be imperceptible and long enough to contain several of the smaller disturbances which dominate the weather: but the precise length of the period is not relevant to the present argument. The important issue is whether an interval, such as 5 days, could be chosen at all which was at a minimum in the spectrum of fluctuations, there being large annual fluctuations and large fluctuations of much shorter period, but no important ones of period close to the interval chosen. Undoubtedly no interval could be found to satisfy this condition always everywhere, but if an interval were once chosen the occasions when it failed could mostly be recognised.

For the sake of argument we may suppose that 5 days is the interval chosen. This done the normal values of all the quantities whose means we shall require would not simply be calculated for a time of year. It would be necessary to define certain weather types and calculate normals for each weather type. We might, for example, calculate the normal value of a term in an equation for seasons colder than usual, or for particular common blocking situations. In principle, instead of lumping all occasions together we would classify them and have normal values for each class: then, when we require to use a normal, we decide that the occasion on which it is to be used falls in one particular class, and we use the corresponding value.

The same procedure might be applied to the coefficient of vertical transport (of water vapour for instance). For a given site experiments might have found a relationship between the wind speed and the transfer coefficient, the relationship depending perhaps upon the lapse-rate of temperature. In using such a coefficient we assume that we are dealing with a large number of the small eddies and only a fraction of a large eddy such as a cyclone: in fact we are working in a region of the spectrum of fluctuations where the amplitude is low. Having measured the lapse-rate and wind speed on a particular occasion we could then apply the coefficient for purposes of prediction. To use a coefficient which depends upon conditions is obviously better than to use a universal one, and in the same way we could, by classification of weather types obtain a normal value more appropriate than an 'all time' normal. The transfer coefficient is completely analogous to any normal value that is any use, and it is only prudent to improve our normals in the same way.

3. The use of normals

In using a transfer coefficient we simply measure on some occasions the quantities it relates and assume its value to be the same when one of the quantities is unknown. Thus, in order to calculate the transfer of heat into the atmosphere by convection it is not necessary to measure the transfer directly if it can be included in an equation in which everything else can be measured. We might, for instance measure the changes in vorticity and deduce the vertical velocity and changes in temperature that result, and compare them with the observed changes, ascribing the rest to convection. Indeed we need not ascribe the rest to anything in particular but simply to everything we cannot measure; and on another occasion when there was one more unknown, we could use the normal value obtained from several similar situations to evaluate the unknown.

To be more specific, let us suppose that we have established an equation

$$Q = A+B+C+ \ldots \qquad (1)$$

Q being the unknown—the quantity to be forecast—while A, B, C, ... are measurable, in theory at least, directly or indirectly.

The instruments making the measurements —barometers, tharmometers, etc.—usually take mean values over a period of perhaps a minute, and from these ordinary charts are obtained. But if we have decided to use 5 day mean charts in order to use normals at all then we must use the equation in the form

$$\overline{Q} = \overline{A} + \overline{B} + \overline{C} + \ldots \qquad (2)$$

the bar denoting a 5 day mean value.

The same equation applies to the normal values (however they have been defined), and using suffix N to denote them we have

$$Q_N = A_N + B_N + C_N + \ldots \qquad (3)$$

The quantities A etc. may be complicated functions of the observations. If r and s are observed quantities we might have

$$A = r \cdot s \qquad (4)$$

whence

$$\overline{A} = \overline{r \cdot s} = \overline{r} \cdot \overline{s} + X \qquad (5)$$

in which X may be complicated expression involving the departures of r and s from their means $\overline{r}$ and $\overline{s}$. The familiar Reynold's stresses are examples of terms like X.

Since X is a term representing the effect of fluctuations we assume that it is the same in every case in which many fluctuations are involved and so

$$A_N = r_N \cdot s_N + X \qquad (6)$$

and then $\overline{Q} = \overline{A} + \ldots$

$$= (\overline{r} \cdot \overline{s} - r_N \cdot s_N + A_N) + \ldots$$

$$= (\overline{r} \cdot \overline{s} - r_N \cdot s_N) + \ldots + Q_N \qquad (7)$$

and so $\overline{Q}$ is known from observations such as $\overline{r}$ and $\overline{s}$ and the normal values

Provided that the terms B, C, etc. do not represent processes which operate largely by means of periodicities nearly equal to the interval over which we have meaned the charts they can, if desired, be treated in the same way as the term X. They may therefore be either long term radiation effects or short term dynamical ones, but we may merely assume that they bring about the same relationship to the measurable quantities and our single unknown as they do between the normal values.

Thus as a first approximation we have $\overline{Q} = Q_N$, i.e. our first forecast is that the quantity will assume its normal value. When we can measure current values of r and s we have

$$\overline{Q} = \overline{r} \cdot \overline{s} - r_N \cdot s_N + Q_N \qquad (8)$$

and if at a later stage we can measure B then

$$\overline{Q} = \overline{r} \cdot \overline{s} - r_N \cdot s_N + \overline{B} - B_N + Q_N \qquad (9)$$

and so on.

There is nothing new in this general principle, but it is now seen in the light of mean values and normals as applied to a turbelent atmosphere.

Clapp's application was simply to use the vorticity equation and obtain.

$$\frac{g}{f} \Delta \frac{^2\partial \overline{z}}{\partial t} = (-\overline{v} \cdot \Delta \overline{\eta}) - (-\underline{v}_N \cdot \Delta \eta_N) \qquad (10)$$

(in the usual notation) assuming $\partial z_N / \partial t$ to be zero. The second term on the right hand side is a first attempt to introduce an estimate of all that was left out in the barotropic vorticity equation, and there is good reason to suppose that if suitable intervals for the mean charts can be chosen, and if normals can be appropriately defined, better approximations can gradually be obtained as it becomes possible to estimate the current values of more terms in the full equation. The limits to this procedure are set by the nature or the spectrum of the actual fluctuations – whether or not it possesses any band of periods of low relative amplitude.

The second question raised is 'what is the appropriate equation to use?' If the forecast is to be considerably better than using an unmodified normal value the equation must contain an expression of what is peculiar to the current situation. The equation must, therefore, deal with the pressure distribution for this is the most important single field that controls weather developments. The reasons which have led workers to handle the pressure field through the equation for the advection of vorticity will govern equally our present choice. It is, in consequence, a reasonable procedure to apply the method here suggested to any equation which experience has shown can be handled usefully; and in the case of numerical forecasting Clapp's choice of the barotropic vorticity equation would be the one to choose on the basis of the experience of other workers, such as Charney and Fjørtoft, in recent years.

The method must be tried because it is a fundamental one. Its success is not to be taken as a judgment upon whether it is appropriate to apply it but as an indication of whether the task is hopeless or not; for if it proves to be of no value it means that the spectrum of atmospheric fluctuations is unbroken in the region where we have tried it and no method can than work better than the simplest—to give the normal as the forecast.

REFERENCE

Clapp, P. F., 1953: Application of Barotorpic Tendency Equation to Medium-Range Forecasting. *Tellus* **5**, No. 1. p. 80.

A Measurement of the Winds Aloft During a Cold Front Passage

By T. O. ERIKSSON, H.Q. Military Weather Service, RSAF

On the island of Väddön in the archipelago of Stockholm (Fig. 1) last summer the ascents of a number of pilot balloons were followed by means of radar. Particularly interesting were the ascents on July 15 because this day the balloons passed through a cold front surface and the wind shift line aloft could be illustrated very clearly.

The wind measurements were made with two radar sets independent of each other and placed, one at Ytterskär and the other at Gåsvik (Fig. 1) at a distance of 5 kilometers from each other.

To obtain an idea of the accuracy of the radar wind measurements, pilot balloons have been followed simultaneously by means of

Fig. 1. The location of the observation points G: Gåsvik; Y: Ytterskär

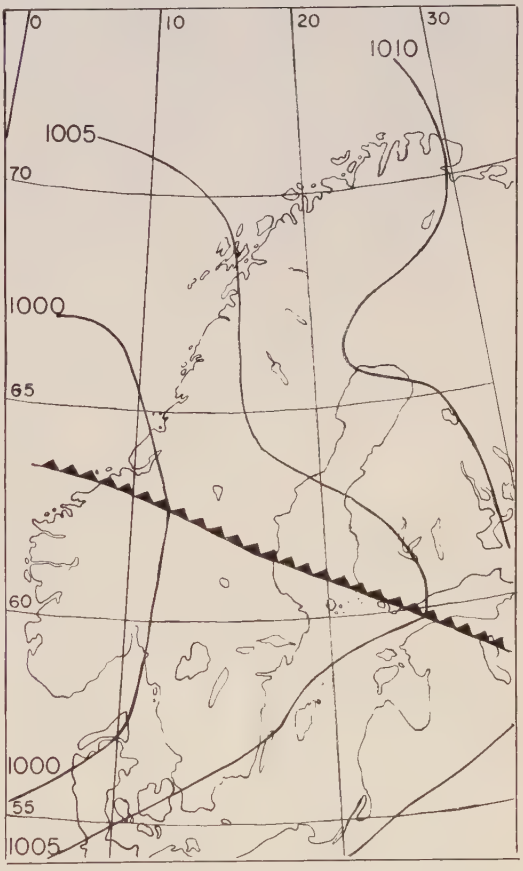

Fig. 2. Location of front and distribution of pressure July 15, 1953, 1300 swedish standard time.

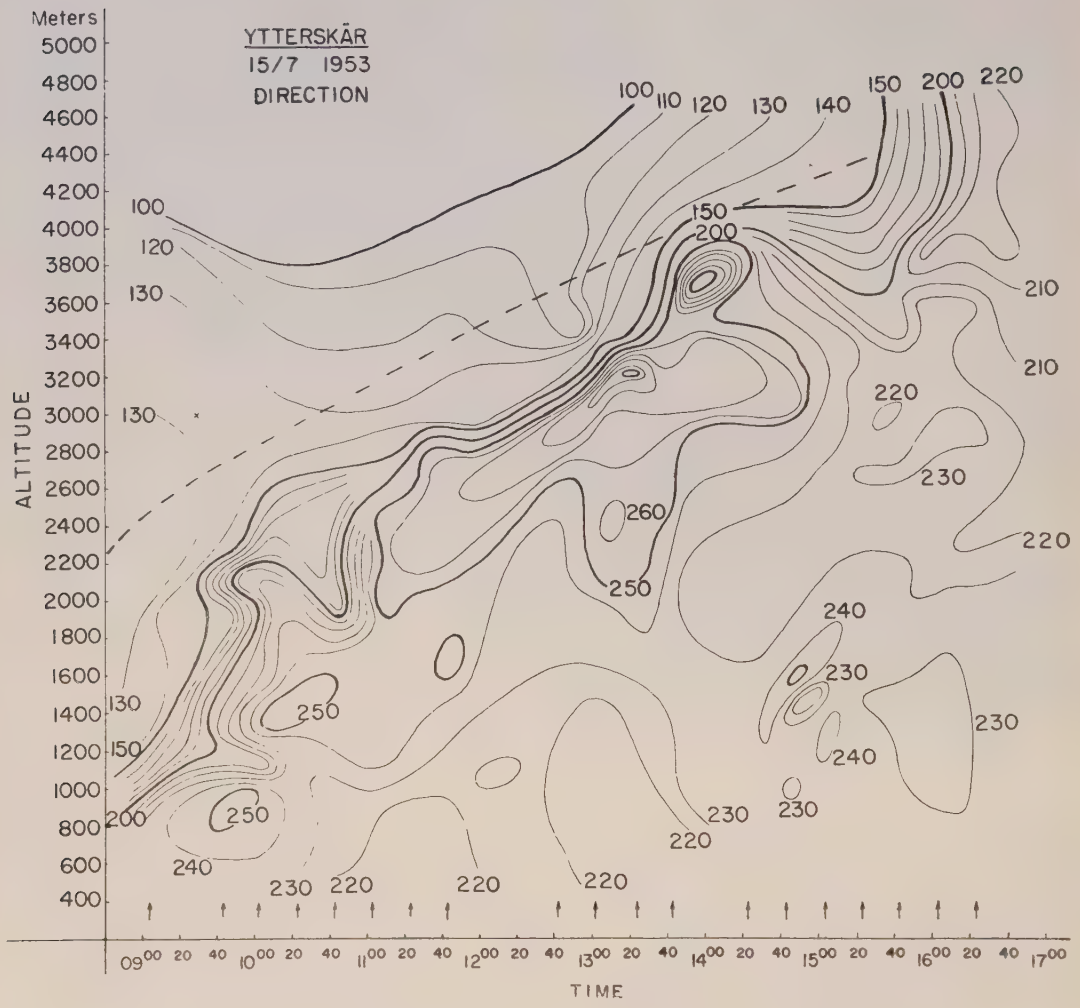

Fig. 3. Time section of wind direction at Ytterskär July 15, 1953, 0900—1620 Swedish standard time. Arrows indicate the time of the ascents.

radar and by using three theodolites. The comparisons between the results of the two methods are not yet finished, but preliminarily one can say that the radar here used gives the wind with errors not exceeding ± 0.5 m/sec in velocity and ± 5° in direction and that the relative error in altitude is ± 2 %.

The weather situation was as follows: On July 14 a cold front type occlusion belonging to a cyclone east of Scottland had moved in over the southern part of Sweden and there, as usual in summer, changed into a cold front. This front passed Väddön about 0730 o'clock, and, as the wind measurements started at about 0900 o'clock, the pilot balloons thus passed right through the cold front surface.

A pilot balloon was sent up about every 20 minutes. The ascent times are marked by ↑ on the time scale in Figures 3—5. The results of the wind measurements are illustrated by means of isopleths for direction and velocity. The isopleths are drawn for every tenth degree, respectively, every m/sec.

Because of a defect of the radar at Gåsvik, the diagrams from this place only show the winds during the afternoon, but the diagrams from Ytterskär (Figs 3—5) show some properties characteristic of a cold front surface such

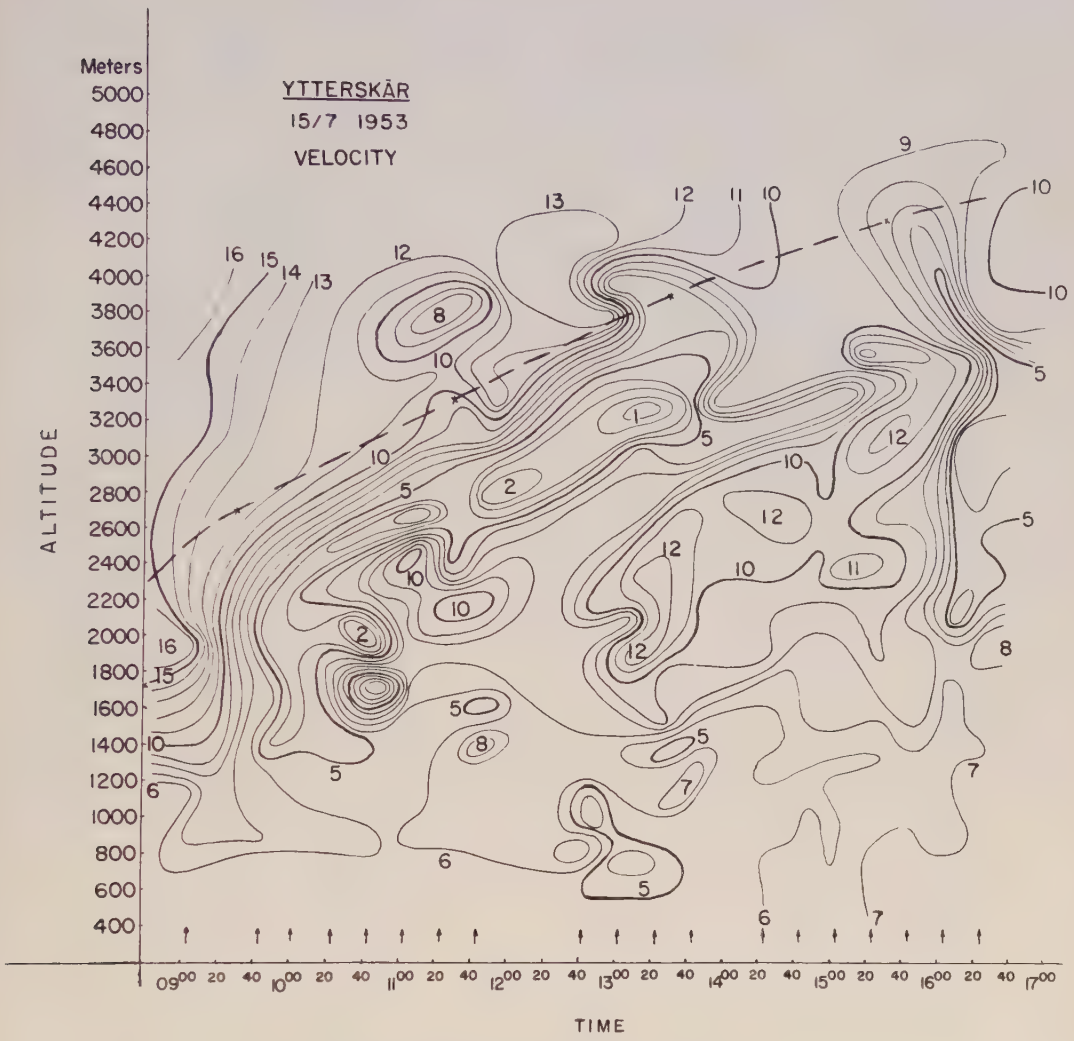

Fig. 4. Time section of wind speed at Ytterskär, July 15, 1953, 0900—1620 Swedish standard time. Arrows indicate the time of the ascents.

as the steep slope in the lower parts, the less steep slope higher up and the increase of wind velocity, when passing through the surface from cold to warm air.

The altitude of the front surface at different places has been estimated from the soundings at Bromma (Stockholm) and at Copenhagen and from weather reports (Fig. 5). In the sounding at Bromma it is evident from wind and Θ_w (wet-bulb potential temperature) that the isothermal layer at 2,500—3,000 m belongs to the front surface. A comparison of the two soundings from Copenhagen indicates that on July 14 at 1600 the front surfaces was at 5,500—5,800 m and that on July 15 at 0400 the temperature had fallen above this altitude to about 9,000 m. Thus it is probable that the position of the front surface on July 15 at 0400 was at about 9,000 m over Copenhagen. Thus the dashed line on Fig. 6 shows approximately the altitude of the front surface. Assuming the shape of the surface to have remained unaltered during the day, the dashed line of Fig. 6 is plotted also on Figs 3—4. The correspondence between this line on Figs 3—4 and the isopleths is not perfect but this may depend on

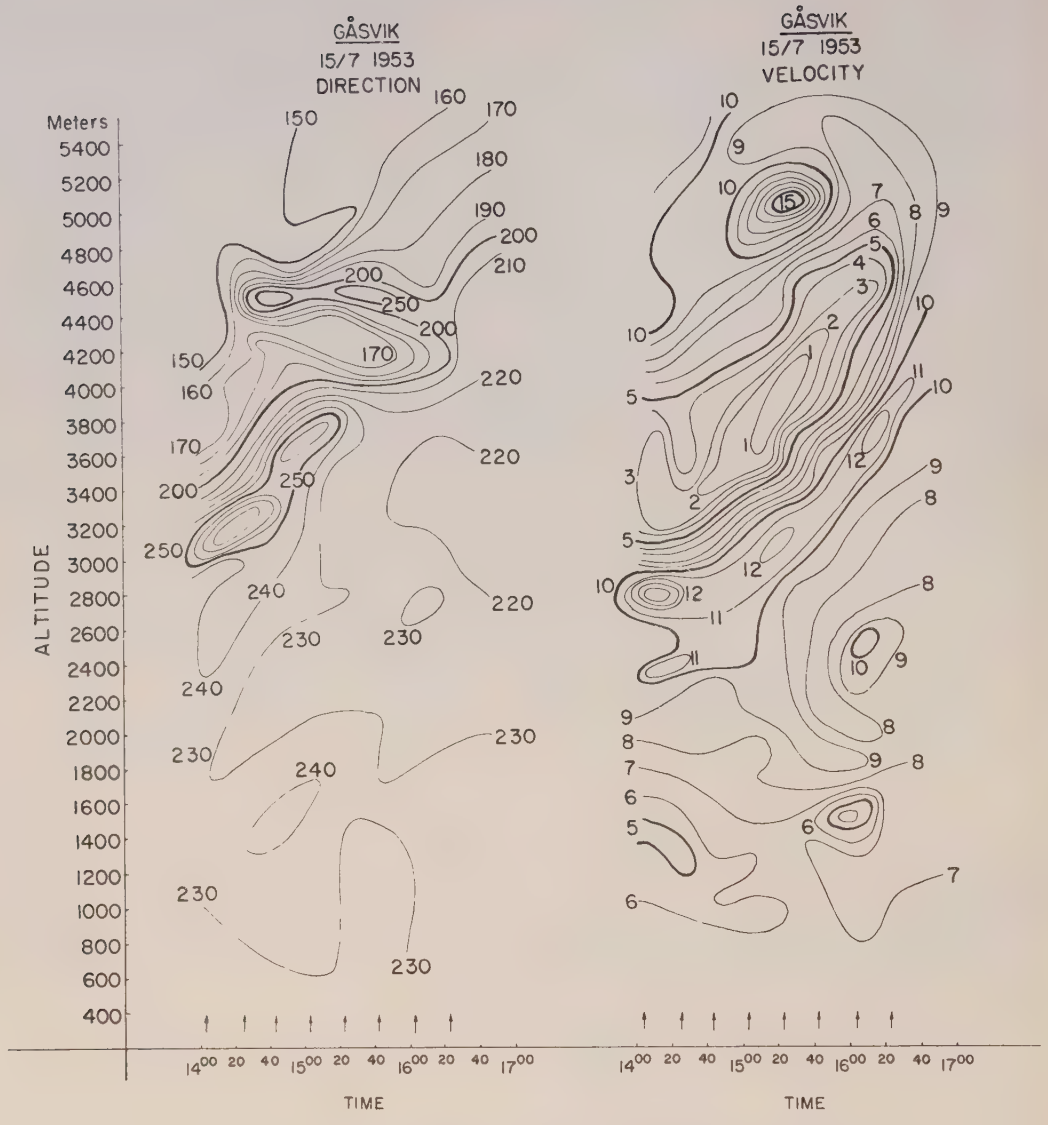

Fig. 5. Time sections of wind direction and speed at Gåsvik July 15, 1953, 1400—1620 Swedish standard time. Arrows indicate the time of the ascents.

the difficulty to determine the exact position of the frontal surface from the soundings and the weather reports available.

Fig. 2 shows the estimated position of the front and the pressure distribution over Scandinavia at 1300 on July 15.

However, it is evident that wind measurements of this kind represent a rather good method to supplement the standard aerological soundings. It is also probable that the position of front surfaces is more easy to determine from wind measurements than from soundings, particularly when the temperature difference between the two air masses is small.

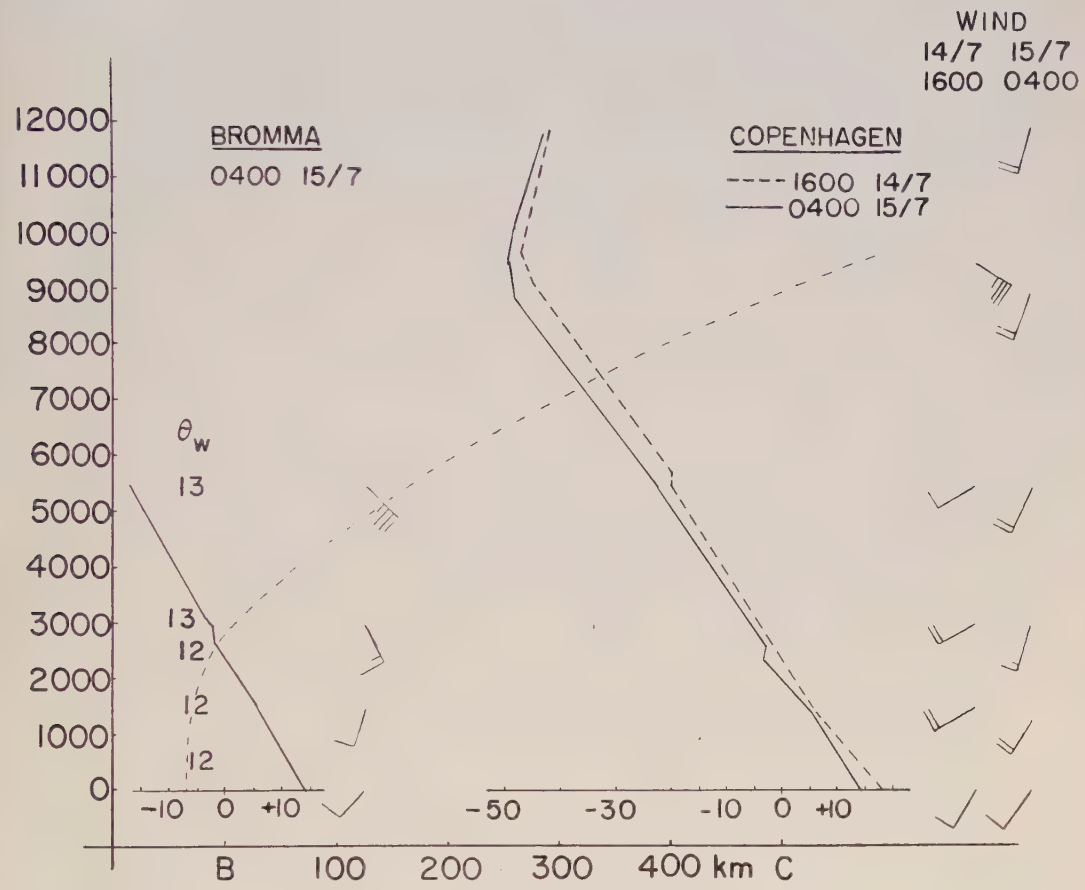

Fig. 6. Radiosonde ascents and winds at Bromma and Copenhagen July 14 and 15, 1953. The slanting curve indicates approximate location of the front.

The Cellular Solution of the Dynamical Equations and the Actual Perturbation of the Westerlies up to 16 km at Valentia

By M. DOPORTO

(Manuscript received 8 July 1953)

Abstract

The cellular solution of the linearized hydrodynamical equations requires the existence of nodal surfaces for the perturbation of air density, pressure and velocity components. When a constant, which appears in the formulae giving the heights of the nodal surfaces, is determined from the observed value of one of them, namely, the first nodal surface of the vertical velocity, all the other heights of nodal surfaces agree within reasonable limits with the heights determined from actual observations by several investigators using very different methods. More than 400 upper wind ascents reaching at least 16 km made by radio wind or radar methods at Valentia Observatory, have been classified according to the sign of the change of pressure at 8 km during the 12 hours prior to the ascent, and average values of the meridional and zonal components of the wind have been computed. The difference at each level between the corresponding average components of the wind when the pressure has increased and when the pressure has decreased gives a good approximation to double the value of the horizontal perturbation of the Westerlies. Applied to this case, the cellular solution requires that the zonal component of the perturbation so determined should be zero at all levels while the meridional component should have nodal surfaces at 4 and 12 km. The observations show that the zonal component is the one having nodal surfaces at the required levels while the meridional component has a maximum value at about 9 km. Taking into account that the equations refer to a single-layer atmosphere and neglect the meridional gradient of temperature, the disagreement between observation and theory appears to be less significant than the confirmation of the existence of nodal surfaces which cannot be explained by the generally accepted exponential solution of the dynamical equations.

1. In the wave theory of atmospheric perturbations, the solution of the linearised dynamical equations leads to the integration of an equation of the second order with constant coefficients. Neglecting the case when the auxiliary equation of the second degree has only one root, the solution may be either exponential, when the roots are real, or cellular, when the roots are imaginary. In the simplest case of an isothermal atmosphere in equilibrium on a flat, stationary earth, the full discussion of the different types of solutions, and therefore of the different possible modes of motion, was given by V. Bjerknes et alia (1934, page 361 and following) who studied them by means of the Lagrangian form of the dynamical equations. The nature of the solution depends on the wave length and period of the waves, the type of transformation the air undergoes, and the height of the homogeneous atmosphere.

In a previous paper the present author (1944) called attention to the fact that for waves of period of the order of one day and greater

and wavelength of a thousand kilometres and longer, i.e. for periods and wave lengths of the kind observed in large-scale motion of the actual atmosphere, the type of solution that obtains is of the cell type. In the case of motion in two dimensions the solution of the Eulerian equations is:

$$u = C_0 e^{\frac{z}{2H}} \frac{\mu\gamma g}{\nu^2 - \gamma g H\mu^2}\left[\left(\frac{1}{2} - \frac{1}{\gamma}\right)\sin \Theta z + \right.$$
$$\left. + H\Theta \cos \Theta z\right] \sin(\mu x - \nu t) \qquad (1\,a)$$

$$w = C_0 e^{\frac{z}{2H}} \sin \Theta z \cos(\mu x - \nu t) \qquad (1\,b)$$

$$p = C_0 e^{-\frac{z}{2H}} \frac{\gamma g \nu \bar{\varrho}_0}{\nu^2 - \gamma g H\mu^2}\left[\left(\frac{1}{2} - \frac{1}{\gamma}\right)\sin \Theta z + \right.$$
$$\left. + \Theta H \cos \Theta z\right] \sin(\mu x - \nu t) \qquad (1\,c)$$

$$\varrho = C_0 e^{-\frac{z}{2H}} \frac{\nu \bar{\varrho}_0}{(\nu^2 - \gamma g H\mu^2) H}\left[\left\{\frac{\mu^2}{\nu^2} g H(\gamma - 1) - \right.\right.$$
$$\left.\left. - \frac{1}{2}\right\} \sin \Theta z + \Theta H \cos \Theta z\right] \sin(\mu x - \nu t) \quad (1\,d)$$

where u and w are respectively the zonal and vertical components of the air velocity with their usual signs; p and ϱ are the perturbation of the pressure and air density; $\bar{\varrho}_0$ the undisturbed surface air density; $\mu = \frac{2\pi}{\lambda}$ and $\nu = \frac{2\pi}{\tau}$ where λ and τ are the wave length and period of the waves, respectively; γ is the ratio of specific heats for air; H is the height of the homogeneous atmosphere; x, z, t, and g have the usual meanings, and

$$\Theta = \sqrt{\frac{\mu^2}{\nu^2}\frac{g}{H}\frac{\gamma - 1}{\gamma} + \frac{\nu^2}{\gamma g H} - \frac{1}{4H^2} - \mu^2}$$

2. The interest of the cell-type solution above is due to the fact that equations (1) show the existence in the atmosphere of nodal and antinodal horizontal surfaces at heights which are dependent on the internal parameters of the atmosphere and on the wave length and period of the motion. The existence of certain nodal (and antinodal) surfaces in the atmosphere has been a well established fact for nearly half a century; evidence of the existence of other nodal surfaces has been accumulated in the last ten years. The importance of this solution is enhanced by the fact that if the value of the constant Θ is determined by means of the height of one of the nodal surfaces, the heights of the others can be computed from the equations (1) and the values so computed agree reasonably well with the heights determined experimentally. Thus —

(a) From equation (1 b) it is deduced that the amplitude of the vertical component of motion is zero for values $z_w = \frac{n\pi}{\Theta}$ where $n = 0, 1, 2 \ldots$

For $n = 0$ this formula re-states the boundary condition.

Nearly forty years ago SHAW (1914) from three days' sounding-balloon observations in Ireland and Great Britain found that the air moves horizontally at a height estimated to be about 8 km. PALMÉN (1932), from a consideration of potential temperatures, deduced that in cases of polar air filling the troposphere the air moved horizontally at about 8 km. The AUTHOR (1943 b, 1952) has shown that if the effects of horizontal advection are neglected it is possible to compute the vertical displacement of the air at different levels from average values of the local variations of pressure and temperature. The method was applied to observations made with radiosondes in 1939 at Thorshavn, and led to the result that there were two surfaces of horizontal motion, one at $z = 8.91$ km, the other at about 16 km. The effect of horizontal advection, which had been neglected, was not expected to be very large especially at the 8—9 km level. The same method applied to radiosonde observations at Sault Ste. Marie and to Valentia gave for the height of the first surface of horizontal motion average values of about 9 km and 9.5 km respectively. FAUST (1952) using radiosonde data at different pressure-levels found that horizontal motion obtains at the level of 240—280 mbs.

From the height of the lowest layer of horizontal motion found at Thorshavn we find

$$\Theta = 3.53 \cdot 10^{-6} \text{ c.g.s.}$$

and therefore the height of the second layer at which horizontal motion should be found is 17.82 km. The estimated value at Thorshavn was about 16 km.

(b) It is also deduced from (1 b) that the vertical component of motion reaches maximum values of opposite signs at 4.46 and 13.37 km.

The vertical displacements of the tropopause and the cloud formation and subsidence in the troposphere support to some extent these results.

(c) From equation (1 d), and giving to the constants the values appropriate to Thorshavn, the amplitude of the perturbation of the air density is zero at heights given by

$$z_\varrho = 8.20 + 8.91\, n \text{ km } (n = 0,\ 1,\ 2 \ldots) \quad (2)$$

Therefore, the first or tropospheric layer would occur at 8.20 km.

WAGNER (1910) was the first to give evidence of the existence of an isopycnic layer at about 8 km from sounding-balloon observations over Germany. SEN (1924) computed the air density in July at different levels from the normal surface isobars and isotherms, assuming the lapse rate to be the same over land and over sea at all latitudes and heights, and found that the air density at 8 km was practically constant all over the world. DOPORTO (1943 a) defined the tropospheric, or first isopycnic layer, as the level at which the standard deviation of air density at the different levels from the respective average is a minimum and found that the Thorshavn data utilised gave a very well defined minimum at 7.80 km. The same results were obtained for Sault Ste. Marie (DOPORTO, 1943 b) and Valentia (DOPORTO and MORGAN, 1947), etc.

On the basis of a discussion of the statical equation the existence of a stratospheric isopycnic layer at an estimated height of 25 km was suggested by DOPORTO (1943 a). This isopycnic layer, found at about 24 km by GOLDIE (1947) corresponds to the value obtained from equation (2) for $n = 2$, namely 26.02 km.

(d) From equation (1 c), it is deduced tha the amplitude of the pressure perturbation should be zero at heights given by

$$z_p = 4.24 + 8.91\, n \text{ km } (n = 0,\ 1.2 \ldots)$$

DINES (1919) anticipated the existence of a layer of constant pressure at 18 or 20 km. For $n = 2$ the above formula gives $z_p = 22.06$ km.

(e) It is also deduced from equation (1 c) that the variability of pressure should have maxima at the surface and at 8.70 km.

Observations show that the interdiurnal variation of pressure is maxima at the surface and about 8 km (HANN-SÜRING, 1938, page 273).

(f) Equation (1 a) gives for the heights where the amplitude of the horizontal component of the perturbed motion vanishes

$$z_u = 4.24 + 8.91\, n \text{ km } (n = 0,\ 1,\ 2 \ldots)$$

which is the same as in (c).

At the heights given by this formula, namely 4.24 for $n = 0$ and 13.15 km for $n = 1$, horizontal divergence should be zero with divergence of opposite signs above and below them. Such a distribution of divergence was found with nodal surfaces at about 4 and 12 km for Saul, Ste. Marie and 7 and 11 km for Thorshavn (DOPORTO, 1943 b) and Valentia (DOPORTO, 1952). FAUST (1952) found that the levels of zero divergence occur to about 500 and 180 mb. In recent literature to which the author has had access it is assumed, on the basis of general considerations, that horizontal divergence is zero at about the 600 mb level (4 km) and 12 km.

3. A similar structure for the arrangement of nodal surfaces was found by the AUTHOR (1944) for the case of an atmosphere in equilibrium with constant lapse rate in the case of a flat, non-rotating earth. The equations giving u, w, p, and ϱ contain, instead of sines and cosines, Bessel functions of a function of z; and by taking four roots, besides the root zero, in the case of the equation giving w, and making the fourth root coincide with the surface and the zero-root with the top of the atmosphere, values for the heights of the nodal surfaces of all variables were obtained which differ but little from the values given in (a) to (f) above.

In the same paper the present author discussed the cases of (i) isothermal atmosphere moving with uniform horizontal velocity over flat non-rotating earth; (ii) atmosphere with constant lapse rate in a similar case; (iii) isothermal atmosphere in equilibrium on a flat, rotating earth; (iv) atmosphere with constant lapse rate in a similar case; (v) isothermal atmosphere moving with uniform velocity over flat rotating earth and (vi) atmosphere with constant lapse rate in a similar case. The solutions differ from those discussed above in that (1) the rotation of the

earth does not allow for cellular motion except for periods shorter than half the pendulum day; (2) the rotation of the earth introduces a separation of the nodal surfaces of pressure and of the horizontal components of the perturbed velocity but for wave-lengths of 1,000 km or greater and for periods shorter, but of the order of the half-pendulum day, the distance between the nodal surfaces for the different elements is negligible; and (3) the solutions in the case of an atmosphere with uniform horizontal zonal motion, referred to axes moving with the undisturbed air, are the same as those for the corresponding case of an atmosphere in equilibrium. This last result makes it possible for an observer stationary on the ground to register cellular motion of an apparent period greater than the half-pendulum day if the waves move, with reference to axes fixed in the unperturbed air, in a direction opposite to the movement of the axes relative to the observer.

There are several other aspects of the cellular solution of the dynamical equations which may provide explanations to other observed facts (DOPORTO, 1944), such as the variation of the tropopause height between 8 and 17 km, etc. but there are also some serious difficulties to overcome before the cellular solution can account for all the dynamical aspects of actual atmospheric perturbations.

4. For the purpose of this discussion the cellular solution for the pressure and wind perturbations may be represented approximately by the following equations:

$$u = A \cos \Theta z \sin (\mu x - \nu t) \qquad (3\ a)$$
$$v = -B \cos \Theta z \cos (\mu x - \nu t) \qquad (3\ b)$$
$$w = C \sin \Theta z \cos (\mu x - \nu t) \qquad (3\ c)$$
$$p = D \cos \Theta z \sin (\mu x - \nu t) \qquad (3\ d)$$

where A, B, C, and D may be considered as positive constants. (The complete solution is given in equations (58) of DOPORTO, 1944.)

Equation (3 d) shows that for $\Theta z = \frac{\pi}{2}$, i.e. at about 4 and 12 km the perturbed pressure should be zero, and that if an anticyclonic situation obtains at the surface there should be a cyclone above it with maximum amplitude at 8 km, the situation reverting to anticyclonic between 12 and 20 km with maximum amplitude at 16 km. This, of course, is not found in the atmosphere. If it is remembered that to reduce the difficulties of the mathematical problem the meridional gradient of temperature has been taken as zero; and that the sloping tropopause has been ignored and the atmosphere treated as a single layer, either isothermal or with lapse rate, the non-existence of the nodal surfaces at 4 and 12 km required by the equation is qualitatively explained. From a consideration of the values of the constants in the complete formula the author indicated that the amplitude of the perturbed pressure should be of the order of a few millibars only. If this is correct, the theoretical opposition of phases of the perturbed pressure due to the dynamics of the motion within the stratum 4—12 km and above and below it would be masked by the statical change of pressure due to the meridional displacements of the atmosphere as a whole, which at the surface is generally greater than 10 mb.

Another difficulty arises from the signs of the coefficients A, B, and D of equations (3). In effect, the motion of the air in throughs and ridges of pressure (or around cyclones and anticyclones), resulting from the combination of signs of A, B, and D in eqs. (3) is contrary to that observed in the actual atmosphere. The horizontal divergence as computed by DOPORTO (1944, 1952) and FAUST (1952), although in agreement with the cellular arrangement, is of opposite sign to that deduced from equations (3).

5. Equations (3 a) and (3 b) indicate that about 4 and 12 km the components u and v of the perturbation change their sign. This is a requirement of the cellular motion which, like those regarding the distribution of divergence and vertical velocity, does not appear in the exponential solution of the differential equations. It has been considered of interest to investigate whether the wind observations in the free atmosphere are in agreement with the theoretical variation with height of the zonal and meridional components of the perturbation of the westerlies.

For this purpose the upper winds observed at Valentia were the only homogeneous mass of data available over a sufficiently long period to give averages which might be of statistical significance.

The upper wind observations utilised in this investigation were carried out with Rawin

equipment No. SCR-658 on loan from the United States between 1/10/46 and 30/6/48 and from 1/7/48 up to 30/9/50 with British radar equipment A.A. No. 3 MK. 2.

The standard daily schedule of observations with the Rawin equipment was two ascents, launched at 10.45 and 22.45 G.M.T. up to 1/1/48 and at 02.30 and 14,30 since that date. However, due to shortage of hydrogen and transmitters there were many breaks in the schedule which could only be maintained by producing hydrogen locally and using transmitters made by the staff of the Observatory. Shortage of hydrogen forced this schedule to be reduced, except in a few cases, to one ascent per day launched at 14.30 G.M.T. as from 30/6/48 when the Radar equipment came into operation. When, due to weather conditions it was considered impracticable to make a combined radiosonde and radiowind launching, an assumed rate of ascent of about 1,400 m/m determined experimentally was used for the computation of the wind.

The computations were in all cases made graphically and the measured wind corresponds to averages of overlapping layers of the order of 800 metres.

All the ascents made between 1/10/46 and 30/9/50, i.e. during four years, were scrutinized and those not reaching 16 km rejected. Also rejected were those ascents which gave winds considered doubtfull by the observer at the time of the computation. These doubtful observations are due mainly to ground reflection of the electromagnetic waves, which occur when the angle of elevation is small and therefore are more frequent with strong winds and for the upper levels of the ascents. The minimum angle of elevation at which reliable observations can be made is never less than 12° for radiowind and 6° for radarwind. The presence of hills up to 300 ms high towards the ESE in the neighbourhood of the observatory raises this minimum angle of elevation in that direction to 20° for radiowind and 12° for radarwind. For each ascent not rejected the direction in degrees true and velocity in knots at 1, 2 . . . etc. km was converted by means of tables to meridional and zonal components.

To find the average components of the perturbation the ascents were then classified in accordance with the only other meteorological variable, namely the pressure, which can give an indication in this respect. An ascent made when the pressure is increasing (decreasing) will, generally speaking, give the vertical distribution of wind in the part of the atmosphere situated between a line of trough (ridge) and the succeeding line of ridge (trough). The facts that the trajectory of the balloon is not vertical, the observation at different heights not simultaneous, and the lines of troughs (ridges) at different levels not in the same perpendicular plane, are here ignored. The average values computed for each of the two groups of ascents given by this form of classification, may be taken as representing the average wind components in the neutral points between a trough and the succeeding ridge, and a ridge and the succeeding trough.

The variation of atmospheric pressure used for the classification of the ascent may, in principle, refer to any level and it would appear that surface pressure values, which are known continuously and with greater accuracy than at any other level, are the most appropriate. However, changes of pressure at the surface are often not representative of the real phase of a perturbation in the atmosphere, due to the influence of erratic, advective changes in the lower layers. Further the writer has shown (1952) that the maximum amplitudes of the average interdiurnal variations of pressure and temperature are greater when the ascents are classified according to the sign of the pressure variation at 8 km and it was expected that this statistical effect would also be operative in the case of wind perturbations. Therefore the variation of pressure at 8 km (to be precise 8 gkm before 1/1/50 and 8 gpkm afterwards) has been used for the classification, although this procedure has resulted in the non-utilisation of some ascents due to lack of pressure data.

The selection of the 8 km level pressure as a basis for the classification introduces also a limitation in the choice of the time interval to which the variation of pressure refers. In effect, radiosonde ascents are made only every twelve hours at Valentia, normally simultaneously with, or in some few cases at very short interval before or after, the radio-wind ascent. It has been considered that to classify the wind data at hour H according to the variation of pressure from $H-12$ hours to

$H+12$ hours, would result in classifying together ascents which in many cases would belong to different halves of the perturbation, due to the short lag with which wind follows the changes of pressure. For this reason it was decided to use the variation of pressure between H and $H-12$ hours.

The values of the pressure at 8 km used for computing the 12-hour variations were obtained by means of Bjerknes' tables and rounded off to whole millibars.

At first only the ascents between 1/10/46 and 31/12/49 were used for this investigation. When they were classified in accordance with the sign of the difference $P_8^{(H)} - P_8^{(H-12)} = \triangle P_8$ between the 8 km pressures at the time of the ascent and 12 hours earlier, it was found that the number of ascents made with increasing pressure was 167 while there were only 85 made with decreasing pressure, i.e. there were approximately twice as many ascents in the group $\triangle P_8 > 0$ as in the group $\triangle P_8 < 0$ (Table 1). This may be due to the wave form of the perturbation having a quick fall and a slow increase of pressure, but it also may be due to a systematic positive error in the values of P_8 during the daytime as a consequence of insufficient ventilation of the temperature element of the radiosonde, and a preponderance of radiowind day ascents (239 including 27 when $\triangle P_8 = 0$) over night ascents (48, including 8 when $\triangle P_8 = 0$).

It was decided then to extend the investigation to cover 4 complete years of observations by considering the ascents made between 1/1/50 and 30/9/50. In this period only day ascents were made, and the proportion of ascents in the groups $\triangle P_8 > 0$ and $\triangle P_8 < 0$ was found to be nearly 3 to 1, i.e. even greater than in the 39 months from 1/10/46 to 31/12/49 considered before.

However, the number of night ascents (21) in the group $\triangle P_8 > 0$ is practically equal to the number of night ascents (19) in the group $\triangle P_8 < 0$ which does not support the hypothesis of a systematic error introducing too large values of P_8 during the daytime.

It is not possible, therefore, to give a satisfactory explanation of the distribution of ascents in the groups $\triangle P_8 > 0$ and $\triangle P_8 < 0$, but as explained in paragraph 7 this distribution is believed not to invalidate the results of the investigation.

6. Table I shows that, in the period of four years to which the investigation refers, there were 405 ascents reaching at least the 16 km level and for which pressure data at 8 km were available for making the classification, and that of these 405 ascents 247 were made when the variation of pressure during the last 12 hours had resulted in an increase at 8 km, 109 when it has resulted in a decrease and 49 when the pressure has not changed. Table II shows the number of selected ascents in each month and season (Winter = December to February, etc.).

The average values in knots of the zonal and meridional component of the wind up to 20 km for the groups $\triangle P_8 > 0$, $\triangle P_8 = 0$ and $\triangle P_8 < 0$ are given in Table III, which refers to the periods 1/10/46 to 31/12/49, and Table IV, which refers to the four-year period 1/10/46 to 30/9/50. From these data Figures 1 and 2, giving the hodographs of the average wind up to 15 km, have been drawn. In these figures the vector wind would be re-

Table I. Number of day and night ascents in the different pressure groups of the classification

	Day ascents			Night ascents			Total		
	1/10/46 to 31/12/49	1/1/50 to 30/9/50	Total	1/10/46 to 31/12/49	1/1/50 to 30/9/50	Total	1/10/46 to 31/12/49	1/1/50 to 30/9/50	Total
$P_8 > 0$.....	146	80	226	21	0	21	167	80	247
$P_8 = 0$.....	27	14	41	8	0	8	35	14	49
$P_8 < 0$.....	66	24	90	19	0	19	85	24	109
Total	239	118	357	48	0	48	287	118	405

Table II. Monthly and seasonal distribution of ascents

Month	J	F	M	A	M	J	J	A	S	O	N	D	Total
Number of ascents	27	23	38	18	54	45	30	37	18	49	39	27	405

Season	Spring	Summer	Autumn	Winter	Total
Number of ascents	110	112	106	77	405

presented, following the meteorological convention, by a straight line drawn from a point of the hodograph to the centre of coordinates. Data up to 20 km have been included in both Tables to illustrate the effect on the average values for the upper four kilometres of a decreasing number of ascents reaching those heights. These data will not be utilized in the discussion. The comparison between the data of Table III and Table IV is also useful in order to estimate the confidence which may be placed in the conclusions derived from them.

The average values of the 12-hour variation of pressure are as follows:

	Period 1/10/46 to 31/12/49	Period 1/10/46 to 30/9/50
$\triangle P_8 > 0$	3.5 mb	3.5 mb
$\triangle P_8 < 0$	3.0 mb	2.9 mb

In Table V and Figure 3 the difference at each height between the respective average wind component of the groups $\triangle P_8 > 0$ and $\triangle P_8 < 0$ for the 39 month period 1/10/46 to 31/12/49 are given. Table VI and Figure 4 refer similarly to the 4-year period 1/10/46 to 30/9/50.

If U and V are the average undisturbed wind components at any level, the average values given in Table III (and Table IV) may be represented by

$$\begin{aligned} U+u \text{ and } V+v &\text{ for } \triangle P_8 > 0 \\ U \text{ and } V &\text{ for } \triangle P_8 = 0 \\ U-u \text{ and } V-v &\text{ for } \triangle P_8 < 0 \end{aligned}$$

where, as before, u and v stand for the perturbation. Therefore the difference between the average values of the wind components

Table III. Average wind components in knots when the pressure variation at 8 km during the last 12 hours has been positive, zero or negative

Valentia. 1/10/46 to 31/12/49

Height km	$\triangle P_8 > 0$			$\triangle P_8 = 0$			$\triangle P_8 < 0$		
	No. of Ascents	$U+u$	$V+v$	No. of Ascents	$U+u$	$V+v$	No. of Ascents	$U+u$	$V+v$
Surface	167	— 1.28	1.80	35	— 2.42	1.16	85	— 0.89	2.75
1	167	— 1.28	4.94	35	— 3.75	4.95	85	0.24	5.52
2	167	1.96	4.07	35	— 1.29	4.41	85	2.31	4.70
3	167	4.72	2.68	35	0.68	2.62	85	4.34	3.78
4	167	5.70	2.46	35	2.06	1.66	85	5.89	5.65
5	167	6.33	2.19	35	2.51	1.95	85	5.67	6.69
6	167	7.38	1.45	35	4.35	2.75	85	5,27	6.58
7	167	9.10	— 0.59	35	4.35	2.67	85	7.22	6.51
8	167	10.16	— 1.48	35	3.75	1.54	85	7.97	7.53
9	167	12.10	— 5.35	35	7.16	0.51	85	8.72	5.89
10	167	13.42	— 7.18	35	10.09	— 0.09	85	10.83	4.47
11	167	14.21	— 7.17	35	11.10	— 0.65	85	13.08	3.59
12	167	14.98	— 6.98	35	14.50	— 0.30	85	14.84	1.99
13	167	15.17	— 5.99	35	15.55	— 1.17	85	15.78	0.32
14	167	13.61	— 4.82	35	16.54	0.06	85	15.61	— 0.16
15	167	13.01	— 2.49	35	14.79	— 1.64	85	15.47	— 0.68
16	167	12.17	— 2.83	35	12.33	— 2.78	85	14.31	0.43
17	126	9.72	— 2.47	24	13.79	— 2.82	59	13.29	— 2.47
18	90	8.90	— 2.34	16	15.75	— 2.62	40	11.46	— 1.00
19	66	7.66	— 2.76	7	10.53	1.87	23	12.28	— 2.03
20	35	5.88	— 1.42	5	3.34	1.66	9	9.03	— 4.30

Table IV. Average wind components in knots where the pressure variation at 8 km during the last 12 hours has been positive, zero or negative

Valentia. 1/10/46 to 30/9/50

Heights km	$\triangle P_8 > 0$			$\triangle P_8 = 0$			$\triangle P_8 < 0$		
	No. of Ascents	$U+u$	$V+v$	No. of Ascents	$U+u$	$V+v$	No. of Ascents	$U+u$	$V+v$
Surface	247	— 0.05	1.92	49	— 0.97	1.95	109	— 0.43	2.53
1	247	0.51	4.21	49	— 1.50	4.20	109	1.55	4.81
2	247	3.55	3.79	49	1.68	5.50	109	3.43	3.93
3	247	6.36	2.61	49	3.83	3.82	109	5.74	2.95
4	247	7.71	2.57	49	5.61	2.86	109	7.27	4.24
5	247	8.67	2.06	49	5.86	2.96	109	6.88	5.16
6	247	9.51	1.37	49	7.85	3.14	109	6.98	4.96
7	247	11.26	0.20	49	8.44	3.28	109	8.71	5.29
8	247	12.72	— 1.03	49	9.29	2.19	109	9.85	5.81
9	247	14.58	— 4.31	49	12.88	1.43	109	11.27	3.79
10	247	15.90	— 6.25	49	14.72	1.83	109	13.17	2.35
11	247	16.35	— 6.11	49	15.39	1.25	109	14.85	1.50
12	247	16.63	— 5.53	49	17.55	1.31	109	16.17	1.00
13	247	16.02	— 4.41	49	18.31	0.88	109	16.77	— 0.23
14	247	14.25	— 3.35	49	17.76	2.09	109	15.58	— 0.60
15	247	13.04	— 1.66	49	15.30	0.45	109	14.61	— 0.86
16	247	12.19	— 2.06	49	13.46	— 0.09	109	13.31	— 0.04
17	195	10.20	— 1.06	37	14.49	— 0.84	80	12.15	— 2.11
18	139	8.69	— 1.38	26	13.28	— 1.53	57	10.11	— 0.73
19	105	7.64	— 2.25	11	10.58	1.88	34	9.65	— 1.52
20	55	4.19	— 0.60	6	12.17	1.95	17	4.46	— 2.10

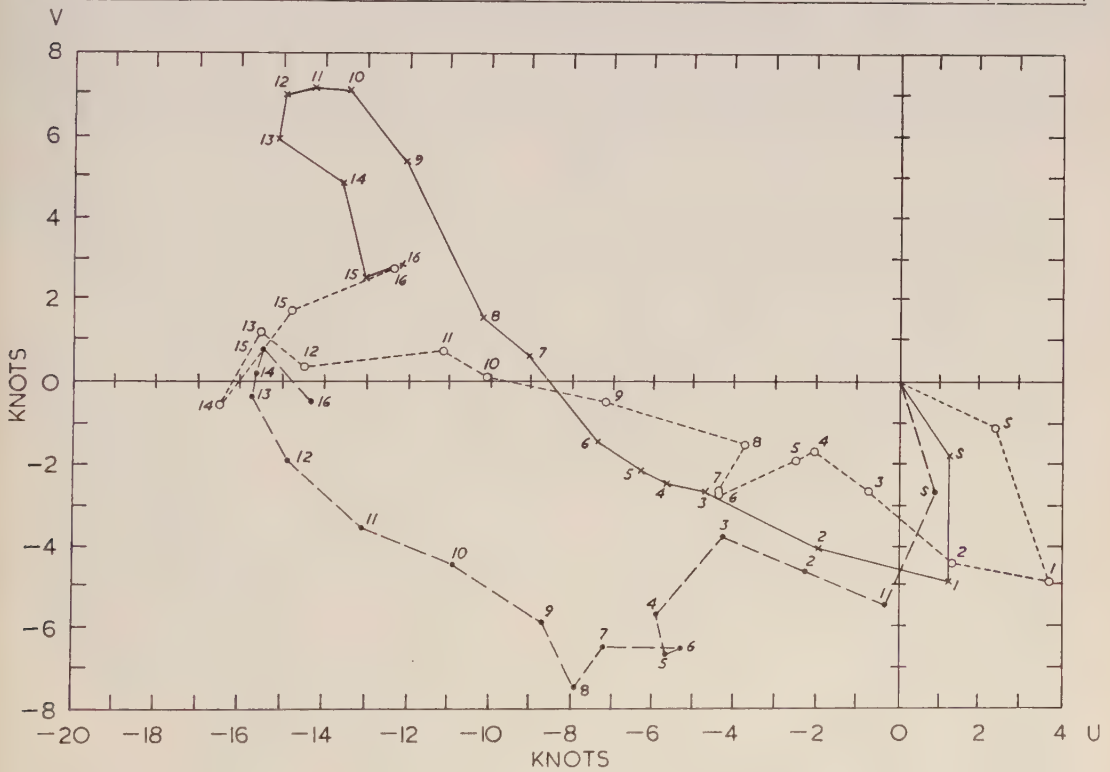

Fig. 1. Hodograph of the average wind when $\triangle P_8 > 0$ (×), $\triangle P_8 = 0$(°) $\triangle P_8 < 0$(·). Valentia Observatory. Period 1/10/46 to 31/12/49. (The vector wind at any height is represented by a straight line drawn from the corresponding point of the hodograph to the origin of coordinates.)

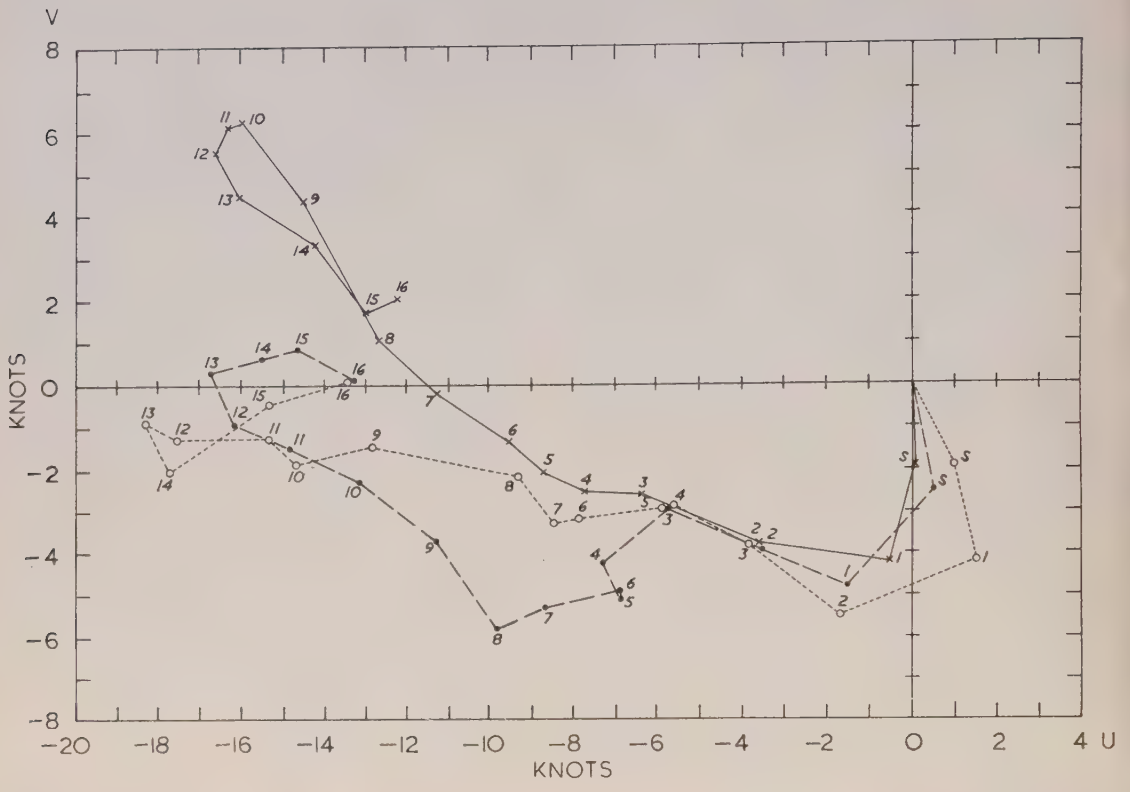

Fig. 2. Hodograph of the average wind when $\triangle P_8 > 0$ (×), $\triangle P_8 = 0$ (°) and $\triangle P_8 < 0$ (·). Valentia Observatory. Period 1/10/46 to 30/9/50. (The vector wind at any height is represented by a straight line drawn from the corresponding point of the hodograph to the origin of co-ordinates.)

for the groups $\triangle P_8 > 0$ and $\triangle P_8 < 0$ gives $2u$ and $2v$ (Tables V and VI and Figures 3 and 4). The relative smallness of the values of U and u is due to the occasional existence of closed circulations, both cyclonic and anticyclonic, at all levels, i.e. the Westerlies at the latitude of Valentia are replaced at times by Easterlies and the algebraic average values of the zonal wind component and of its perturbation are reduced accordingly.

Tables III and IV and Figures 1 and 2 show that the average values of the components for the group $\triangle P_8 = 0$ do not fall as they should between the corresponding values for the groups $\triangle P_8 > 0$ and $\triangle P_8 < 0$. Apart from the large difference between the number of ascents from which the averages have been computed, it is necessary to remember that periods of 39 and 48 months are not long enough to obtain for most meteorological observations average values which may be considered as good approximations to normal values.

For the purpose of this investigation, however, the values of the wind at different levels are not as important as the differences between corresponding wind components at the same level for the groups $\triangle P_8 > 0$ and $\triangle P_8 < 0$ and the variation of these differences with height. Although the corresponding values of these differences given in Tables V and VI show in some cases large variations the general form of the curves in figures 3 and 4 are fairly similar. Only at the lower levels, where the wind circulation is affected by the rugged topography of the Kerry Mountains is the agreement not so good. At other levels the differences between the curves are due, not only to the different number of ascents used for the computation of the average values of the components in the two groups for both periods, but also to the error inherent to the

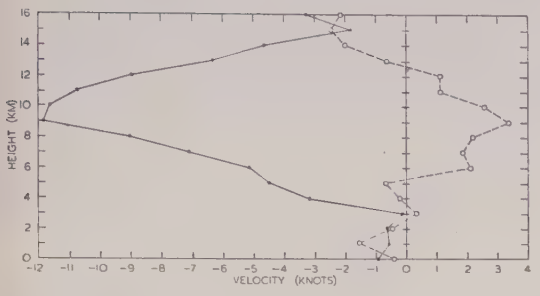

Fig. 3. Variation with height of twice the meridional (·) and zonal (°) components of the vector difference between average winds when $\triangle P_8 > 0$ and $\triangle P_8 < 0$. Valentia Observatory. Period 1/10/46 to 30/12/49.

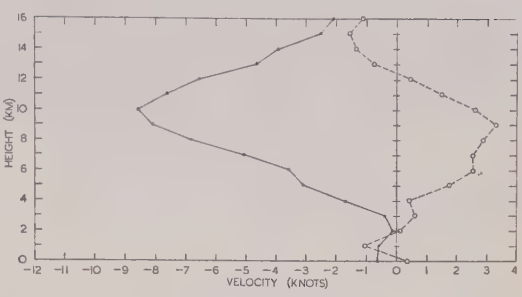

Fig. 4. Variation with height of twice the meridional (·) and zonal (°) components of the vector difference between average winds when $\triangle P_8 > 0$ and $\triangle P_8 < 0$. Valentia Observatory. Period 1/10/46 to 30/9/50.

method of observation. Whatever the claims made regarding the accuracy of the observations by Rawin and radar methods it appears that the average error of individual observations made at Valentia may be in both techniques as large as 5 knots for each component. If this figure is adopted, the average value of the error for the average component would be about 0.4 knots for the $\triangle P_8 > 0$ group and about 0.6 knots for the group $\triangle P_8 < 0$ and, therefore, about 0.7 knots for the differences.

It appears from Figures 3 and 4, and from the above considerations regarding the average errors that

(1) The zonal perturbation, u,
  (a) has opposite directions above and below about 12 km.
  (b) decreases the westerlies, above 12 km and reinforces them below 12 km when the pressure at 8 km in the previous 12 hours has increased. The reverse happens when the pressure has decreased.
  (c) has a zero value at about 4 km and
  (d) has below 4 km the opposite sign to that in the stratum 4—12 km.

(2) The meridional perturbation, v,
  (a) has a maximum value at about 9 km.
  (b) is very small between the surface and 3 km.
  (c) is directed towards the South when the pressure at 8 km has increased during the previous 12 hours. The reverse happens when the pressure has decreased.

7. If the large difference of the number of ascents classified in the groups $\triangle P_8 > 0$ and $\triangle P_8 < 0$ is due to the form of the wave length of the perturbation of pressure at 8 km these results need not be modified. If, as discussed before, this difference were due to a systematic error in the observed pressure at 8 km during daytime, the classification of the ascents into the three groups would no longer be valid; the conclusions, however, would, most likely, be an understatement of the true facts. In effect the averages of the group $\triangle P_8 > 0$ for instance would be based not only on ascents belonging in fact to this group but also on others which more properly would belong to the groups $\triangle P_8 = 0$ and $\triangle P_8 < 0$; therefore the values obtained for the perturbation would be less than the actual values and it would only be necessary to change slightly the heights at which the zonal perturbation is zero.

These observed values of the component of the perturbation of the Westerlies at Valentia show that the exponential solution of the dynamical equations fails in this case, as also in those referring to the existence of nodal and anti-nodal surfaces of the other variables, to account for the data derived from the observations.

The cellular solution, on the other hand, explains the existence of nodal and anti-nodal surfaces of the components of the wind perturbation at heights which are in agreement with the result of the observations. As in some other cases referred to above, the cellular solution, however, fails to give a correct interpretation of the observed circulation.

Taking into account the fact that, neglecting the slant of troughs and ridges, the average values of the components for the group

Table V. Components in knots of the vector difference between the average winds when the pressure variation at 8 km during the last 12 hours has been positive and when it has been negative. (This difference is approximately twice the perturbation components.)

Valentia 1/10/46 to 31/12/49

Height	$2u$	$2v$
Surface	—0.39	—0.95
1	—1.52	—0.58
2	—0.45	—0.63
3	0.38	—0.10
4	—0.19	—3.19
5	—0.66	—4.50
6	2.11	—5.13
7	1.88	—7.10
8	2.19	—9.01
9	3.38	—11.84
10	2.59	—11.65
11	1.13	—10.76
12	1.14	—8.97
13	—0.61	—6.31
14	—2.00	—4.66
15	—2.46	—1.81
16	—2.14	—3.26

Table VI. Components in knots of the vector difference between the average winds when the pressure variation at 8 km during the last 12 hours has been positive and when it has been negative. (This difference is approximately twice the perturbation components.)

Valentia. 1/10/46 to 30/9/50

Height	$2u$	$2v$
Surface	0.38	—0.61
1	—1.04	—0.60
2	0.12	—0.14
3	0.62	—0.34
4	0.44	—1.67
5	1.79	—3.10
6	2.53	—3.59
7	2.55	—5.09
8	2.87	—6.84
9	3.31	—8.10
10	2.63	—8.60
11	1.50	—7.61
12	0.46	—6.53
13	—0.75	—4.63
14	—1.33	—3.95
15	—1.57	—2.52
16	—1.12	—2.10

$\triangle P_8 > 0$ may approximately be equated to the values of these components at the neutral point between a trough and the next ridge, and those for the group $\triangle P_8 < 0$ to the values for the neutral point between a ridge and the next trough, equations (3 a) and (3 b) indicate that the differences of the average components given in Tables V and VI should be:

for the Zonal component, $2u = 0$
for the Meridional component,

$$2v = -2B \cos \Theta z.$$

It is obtained, however, both from Table V and from Table VI, that it is the zonal component, and not the meridional, that shows nodal surfaces at about 4 and 12 km, while the sign is opposite to that required by the equations. It might be expected in view of this result that the observed meridional component would be zero, as the theory requires the zonal component to be; however the observed meridional component shows a very well defined maximum at about 9 km. Whether this result, together with the sign of the circulation, might be explained by integration of the dynamical equations for a two-layers atmosphere, with sloping tropopause and meridional gradient of temperature, is a problem which awaits the enterprise of a meteorologist who is also an expert mathematician or of a mathematician with an interest in Meteorology.

Acknowledgments: Many of the computations have been carried out by Messrs J. B. O'Sullivan and J. Byrne. Messrs P. M. A. Bourke, W. A. Morgan, and F. E. Dixon have been kind enough to help in the preparation of the text. The author wishes to express his gratitude to them.

REFERENCES

Bjerknes. V., Bjerknes, J., Solberg, H., Bergeron, T., 1934: *Hydrodynamique Physique.* Paris. Les Presses Universitaires de France. 864 pages.

Dines, W. H., 1919: The characteristics of the free atmosphere. *Geoph. Mem.* No. 13, London, pages 47—76.

Doporto, M., 1943 a: The computation of Atmospheric Pressure at the 8 km level of constant Air Density. *Irish Meteorological Service, Technical Note* No. 1. Reprinted as *Geophysical Publications* Vol. III, No. 4. 1951.

— 1943 b: Dynamical aspects of the constancy of Air Density at 8 km. *Irish Meteorological Service, Technical Note* No. 2. Reprinted as *Geophysical Publications* Vol. III, No. 6. 1951.

— 1944: Cell Motion in the Atmosphere. *Irish Meteorological Service, Technical Note* No. 6. Reprinted as *Geophysical Publications,* Vol. III, No. 7. 1951.

— and Morgan, W. A., 1947: The significance of the Isopycnic Level. *Quart. J. R. Meteor. Soc.* **73**, p. 384.

— 1952: Vertical Motion and Divergence computed from Upper Air Variations of Pressure and Temperature at Valentia. *Ber. Dtsch. Wd. US-Zone* No. 35, p. 103.

Faust, H., 1952: Zur Dynamik der Hoch- und Tiefdruckgebiete. *Ber. Dtsch. Wd. US-Zone* No. 35, p. 92.

Goldie, A. H. R., 1947: The Upper Atmosphere Estimated Distribution of Temperature, Pressure and Wind up to the 45 km level. *Meteorological Research Paper* 360. Air Ministry, London.

Hann, J. von and Süring, R., 1938: *Lehrbuch der Meteorologie,* Leipzig. Willibald Keller.

Palmen, E., 1932: Versuch zur Analyse der dynamischen Druckschwankungen in der Atmosphäre. *Beitr. z. Phys. d. fr. Atm.* **19**, p. 55.

Sen, S. N., 1924: On the distribution of air density over the Globe. *Quart. J. R. Meteor. Soc.* **50**, p. 29.

Shaw, Sir N., 1914: Upper-Air Calculus and the British Soundings during the International Week (May 5—10) 1913. *Jour. Scottish Met. Soc.* **16**, p. 167.

Wagner, A., 1910: Die Temperaturverhältnisse in der freien Atmosphäre *Beitr. z. Phys. d. fr. Atm.* **3**, p. 57.

Measurements of solar radiation at Lövånger in Sweden during the total eclipse 1945

By N. JERLOV, Fishery Board of Sweden, Gothenburg
H. OLSSON, TAM Airport, Bagdad
W. SCHÜEPP, Service Météorologique, Levpoldville

(Manuscript received November 15, 1953)

The meteorologic work at Lövånger (64° 22′ N, 21°19′ E) during the total eclipse on 9 July 1945 included continuous observations of the solar radiation. A Moll thermopile with 80 sets of junctions was used for measuring the radiant energy in different parts of the visible region. It was provided with a cylindrical screen at the upper end of which colour filters were introduced in succession. The device has been earlier described in detail (JOHNSON and OLSSON, 1944). Infra-red screening was achieved by means of the Schott and Genossen filter BG 19 in order to attain a high degree of accuracy in the visible range.

The experiments were conducted under favourable conditions with a clear sky and no wind. At 13: 10 and 13: 30 before and at 16: 15 and 16: 25 after the eclipse, complete measurements were carried out, *i. e.* with the whole set of 12 colour filters as well as without filter. During the eclipse, when quick observations were desirable, only 5 filters were used, *viz.* RG 8, RG 1, OG 2, VG 9, and BG 12. Thus a series of readings was accomplished every fifth minute from 13: 50.5 to 16: 04.5. The duration of totality was from 15: 01.5 to 15: 02.1.

These records of the sun's spectral energy are expected to contribute some information about a possible change in atmospheric conditions during the eclipse. The extinction of solar radiation is made up of three components. One is due to molecular scattering, the second to absorption and scattering by liquid and solid particles, and the third to absorption by atmospheric gases, chiefly water vapour and ozone.

According to a method elaborated by ÅNGSTRÖM (1929) and later revised by SCHÜEPP (1949) the extinction caused by particles is expressed by the formula

$$m_h \beta (2\lambda)^{-\alpha},$$

where β is the extinction coefficient for $\lambda = 500$ mμ and for the relative air-mass $m_h = 1$, and α is an exponent indicating the dependence of scattering on wave-length.

Values of α and β have been derived from the observations. The factor α shows small irregular variations with the time which are, however, within the experimental errors. On an average α amounts to 2.0. The trend of the extinction coefficient, β, is a slow decrease (fig. 1) which is probably associated

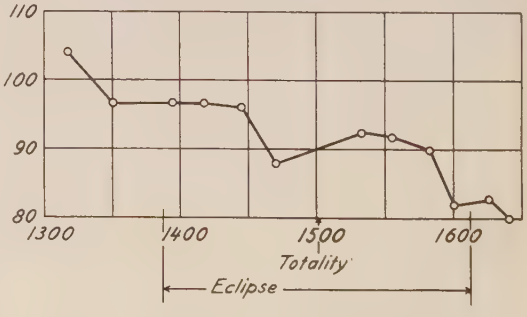

Fig. 1. The extinction coefficient $\beta \cdot 10^3$.

with an observed dissolution of the inversion at an altitude of 1,000 m. The irregularity in β near the totality may suggest that this dissolution, caused by the rising temperature in the low air layers, was retarded during the eclipse.

Following Schüepp's procedure it is possible to arrive at a determination of water vapour on account of its selective absorption in the spectral range 625 – 3,000 mμ. The actual observations do not clearly establish any alteration in the content of water vapour during the eclipse.

Furthermore the amount of ozone has been estimated from wave-lengths within the Chappuis bands (fig. 2). Although the resulting values are not obtained with a high exactitude it is established that an appreciably lesser quantity ozone was present in the atmosphere after the eclipse (0.2 cm) than before it (0.3 cm). Whether this is an effect of the eclipse or due to a normal weather change is thus far an open question.

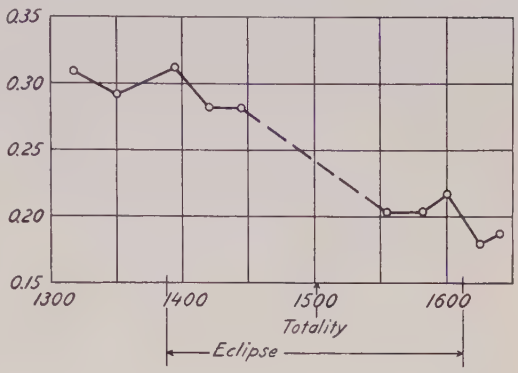

Fig. 2. The content of ozone.

REFERENCES

Ångström, A., 1929: On the atmospheric transmission of sun radiation and on dust in the air. *Geogr. Ann.*, p. 156.

Johnson, N. G. and H. Olsson, 1943: On the standardization of photo-electric elements by means of solar radiation. *Geogr. Ann.*, H. 3.

Schüepp, W. 1949: Die bestimmung der Komponenten der atmosphärischen Trübung aus Aktinometer-Messungen. Diss., Wien.

Average Temperature and Salinity at a Depth of 200 Meters in the North Atlantic[1]

By F. C. FUGLISTER, Woods Hole Oceanographic Institution

(Manuscript Received October 20, 1953)

Abstract

New charts are presented showing the average temperature and average salinity at a depth of 200 meters in the North Atlantic. These are compared with charts published by WÜST and DEFANT in 1936 and it is shown that, over most of the ocean, conditions are nearly constant at this depth. Attention is focused on the areas of changing temperature where the major ocean currents exist. It is shown that important details are obscured by the averaging process. The range of observed temperature is charted and supplements the information given by the average charts. The standard deviation from the mean temperature, calculated for two portions of the Gulf Stream System, indicates that when more observations are available such calculations may be of use in studying the major ocean current systems. Temperature anomalies from the mean for each degree of latitude are plotted and compared with data published by WÜST in 1937.

Introduction

The best source of information on the subsurface temperature, salinity and density distribution in the North and South Atlantic is the atlas to volume six of the Deutsche Atlantische Expedition Meteor (WÜST and DEFANT, 1936). The atlas contains charts of average conditions for various standard depths from 200 meters to 5,000 meters. These charts represent the mean state or yearly normal and were based on all available data regardless of date. The charts are printed in colors and are large, clear and easy to read. Because virtually all studies of the general circulation of the oceans are based on what is known of the temperature, salinity and density distribution and also because of its exceptional quality this atlas should be a standard reference on the subject.

Since the date of publication of the Meteor Atlas many observations, especially of subsurface temperatures, have been made in the North Atlantic. The files of the Woods Hole Oceanographic Institution contain 210,000 records of subsurface temperatures obtained with the bathythermograph and 37,000 serial observations of subsurface temperature and salinity obtained by the Nansen bottle method. All of the bathythermograph and approximately 50 % of the serial observations were made after 1934. With these new data on hand the question arises as to whether or not that part of the Meteor Atlas that deals with the North Atlantic is obsolete.

The task of producing a new atlas in any way comparable to the German one would

[1] Contribution No. 668 from the Woods Hole Oceanographic Institution.

This research was sponsored by the Office of Naval Research under Contract Nonr-683 (00) (NR-083 – 019).

be an expensive and large undertaking. If it should prove desirable at this time, then the U.S. Navy Hydrographic Office with its punch card system and complete file of data would be best able to do this work. This paper is intended as an investigation of the problem of whether or not a part of the Meteor Atlas is obsolete and it may serve as a supplement to that atlas. Only the 200 meter depth is considered, partly because there are more new data for this than for any other depth represented in the German Atlas and partly because the temperature conditions at this depth have been of special interest in various studies of the Gulf Stream System, (Wüst, 1937) (Fuglister, 1951). Problems that arose in the averaging process will be discussed and the need for other than average charts examined.

Chart Construction

Of the available temperature observations, 40,000 reached to a depth of 200 meters and were used in constructing the accompanying 200 meter average temperature chart (chart 2); 14,000 salinity observations were available for the 200 meter average salinity chart (chart 4). This is approximately 10 times as many temperature observations and 4 times as many salinity observations as were available for the construction of the German Atlas Charts (here copied as charts 1 and 3). Lest it is felt that the saturation point of observations in the North Atlantic is being approached, chart number 5 has been drawn up to show the large portions of this ocean for which our files contain no data for the 200 meter depth.

In the process of averaging, the unit of area used was the one degree field. All observations from one month, regardless of year, were averaged and then these monthly values were in turn averaged to obtain a yearly normal. This system tended to decrease the weight of numerous observations made by one ship at one time in a unit area as it increased the weight of scattered "off season" observations. The temperature and salinity values from serial observations were, in many cases, interpolated values. The tabulations for each unit area included, besides the average temperature and salinity, the total number of observations, the months represented, the maximum and minimum observed values and the range. In order to compare the 200 meter temperature data with some results published by Wüst (1937), the average temperature for each degree of latitude was calculated and the temperature anomalies for each one degree field were tabulated. In these computations the Mediterranean data were excluded.

After the various tabulated values were plotted on the charts an important decision had to be made. Should the isopleths be drawn to follow the plotted values exactly or should some smoothing of the resulting irregular curves be done? Once a smoothing process of this sort is started it is difficult to know where to stop. Rather than risk misinterpreting the data, the decision was made to make every effort to follow the data exactly. An exception was made in a few cases where separate isopleths would have been required to represent a single value unsupported by the values in adjacent one degree fields. Some interpretation and interpolation of the data was, of course, necessary in order to make the isopleths continuous over the areas devoid of data.

A Comparison with the Meteor Atlas Charts

A superficial comparison of the new and older charts will give the impression that they are radically different. However, a closer study shows that, except for the addition of new areas and the introduction of numerous irregular lines instead of long smooth curves, there is remarkably little difference in the two sets of charts. In many instances the isotherms and isohalines of the German Charts are a smooth or average representation of the more complicated curves of the new charts. This suggests that the Meteor Charts, although based on far fewer observations, are in fact more nearly correct representations of the average conditions in the North Atlantic than are the new charts. It suggests that the method of drawing the isopleths on the new charts tends to confuse the average picture and the curves should have been smoothed, that is, an averaging process should have been employed in drawing the isopleths. Although it is quite possible that the German Charts

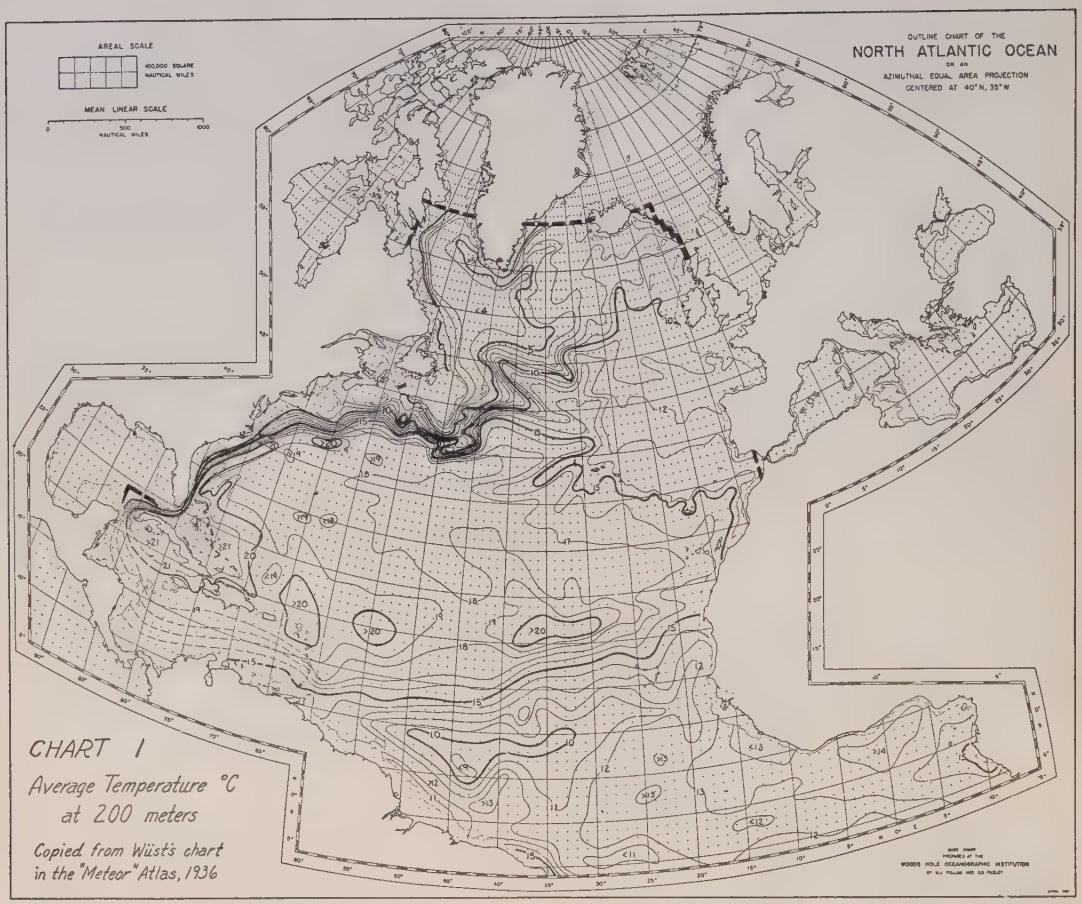

Chart 1. Average Temperature (after Wüst).

approximate the true average condition, the new charts have the advantage of showing some of the complexities and details (which may or may not be significant) and of allowing the reader to interpret and smooth the results for himself.

A comparison of these charts brings out the important fact, that over most of the vast extent of the North Atlantic conditions at 200 meters must be very nearly constant. The complex areas on all the charts are confined to certain portions of the ocean and it is evident that in these areas the major ocean currents exist. Most of what follows will be a discussion of the details in these complex areas and, because of the better distribution of temperature data, attention will be focused on the new 200 meter average temperature chart.

The 200 Meter Average Temperature Charts

The new 200 meter temperature chart shows many interesting details not appearing on the German Chart. Since it is almost impossible to discuss these details without referring to currents, the general assumption will be made here that the positions of the major ocean currents coincide with the positions of the pronounced horizontal gradients of temperature at 200 meters. Also, the assumption is made that the current directions are such that the warm water is to the right facing downstream. Because of the fresher water in the following areas the direction of flow is reversed with warm water to the left: in a narrow belt just off the continental shelf from the tail of the Grand Banks northward to Baffin Bay, and similarly from Cape Farewell

Chart 2. Average Temperature.

at the southern tip of Greenland northward along the east coast of Greenland to the Polar Sea.

The most pronounced gradient on both temperature charts is the one associated with the Gulf Stream. Between the Florida Straits and the 65th meridian the temperature contrast on the new chart is 2 to 3 degrees centigrade less than on the older chart. In the region between Cape Hatteras and the Grand Banks the zone of maximum temperature, south of the gradient, is displaced further to the south. Both of these changes can be explained in the following manner. If the current is continually shifting its geographical position and we assume the cross-current gradient to be constant then, up to a certain point, an increase in the number of observations averaged in the area will tend to spread out the gradient, decrease the total range of temperature across the gradient, and displace the maximum value to the right, facing downstream. If, as shown in Figure 1, the solid line represents the normal

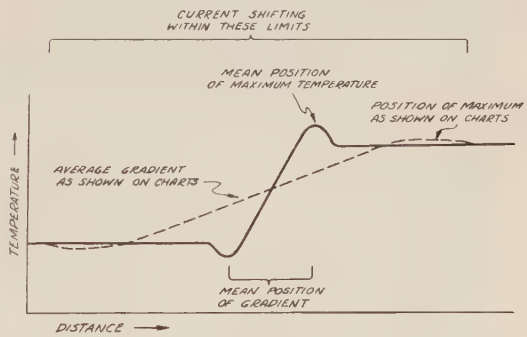
CURRENT SHIFTING WITHIN THESE LIMITS
MEAN POSITION OF MAXIMUM TEMPERATURE
POSITION OF MAXIMUM AS SHOWN ON CHARTS
AVERAGE GRADIENT AS SHOWN ON CHARTS
TEMPERATURE
MEAN POSITION OF GRADIENT
DISTANCE

Fig. 1. Schematic cross-current profile of 200 meter temperature.

4—305658

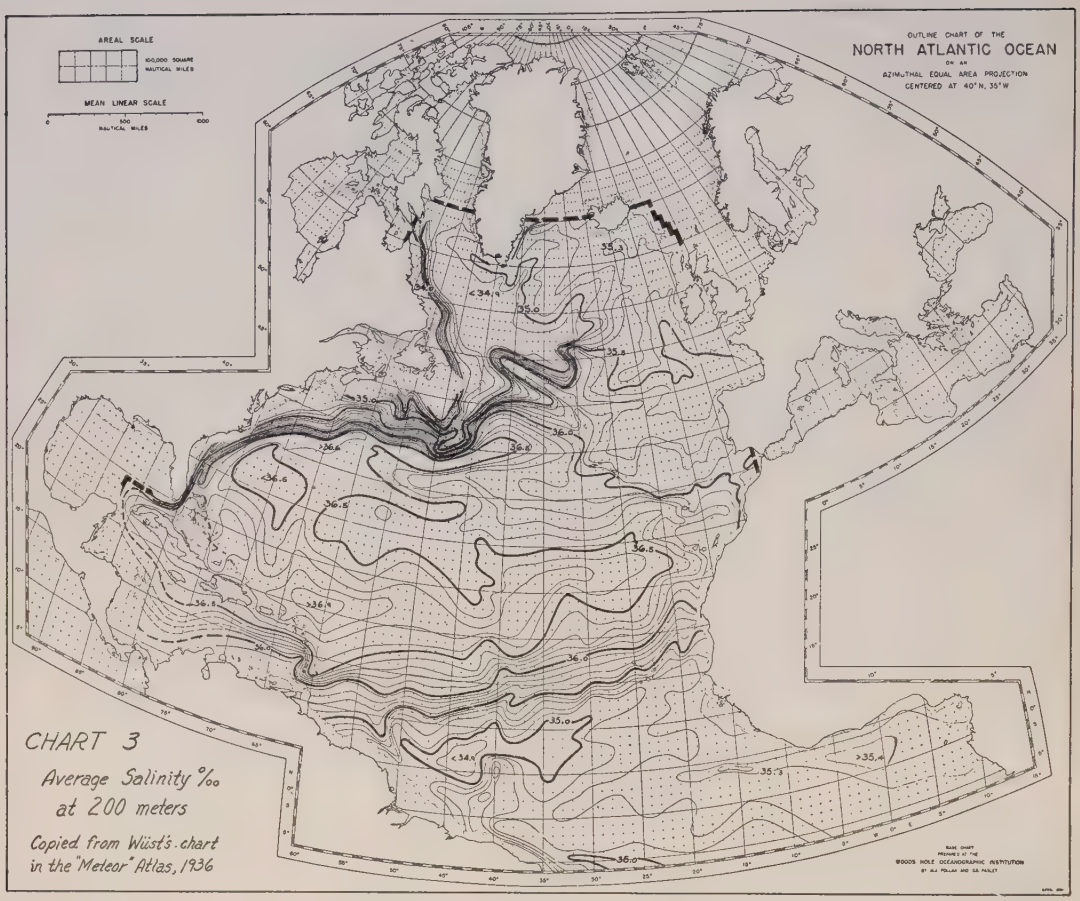

Chart. 3. Average Salinity (after Wüst).

temperature gradient across the current and the current shifts between the limits shown, then the average chart will show the more gradual gradient and the less pronounced maximum and minimum values as represented by the dashed line.

In the area to the south of Nova Scotia and Newfoundland there is what might be termed an intermediate development of the average in the Gulf Stream zone. The single gradient that appears on the German Chart is now broken down into at least two separate gradients. Although this separation of the isotherms appears to support the theory of multiple currents in the area (FUGLISTER, 1951) it is possible that increasing numbers of observations may again blend the picture and eventually show a single, gradual gradient across the zone. Much of the complicated pattern of isotherms on the new chart, in the Gulf Stream area in particular, but also to some extent in the equatorial regions, may be interpreted as showing the non-continuity or multiple current characteristics of the major ocean currents. This characteristic is not suggested by the German Chart, except perhaps in the area to the east of the Grand Banks, and it may not be indicated again when an average chart based on many more thousands of observations is produced.

The most confused area on the new charts is in the portion of the Gulf Stream System to the east of the Grand Banks. Disregarding the complex details for a moment, it is obvious that the many new observations in this area show that the warm water ($> 10°$ C) flows closer to Flemish Cap and further to the north and west than is indicated on the Meteor

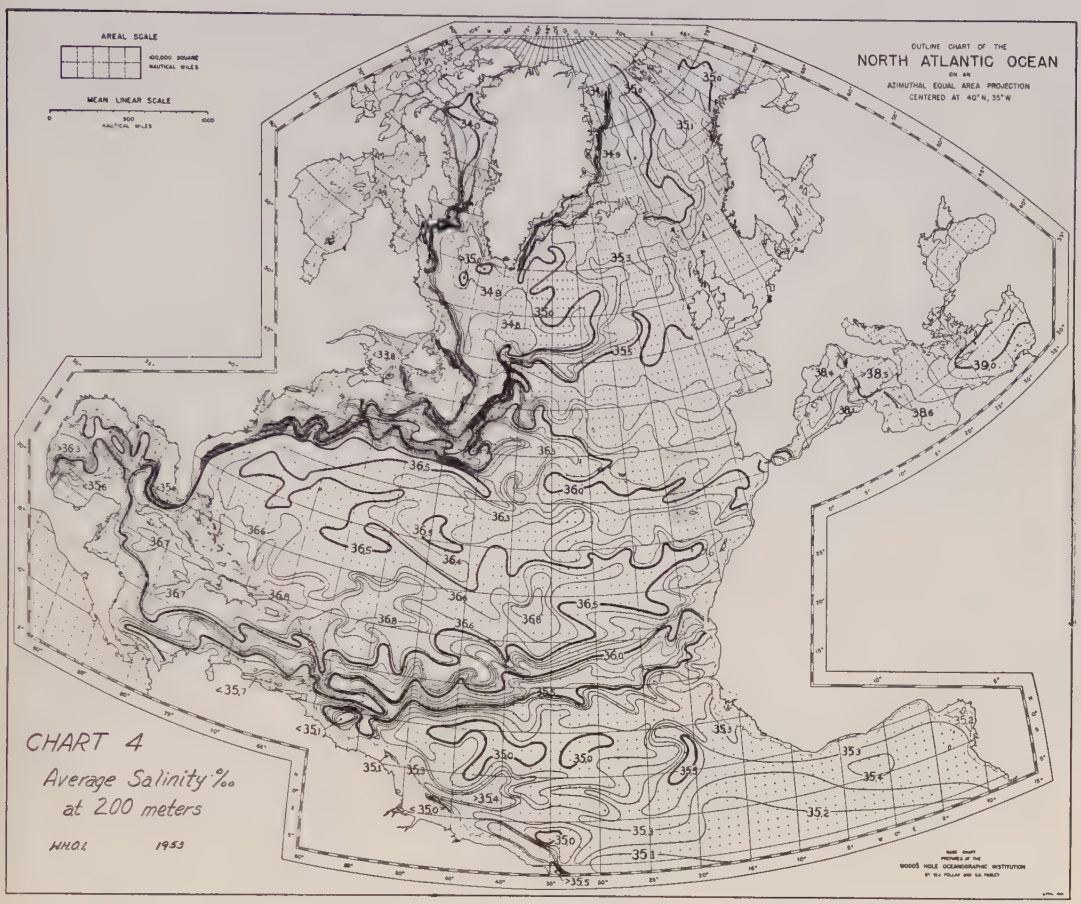

Chart 4. Average Salinity.

Chart. The pronounced gradient, indicating a northwesterly current, which turns abruptly towards the east near 50° north latitude is one of the most interesting features shown on either chart. One may be tempted to say that it is the bottom topography in this area that is the controlling factor but then it would be necessary to explain how bottom contours at depths of 4,000 meters could affect the course of a current which, according to its density structure, does not extend deeper than 1,500 meters.

To return to the details shown on the new chart in the region to the east of the Grand Banks we see that there are several isolated areas of maximum and minimum temperatures. If this were a truly average picture of the temperature conditions in the area we would interpret these areas as the locations of permanent eddies in the system. A more logical explanation is that this is a region of shifting currents and countercurrents and the distribution of observations is such that the resulting picture is a combination of average and instantaneous values. As we approach the Grand Banks from this area the number of observations increases and the isotherms smooth out.

East of the 30th meridian neither chart defines the area of the Gulf Stream System. The new chart shows a pronounced gradient in the eastern Norwegian Sea but there is no recognizable connection between it and the gradients in the area east of the Grand Banks. If the cross-current gradients decrease in magnitude and the currents shift over wide areas in the northeastern Atlantic then we can expect to find a widespread gradient on the average.

However, as will be shown later, no gradient of as much as 2° C. in a one degree field has ever been observed in the area southeast of the Faeroe-Shetland Channel where the northern branch of the Gulf Stream System presumably flows toward the Norwegian Sea. More will be said on this subject in connection with the discussion of the temperature range and temperature anomaly charts.

In the Norwegian Sea there is a scarcity of data north of the latitude of Jan Mayen (66° N) but in the southern portion, especially in the east, there is an excellent distribution of observations. The most interesting feature is the indicated current area extending northward along the Greenwich Meridian. The Norwegian Current is generally depicted as flowing along the coast of Norway and it is surprising that the chief concentration of gradients lies so far to the west. The pronounced gradient area along the southern boundary of the Norwegian Sea is evidently associated with the ridge that separates the Norwegian Basin from the main body of the North Atlantic. These gradients define a frontal zone and must be associated with relatively permanent currents, but because of the salinity gradients near the Greenland end of the ridge and the generally shoal depths several interpretations of current direction are possible.

In the north equatorial regions the principal differences between the new and the old charts appear in the area near the West Indies and off the coast of South America. The maxima and minima in these areas can be explained in the same way as were those phenomena in the area east of the Grand Banks, that is, the new chart represents a combination of average and synoptic data. As in the Gulf Stream the gradient across the north equatorial current has decreased slightly, the zones of 20° water to the north of the current have disappeared and the area of $< 10°$ water to the south has become smaller.

The Equatorial Countercurrent is only vaguely suggested by the 200 meter temperature distribution except in the western area, around 8° N, 50° W, where a pronounced gradient appears on the new chart. There is no evidence of the existence of the Antilles Current on either the new or the old chart.

In the Mediterranean Sea there are no pronounced gradients of temperature at 200 meters. The positions of the few isotherms on the new chart are somewhat doubtful but it is evident that conditions are relatively uniform with a slight increase in temperature toward the east and south across this sea.

To conclude this discussion of the 200 meter average temperatures, it is evident that a new chart, based on ten times as many observations as were used in the Meteor Atlas, does not alter the general picture as shown by that atlas. Except for a few significant detailed changes the new chart only confirms the average conditions as depicted by Wüst and Defant. The implication that the 200 meter temperature chart may serve as a useful tool in the study of the major ocean currents appears to be sound and, as we have seen, it does raise some interesting and provocative questions.

Range of Observed Temperatures

Chart number 6 shows the range of observed temperatures at a depth of 200 meters in the North Atlantic. These ranges are the maximum minus the minimum observed temperature within each one degree field regardless of the date of the observation. The total range was calculated in order to show where, in the North Atlantic, pronounced horizontal gradients of the temperature at 200 meters have been observed. The assumption is made here that, except for slight seasonal changes, the temperature at 200 meters does not gradually change with time and any marked differences in observed temperatures in a unit field indicate that a pronounced horizontal gradient has existed in the area. Since no averaging process is involved in the production of this chart it should prove useful as a supplement to the average temperature chart in studying the major ocean current of the North Atlantic.

In general the maximum range of temperature occurs in those regions where the average temperature chart shows the maximum horizontal gradients. The highest values occur in the area shown in black off the northeast coast of North America where ranges of from 10° to as high as 16° have been observed. Over most of the ocean the range is less than 2°. Calculations of the seasonal varia-

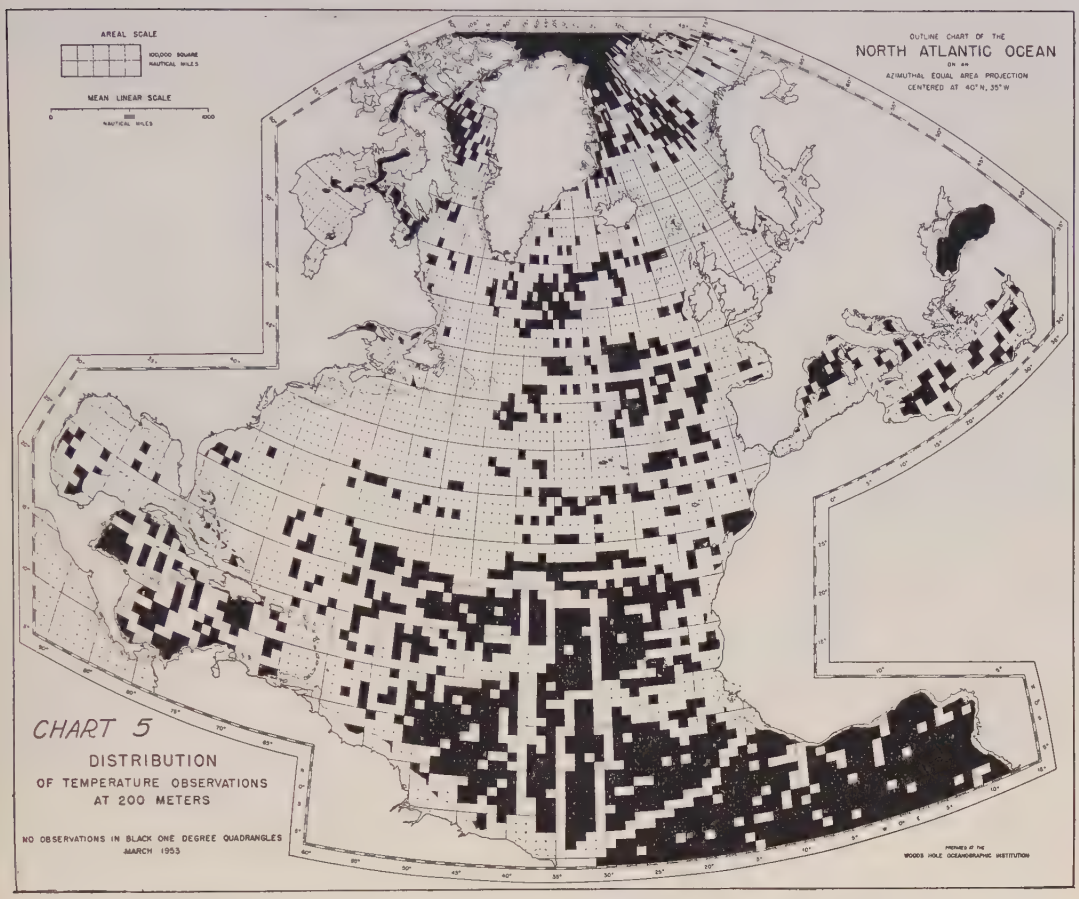

Chart 5. Distribution of Temperature Observations.

tions in the 200 meter temperature, in a few areas where observations are available for all months of the year, indicate that this variation is between 1° and 1.6°. We may assume then that changes in temperature, that we associate with currents, occur in all the areas where the range is greater than 2°. These areas are shaded or black on chart number 6.

The most interesting feature on the range chart is the four prongs of $> 2°$ ranges extending eastward from the Grand Banks area and the fact that the northernmost prong does not extend to the Norwegian Sea. In the area southeast of the Faeroe-Shetland Channel (54° to 61° N. Lat., 9° to 20° W. Long.) there are 402 observations giving range values in 66 of the 77 one degree fields. The seven months from May through November are represented. If a major ocean current exists in this area it is indeed surprising that this number of observations could have been made without once showing a temperature gradient of more than 2° in a unit area.

Unlike the average temperature chart the range chart does indicate the existence of current in the Antilles region. Unfortunately there are too few observations in the eastern equatorial area, in the Caribbean and in the western Norwegian Sea to determine the ranges. It may be argued that the calculation of the total, or maximum, observed range in temperature is too crude a method of study. The range is calculated from only two observations in each unit field and these observations, the maximum and minimum observed temperatures, are the ones most likely to be in error. Of course, every effort has been made to

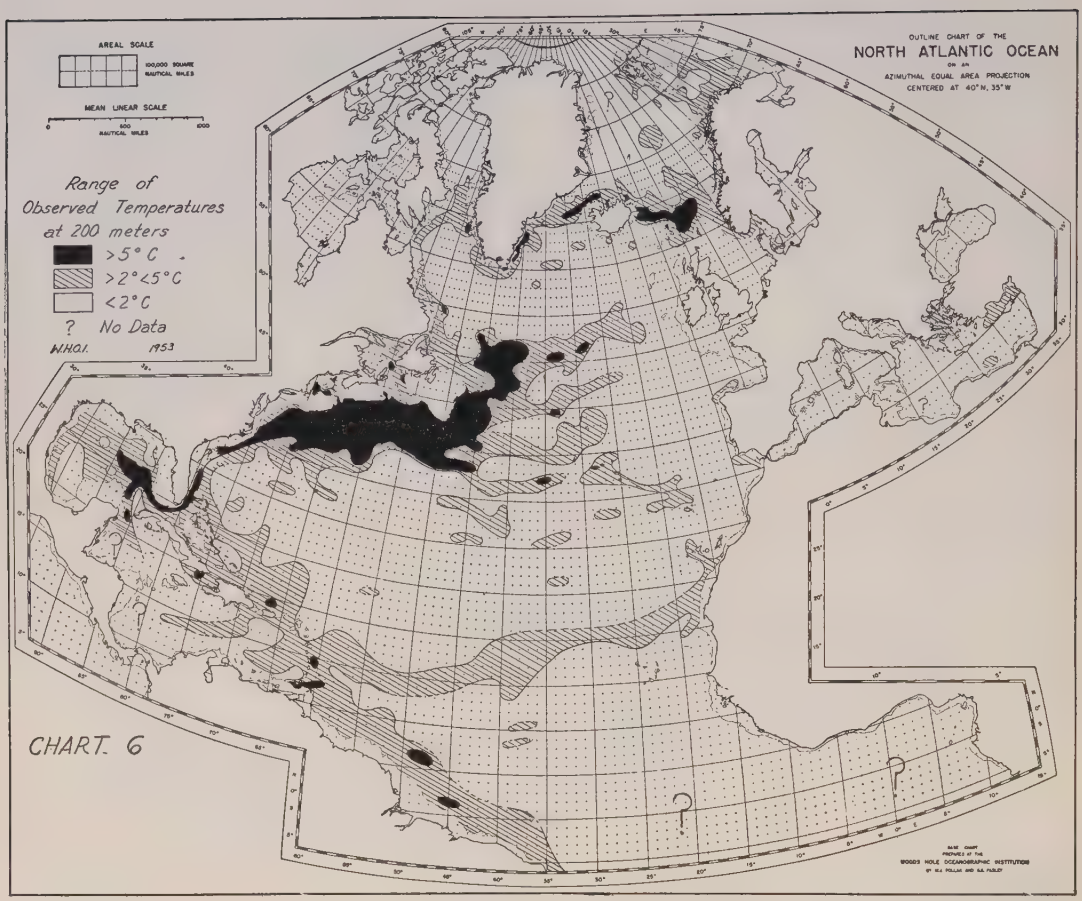

Chart 6. Range of Observed Temperatures.

remove from the files any data that could be shown to be in error but, in many cases, no such check was possible. The scarcity of observations in many areas is a more serious drawback than the inclusion of occasional errors. Nevertheless, the range chart produced here achieves a continuity that appears to be reasonable in the light of what is known about the North Atlantic circulation.

Standard Deviation from the Mean Temperature

The standard deviation from the mean temperature could be calculated for each unit area in order to show the probable variation (and to minimize the effect of errors in the extreme values). These calculations were not carried out for the North Atlantic chiefly because of the amount of labor involved but also because the number of observations over large areas did not warrant this approach. The standard deviation was calculated for two areas in the Gulf Stream region in order to compare the results with the average temperature and the range of temperature.

The first area contains the one degree fields that fall on a line between Bermuda and the continental shelf off Long Island. Figure 2 A shows the latitude and longitude of each degree field, the number of observations, the number of months, the average temperatures, the ranges and the standard deviation. The average temperature curve shows that the maximum gradient (the Gulf Stream) lies between the unit fields whose centers are at 37° 30′ and 38° 30′ north latitude; the standard deviation is highest in the unit field

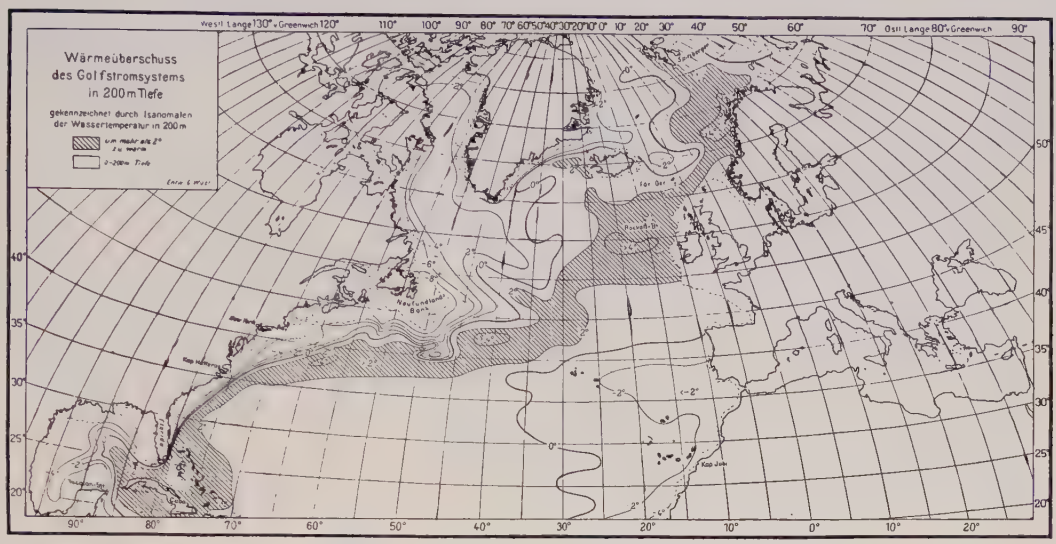

Chart 7. Temperature Anomalies (after Wüst)

centered at 37° 30′ N and the high ranges are spread over three unit fields from 36° to 39° north latitude. We can interpret the standard deviation curve as showing that there is one major current in the area and that its mean position is at about 37° 30′ N. The range curve can be interpreted as showing that the major current in this area varies in position between 36° and 39° north latitude.

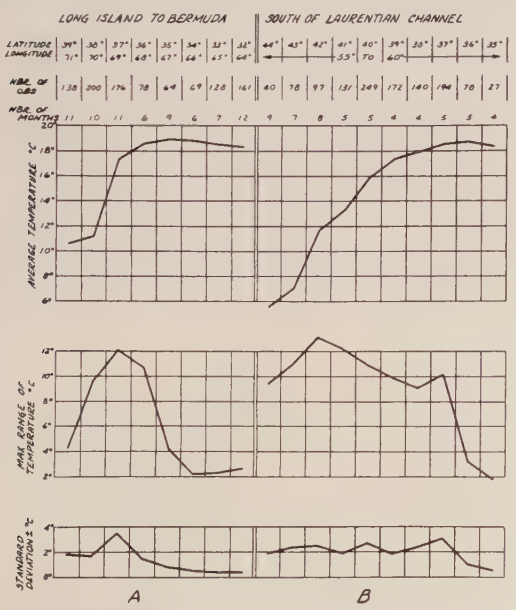

Fig. 2. 200 meter profiles across the Gulf Stream region.

In the second example shown in Figure 2 B the unit fields were enlarged to include five degrees of longitude. The area extends from the continental shelf south to 35° N crossing the Gulf Stream between 55° and 60° west longitude. The average temperature curve shows the maximum gradient between 40° and 44° N. The standard deviation is highest at 37° 30′ N with secondary maxima at 40° 30′ N and 42° 30′ N. The high ranges are spread over eight unit fields from 37° to 45° N. The average temperature curve indicates that the Gulf Stream has become wider in this zone, with perhaps two branches both north of 40° north latitude. The range and the standard deviation curves both show high values for all the area north of 37° north latitude. The standard deviation curve may be interpreted as showing three zones of maximum gradients.

Temperature Anomalies

In order to show the continuity of the Gulf Stream and the Norwegian Current, Wüst (1937) calculated the zonal mean temperatures at a depth of 200 meters for each $2\frac{1}{2}°$ of latitude from 20° to 75° north latitude in the North Atlantic. From these mean temperatures he calculated the anomalies. He considered that the areas showing a positive anomaly of greater than 2° defined the position

of the Gulf Stream System. The chart that Wüst published is reproduced here as Chart 7.

On the bases of the 40,000 observations now available the zonal mean temperature for each one degree of latitude was calculated. These values are plotted in Figure 3, the values obtained by Wüst are shown on the diagram by × marks and it can be seen that there is a surprising agreement in the two sets of zonal averages.

The temperature anomalies as calculated from the zonal averages (for every 2° temperature difference) are shown on Chart 8. Here it is apparent that the new chart differs from Wüst's in several respects and this in spite of the fact that the zonal averages used were virtually the same. In the Gulf Stream area south of 40° north latitude the changes appearing on the new chart may be attributed to the effects of averaging. This was discussed on page 49 where it was pointed out that when averaging many observations in an area of a shifting current the zone of maximum temperature is displaced to the right — facing downstream — and the maximum temperature values are decreased. This may account for the break in the shaded zone (> 2° positive anomalies) off Florida and the very nearly broken segment south of the Grand Banks. To the east of the Grand Banks the shaded zone is much more extensive on the new chart. This is due to the fact that at the time when Wüst made his chart there were very few observations in the region between 35° and 45° west longitude and 40° and 50° north latitude and the new data show that warm currents exist in the northern portion of this area.

In connection with the discussion of the continuity of the Gulf Stream System in the northeastern Atlantic, the difference between the two anomaly charts in the area southeast of Iceland is of particular interest. Wüst's chart shows a pronounced flow of warm water into the Norwegian Sea, through the Faeroe-Shetland Channel, with only a suggestion of a branch of warm water pointed toward the west of Iceland. The new chart reverses this picture, most of the warm water is concentrated to the south and west of Iceland with only a suggestion of flow into the Norwegian Sea along the European continental shelf. This difference in the two

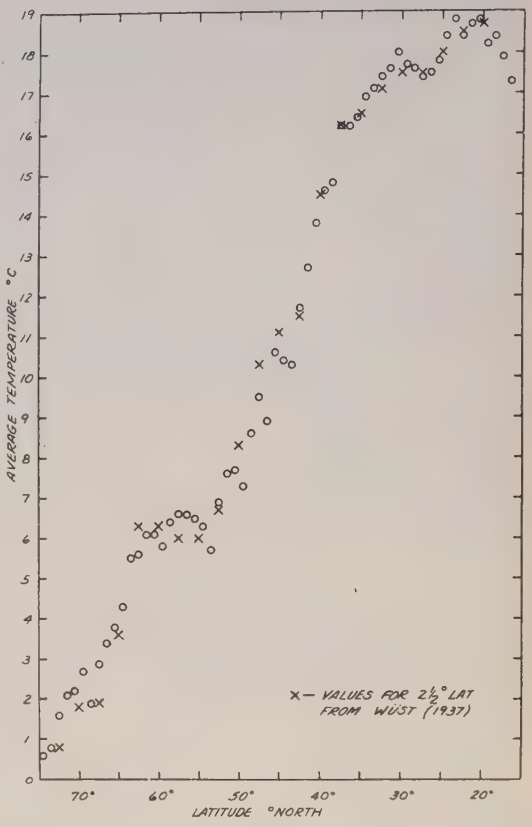

Fig. 3. Average temperatures at a depth of 200 meters for each degree of latitude for the North Atlantic Ocean.

charts may be interpreted in various ways, as in fact the entire subject of temperature anomalies may be, but taken together with the evidence of the average temperature chart and the range chart it does suggest that the high positive anomalies in the eastern Norwegian Sea are not entirely the result of a flow through the Faeroe-Shetland Channel. It is interesting to speculate on what these anomalies would be if the Norwegian Sea was entirely disconnected from the Atlantic.

The 200 Meter Salinity Charts

Although the new salinity chart (Chart 4) is based on far fewer observations than the new temperature chart the same trend of differences from the Meteor Atlas Chart (Chart 3) is evident. Virtually all the statements made concerning the new average temperature chart can be applied to the new salinity chart.

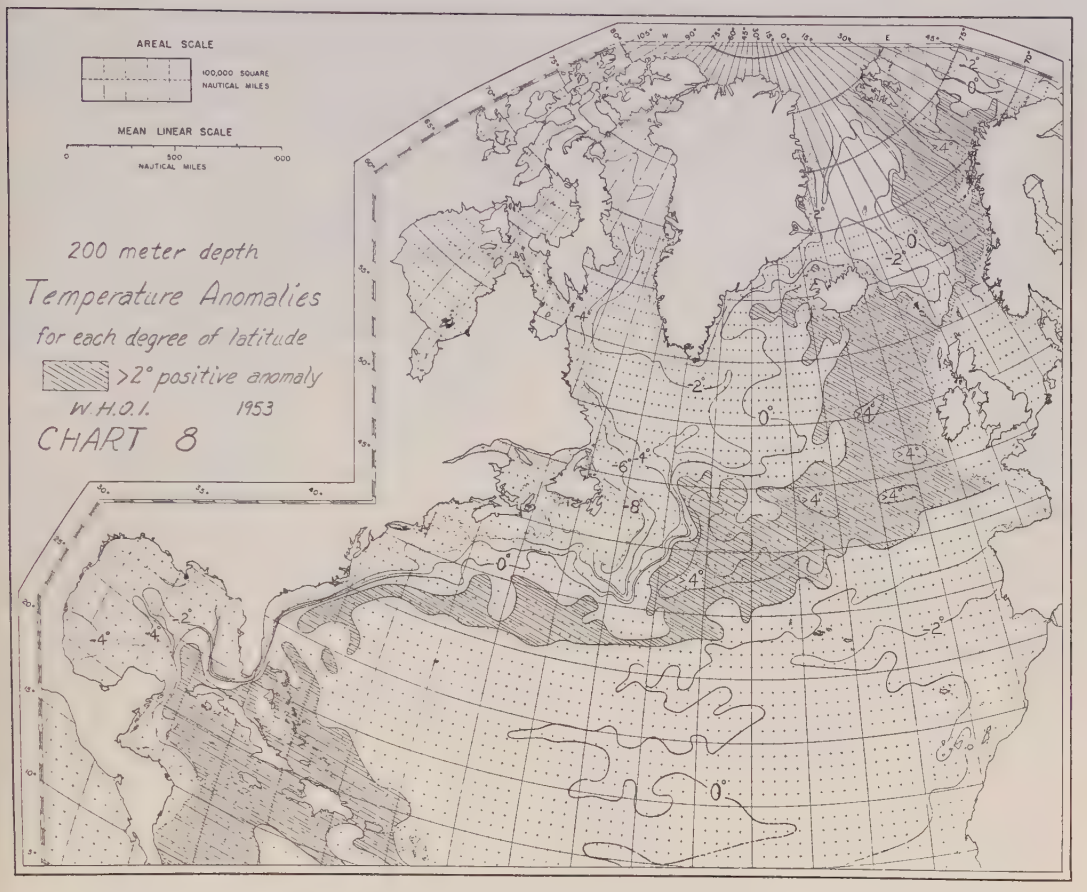

Chart 8. Temperature Anomalies.

However, no attempt has been made here to correlate the new temperature and salinity charts; each chart was drawn independently even though there were many areas where no salinity data were available and the placement of the isotherms. may have been used to determine the position of the isohalines.

Conclusions

It is quite apparent from the foregoing that, far from being obsolete, the charts in the Meteor Atlas that deal with conditions at a depth of 200 meters in the North Atlantic are still to be considered as accurate representations of the mean state. This atlas shows, as we might expect, a certain continuity of conditions with increasing depth and, therefore, we may assume that all the charts in this atlas are equally reliable. The major drawback of the Meteor Atlas is that it does not cover the Norwegian Sea, the Gulf of Mexico, the Mediterranean Sea and Baffin Bay.

The new set of charts presented with this paper show that, although much can be learned from studying the average conditions as depicted in the Meteor Atlas, if we wish to study the major ocean current systems the average picture is somewhat misleading. The value of charts showing the mean state can be greatly increased if they are supplemented by charts showing the range of conditions and the standard deviations from the mean. However, it is obvious that it will be many years before enough observations are obtained to do this for any depths greater than 200 meters. Even at this depth the distribution of observations over the North Atlantic

is too uneven to make such charts completely reliable.

It may seem a paradox but the chief value of the new 200 meter average temperature chart, aside from the fact that it covers a more extensive area in the North Atlantic than the Meteor Atlas, is the fact that it does not represent a true average picture. Because of the uneven distribution of data and the non-averaging system of drawing the isotherms this chart focuses the attention on many details that would not exist on a chart more truly representative of the average. This is especially evident in the major ocean current areas.

Several interesting questions are posed if the new 200 meter temperature chart, supplemented by the range chart, is used as a current chart. Why does the Gulf Stream break down into more than one current long before it reaches the longitude of the Grand Banks and why does the system break down so much more rapidly into at least four currents after it has passed this longitude? Why is there no pronounced current extending from this system in mid-Atlantic to the Norwegian Sea and is the circulation in that sea largely self-contained? Why is the Antilles Current only vaguely suggested on the range chart and not at all on the average temperature chart? How far does the current that passes through the Yucatan Channel penetrate into the Gulf of Mexico before turning about to flow out through the Straits of Florida? Why is there so little evidence of an anticyclonic current system over the main body of the North Atlantic?

No attempt is made here to answer these questions. It has been assumed that a cross-current temperature gradient at a depth of 200 meters exists wherever there is a major ocean current. If this assumption is wrong then the above questions are meaningless. But if it is a justified assumption then these questions are valid and should be of considerable interest.

REFERENCES

Wüst, Georg, and Albert Defant, 1936: Atlas zur: Schichtung und Zirkulation des Atlantischen Ozeans. Deutsche Atlantische Expedition Meteor 1925 – 1927, Wiss. Erg. Bd. VI, Berlin.

Wüst, Georg, 1937: Recent Conceptions of the Nature of the Gulf Stream System and the Nomenclature of its Parts. *Der Seewart*, Heft 10, pp. 359 – 367, Hamburg.

Fuglister, F. C., 1951: Multiple Currents in the Gulf Stream System. *Tellus*, **3**, 4, pp. 230 – 233, Stockholm.

A Practical Method for the Prediction of the Surface Currents of the Ocean[1, 2]

By LOUIS A. POST, Oceanographer U.S. Navy Hydrographic Office

(Manuscript received June 24, 1953)

Abstract

A method is advanced for the prediction of surface currents based on the stability of computed dynamic currents. Wherever the latter are known and simultaneously the measured (geomagnetic) current and local wind direction, speed, and duration are known, the vector difference between the measured and the computed currents is assumed to be the portion of the current induced by the wind.

The hypothesis is demonstrated empirically by a correlation of the above factors based on data obtained during a recent oceanographic survey. The predicted surface current vector is shown to be the resultant between a forecast wind-current and a permanent dynamic current.

A new type of survey is proposed to make feasible the complete correlation of these factors.

Introduction

The principal obstacle to the investigation and interpretation of many of the observed properties of the ocean is ignorance of the limits of a "normal" condition as a frame of reference to which the observed properties are related.

Techniques for establishing the normal condition of ocean currents have so far been limited to methods for obtaining the average of conditions from a large number of observations. This average is by no means adequate to define a normal or fixed condition upon which we may superimpose predictable variables, for it already includes the average of all possible variables.

A frame of reference: It is important to consider to what extent an adequately fixed condition, unaffected by such surface variables as wind, is afforded by the dynamic topography of the sea surface. It is generally conceded by oceanographers that the oceanic circulation derived from dynamic sections results purely from the distribution of mass within the ocean. Disturbances in the equilibrium of water masses give rise to "density" currents varying in direction and velocity, and it would appear that the currents so produced can reflect only forces of sufficient permanence to create and maintain the disturbances. Such forces apparently do not include the transitory local, or even seasonal variables of wind although these do alter the actual, observed current velocity and direction.

[1] The writer wishes to thank Dr C. O'D. Iselin for reading this paper and suggesting several important improvements.

The opinions expressed in this paper are solely those of the author and do not necessarily reflect the opinions of the Hydrographic Office or U.S. Navy.

[2] 1. Normal: basic, as "a basic condition", exclusive of superimposed variables — not an average.

2. Dynamic current: The component of ocean currents derived from the dynamic topography and resulting from the distribution of mass within the ocean; also "permanent current".

3. Stability: state of being unaffected by external influences, as the stability of dynamic current with respect to wind.

Thus, Stommel (1951), writes that "although fluctuations of the global wind system of periods of a week or longer can induce measurable changes in both the velocity and surface levels of the ocean, an adjustment of the density distribution over the whole ocean cannot occur for periods of less than 30 years." And further, "seasonal fluctuations of oceanic circulation cannot be discovered by the usual methods of dynamic computation."

The permanent effect of wind upon dynamic topography would thus appear to be cumulative for long periods over the ocean as a whole; locally, wind would not seem to be detectable in the dynamic topography.[1] Although there are certain known conditions under which great fluctuations in dynamic topography occur, Parr (1938), these do not appear to depend upon the wind, locally or seasonally.

The present study makes an attempt to answer two questions: (1) What evidence exists that ocean currents, dynamically computed, provide a nearly fixed frame of reference, a constant integrant of surface flow though not always identical with it, a sort of "ecliptic" of oceanography upon which we may superimpose the other variables? A question which naturally follows is (2) Can these variables be accurately predicted? The writer suggests that such changes as the result of fluctuations in the wind system, superimposed upon relatively established (dynamic) surface currents of the oceans, are both measurable and predictable.

To demonstrate this concept, the following method is advanced to determine (a) the stability of dynamic currents with relation to observed (electromagnetically measured) and wind-driven currents, and (b) the amounts of wind-driven currents induced by different velocities of wind.

The Method

Stability of dynamic currents with relation to observed and wind-driven currents: This method may be used wherever three factors have been determined simultaneously for a series of stations; (1) the dynamic or density current speed and direction, (2) the observed (geomagnetic) current speed and direction, and (3) the wind speed, direction and duration.

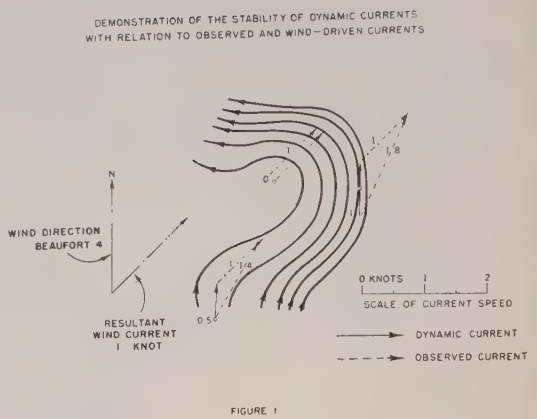

FIGURE 1

Fig. 1.

Contours of dynamic height anomalies are drawn for the sea surface over a practically level isobaric surface. Dynamic current velocities and directions may be thus determined for a number of adjacent oceanographic stations. Vectors are drawn as in figure 1 (hypothetical). Similarly, vectors are drawn to represent currents measured by the Geomagnetic Electrokinetograph, von Arx (1950), just before or after the stations. The third factor is the wind speed, direction and duration at each station.

When the dynamic currents are subtracted vectorially from simultaneous observed currents, the resultant wind-driven currents should be to the right of the wind (in the Northern Hemisphere), Ekman (1928) and should be proportional to the observed wind if indeed dynamic currents, as defined above, remain unaffected by local wind.

It can be seen from figure 1 that the observed current includes the same component of wind-current (1 knot) at every station at which the same wind speed and direction prevail, even where the dynamic current indicated is nil. At the same time the dynamic current component remains unaffected by the wind.

Example

The hypothetical relationship shown in figure (1) cannot at present be fully utilized to determine wind-currents for all the forces of wind on the basis of observed data. There is a scarcity of synoptic material necessary to

[1] The fact that icebergs more often follow the computed currents than the winds has been frequently noted.

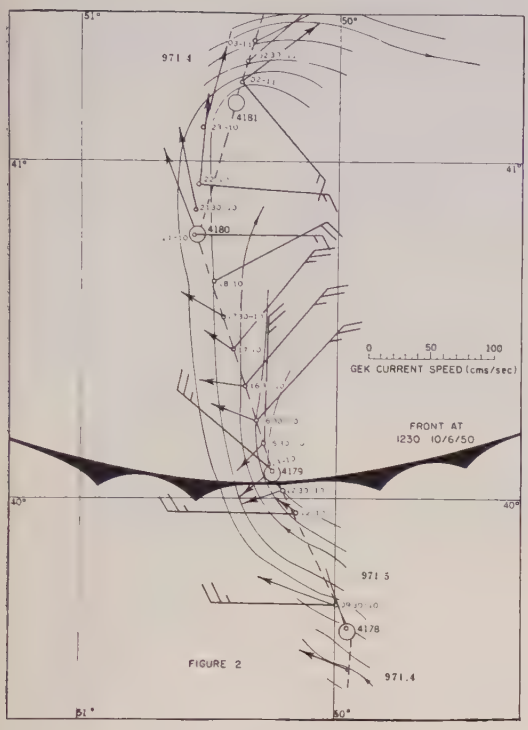

Fig. 2.

prepare a complete correlation of the three factors, dynamic current; observed current; and wind direction, speed and duration.

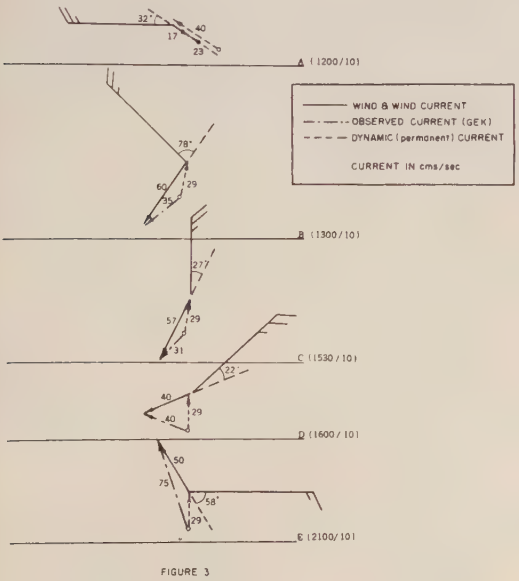

Fig. 3.

The dynamic current at 1200/10 (40 cms/sec.) is an average value derived from the difference in dynamic height between stations 4178 and 4179. The value from 1300/10 to 2100/10 (29 cms/sec.) is derived from the dynamic height difference between stations 4179 and 4180. This value was necessarily used at all points between stations, since a somewhat different spacing of lines than in figure 2 would have been equally valid. (The topography is drawn in figure 2 as it appears in figure 18, Bulletin 36, International Ice Patrol.)

Figure 2 is not an ideal example from the standpoint of the location and spacing of the stations, but it was the best one available to the writer having the necessary simultaneous observations and during which a significant change transpired in the local wind.

However, a sufficient quantity of simultaneous wind and surface current measurements, together with dynamic topography, is now available to demonstrate the hypothesis empirically.

Figure (2) represents the dynamic topography from oceanographic data obtained by the U.S.C.G.C. EVERGREN on June 9—10, 1950. Simultaneous surface current vectors, measured between the stations at half-hourly intervals with the GEK[1], VON ARX, (1950) have been superimposed on the topography.

The occurrence of deviations between currents measured by the GEK and the dynamic currents is clearly coincident with the location and time of change in wind force and direction following frontal passage as indicated, while the dynamic currents appear to have remained constant.[2] As assumed previously, the amount of this deviation (the wind current vector) should be proportional in both direction and speed to that of the observed wind.

In figure (3), showing the effect of wind change during the frontal passage in figure (2), the wind current vectors, though only roughly proportional, demonstrate the rapid responsiveness in the surface current to short period changes in the wind.

Evidence of the Ekman Spiral appears in the deflection of the wind current to the

[1] GEK data used in figure 2 have been furnished by W. S. von Arx, Woods Hole Oceanographic Institution. Wind data and the dynamic topography were supplied by Floyd Soule, Woods Hole Oceanographic Institution.

[2] At least the net transport of the relative surface current indicated between stations 4179 and 4180 is in a northerly to easterly direction while the currents measured by the GEK are in a southwesterly to northwesterly direction.

right of the wind. It is probable that some inconsistency in the amount of this deflection results from inexactness in the permanent currents prepared from the dearth of dynamic data available for synopsis. Detailed information as to the depth of change in the observed current is also lacking.

These inaccuracies can be overcome only by the conduct of controlled oceanographic surveys, involving at least three, closely spaced survey vessels, operating simultaneously preferably at anchor station in areas of generally weak permanent currents, for sufficient time to experience and record the effect on the current of any force and duration of wind. Continuous oceanographic stations will establish closely the permanent current topography between the vessels and will also readily expose the effects of internal wave or other related phenomena. Simultaneous observed currents measured with the GEK together with area weather patterns and accurate wind observations will complete the necessary data.

The present study is offered in support of this proposal. Despite discrepancies in existing data that are too large for statistical analysis, the present study at least qualitatively supports the method and illustrates the responsiveness of the observational techniques employed.

Methods in present use for the prediction of wind-current from observed wind speed have been based on averages of drift observations where permanent currents were supposed to have been weak or non-existent, and where the sole drift experienced was attributed to wind.

An accurate prediction table for wind current will become possible when sufficient numbers of wind-current vectors for each force interval of wind have been determined as in figures (1) and (2) and tabulated. Current vectors, so determined for an observed or predicted wind, may be directly superimposed on specially prepared surface dynamic current charts at any point.

The resultant will be the predicted current at that point and should prove invaluable to the solution of problems of precise navigation, including those of rescue operations for which the area of search will be measurable reduced.

The proposed type of survey will provide a truly synoptic basis for the analysis of wind current versus wind force and duration. It will provide the basis for prediction tables for ocean currents, subsurface as well as surface, and will utilize empirical knowledge beyond the reach of any existing data, which are too widely spread in space and time to determine the interrelationship of wind and currents.

Conclusion:

1. Averages of ocean current data are considered to be unsuitable as a basis for the prediction of currents, because they include, together with the permanent current, all of the variables on which prediction depends.

2. A method is advanced for testing the stability of the surface dynamic topography. Where this is constant, the difference between the measured (geomagnetic) current and the dynamic current should be proportional to the local wind speed, direction and duration.

3) An empirical check on the above relationships, based on data from a recent oceanographic survey, supports the thesis that dynamic topography is unaffected by fluctuations of local wind, whereas the measured (GEK) surface current is observed to depart from the topography by amounts approximately proportional to observed short period changes in the wind.

4. A new type of survey is proposed by which the rising stage of wind-driven currents can be studied comprehensively from the simultaneous and continuous measurement of dynamic current, observed current, and wind velocity and duration.

REFERENCES

Ekman, V. Walfrid, 1928: A Survey of some theoretical Investigations on Ocean Currents. *Journal du Conseil*, **3**, 3.

Parr, Albert E., 1938: On the Validity of the dynamic topographic method for the determination of ocean current trajectories. *J. Marine Research*, **1**, 2, pp. 119—132.

Stommel, Henry, 1951: On the mutual adjustment of the velocity and pressure fields in the ocean under the influence of a fluctuating wind stress. *WHOI tech. Rept.* 51—57.

U.S. Navy Hydrograhic Office, 1944: Methods for locating survivors adrift at sea on rubber rafts. *H. O.* No. 235.

von Arx, William S., 1950: An electromagnetic method for measuring the velocities of ocean currents from a ship under way. *Papers in phys. oceanography and meteorology*, **11**, 3.

A Study of *T* Phases Recorded at the Kiruna Seismograph Station

By MARKUS BÅTH, Meteorological Institute, University of Uppsala

(Manuscript received June 15, 1953)

Abstract

Five cases of clear *T* phases from earthquakes in the Norwegian Sea recorded at Kiruna since 1951 are studied. To the author's knowledge these observations are the first of this kind in Europe and also the first so far to the north – on the borders of the Arctic Ocean. It is verified that *T* propagates as a sound wave through the water. Different phases, constituting *T*, have been identified, travelling along the land path as P_g, S_g, and a third wave with a land velocity of 2.7 km/sec, probably an *S* wave in more superficial layers than granite. The conditions for sound-channel transmission in the ocean are studied. The efficient use which can be made of the *T* phase in epicentre locations is illustrated with a particular case. The period of *T* is remarkably constant and equal to 0.5 sec. By amplitude calculations it is shown among other things that different submarine earthquakes are not equally efficient in producing a *T* phase; reasons for this behaviour are discussed. A theoretical explanation is given for the fact that at the same time as the amplitude of *T* may be larger than that of *P* at Kiruna, there is no *T*, but a clear *P* recorded at Uppsala.

1. Introduction

T phases (from submarine earthquakes) were first reported as observed at a few seismological stations in North America, namely Weston, Fordham, Ottawa, and Harvard for Dominican Republic and North Atlantic shocks and at stations on or near the Pacific coast for Japanese and Aleutian shocks (see TOLSTOY and EWING, 1950, and LEET, LINEHAN, and BERGER, 1951). Observations of *T* phases at the Honolulu seismograph station and at two SOFAR stations in the Pacific for circumpacific-belt shocks have been studied by EWING, PRESS, and WORZEL (1952). *T* phases have also been observed at Brisbane and at Bermuda. Observations at Morne des Cadets, Martinique, of Dominican Republic shocks by COULOMB and MOLARD (1949) also refer to the *T* phase. Recently WADATI and INOUYE (1953) have reported observations of *T* phases at Japanese seismograph stations for earthquakes in the Japanese waters.

The present paper is a report of a study of records of *T* phases obtained by means of a short-period vertical seismograph, type Grenet-Coulomb, at the Kiruna seismograph station. Kiruna is situated in North Sweden at 67° 50′.4 N, 20° 25′.0 E (see map Fig. 1). The station was installed in the summer of 1951 and since that time five clear cases and one doubtful of

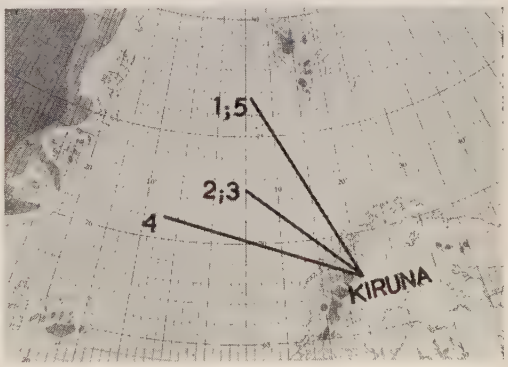

Fig. 1. Location of epicentres 1—5 (at the ends of the lines) and the paths to Kiruna.

Table 1. Observations of *T* phases.

Earth-quake No.	Date	Origin Time[1] G.M.T.	Epicentre	Distance to Kiruna km			*P* (Kiruna)	Observed arrival times of *T* (Kiruna)	Remarks
				Total path	Water path	Land path			
1	1951, Oct. 16	06.54.33* (USCGS) 06.54.30 (BCIS)	76° N, 5° E (USCGS) 77° N, 6° E (BCIS)	1,070	830	240	06.56.50	i_1 07.04.44 i_2 07.05.33	i_1 has a sharp beginning. Su face waves very well dev oped. A position of epicen between the two determin tions has been adopted.
2	1952, Feb. 10	06.10.05* (USCGS) 06.10.03 (BCIS)	72°½N, 2° E (USCGS) 73° N, 0° (BCIS)	780	530	250	06.11.52	i_1 06.16.47 i_2 06.17.07 i_3 06.17.45	Epicentre location has be redetermined to be at 72°½ 5° E.
3	1952, Apr. 28	01.15.15 (USCGS)	500 km NE of Jan Mayen	780	530	250	01.17.01	i_1 01.22.13 i_2 01.22.46	Same epicentre as in 2.
4	1952, Dec. 10	05.58.06 (USCGS)	71° N, 7° W (USCGS)	1,110	850	260	06.00.31	e_1 06.08.25 i_2 06.09.18 i_3 06.09.40	Beginning of e_1 uncerta disturbed by preceding m tion. Very well develop surface waves of long dur tion (up to 07^h).
5	1953, Apr. 24	02.09.44* (USCGS) 02.09.42 (BCIS)	76°½N, 6°E (USCGS) 77°½N, 6°½ E (BCIS)	1,070	830	240	02.12.07	e_1 02.20.08 i_2 02.20.39 i_3 02.20.45 i_4 02.21.16	Same epicentre as in 1 h been used.

[1] In case more than one value is given, a star indicates which value has been adopted.

T phases have been obtained.[1] They are all due to submarine earthquakes in the area from Jan Mayen to Spitzbergen. To the author's knowledge these observations are the first of this kind in Europe and also the first so far to the north on the earth – on the borders of the Arctic Ocean.

2. Arrival times of *T*

Typical cases of *T* phases recorded at Kiruna are shown in Fig. 2. The *T* phase begins with small amplitudes, often gradually, and the largest amplitudes are later. In all cases several phases could be distinguished within the *T* group and they have all been measured. Table 1 gives the measured arrival times and other necessary data for the earthquakes. Reference is made to the Kiruna seismic bulletins for the usual analyses. All measurements of the *T* phases were made before I had any knowledge whatsoever where to expect them; this is of essential importance, especially in the case of gradually beginning phases.

[1] Note added in proof: Another five cases of *T* phases have been recorded up to January, 1954.

The observed phases are definitely not *PcP*, *PcS*, or *ScS*, as the expected arrival times of these phases deviate by far too much from the observed times. Nor are the observed phases due to aftershocks or other earthquakes as in that case the very striking regularities in the arrival times and computed velocities (see below) would not be obtained.

It has been demonstrated conclusively by Ewing, Press, and Worzel (1952) that the *T* phase propagates as sound through the water and as body waves over the land path from the coast (or continental shelf) to the station. I therefore started with this assumption and computed the total travel times t simply from the equation

$$t = \frac{a_1}{v_1} + \frac{a_2}{v_2},$$

where a = the length of path, v = the corresponding velocity, and index 1 stands for water and 2 for land. The values of a_1 and a_2 are given in Table 1 as measured on a map (compare Fig. 1), assuming the transition to take place close to the actual coast. This seems justified as the sea is rather deep right up to the

5—305858

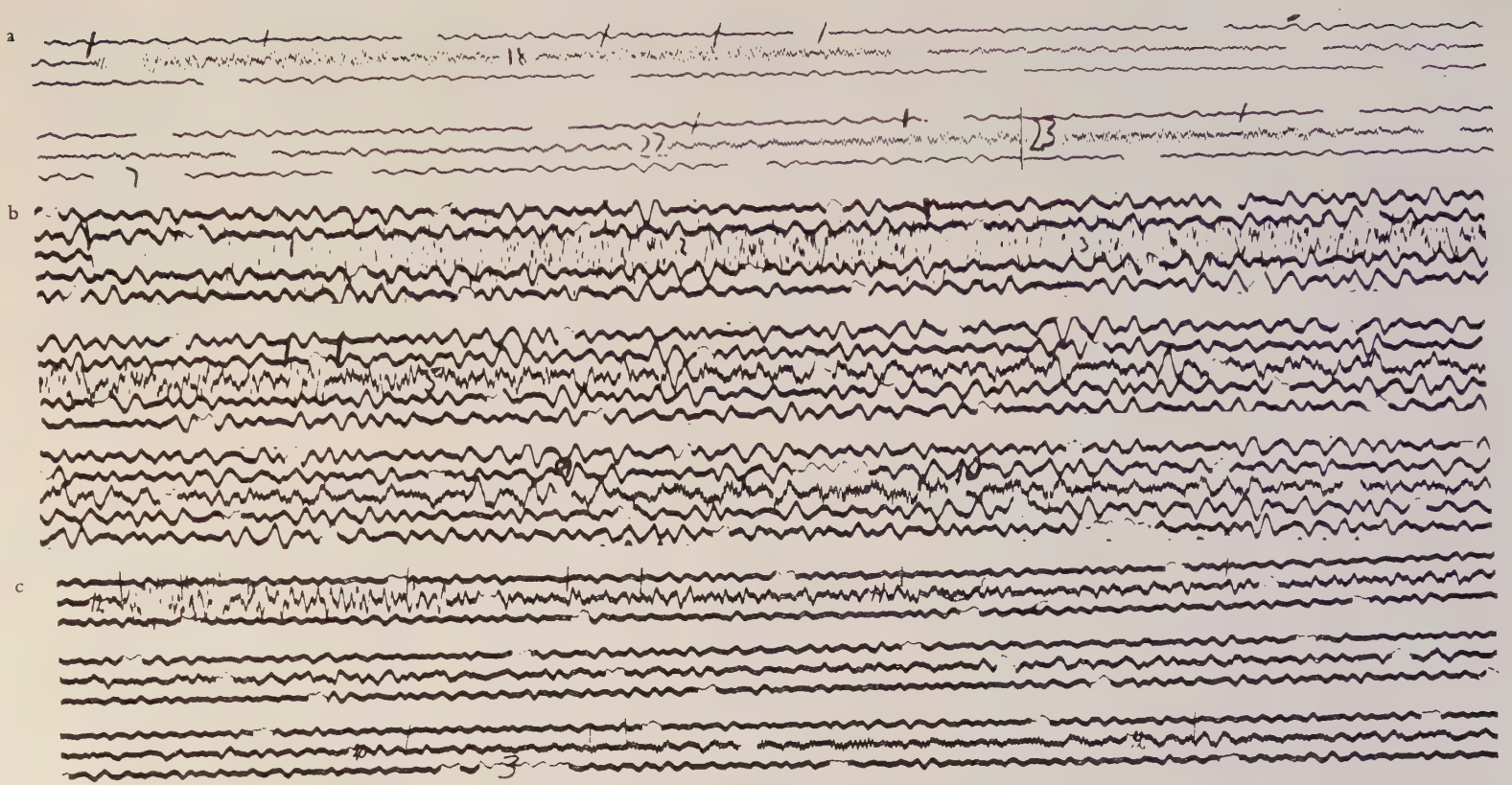

Fig. 2. Examples of records of earthquakes with *T* phases at Kiruna. In each case the record begins with the *P* phase in the uppermost figure. The *T* phases are visible on the central line of the lowest figure in each case. For details compare Table 1.

a. April 28, 1952.
b. December 10, 1952.
c. April 24, 1953.

coast and the limit of the continental shelf coincides practically with the coast for cases 2—4; for 1 and 5 the path is to a large extent along the continental shelf, which passes from the northern part of the Norwegian coast towards NW just SW of Spitzbergen. For v_1 the value 1.45 km/sec was used. In our conditions this value is the most likely (see Table 5 below). Depending on the angle of incidence of the sound wave in water on to the solid ground, it is just as likely to get S waves as P waves in the crust. Detailed energy computations of interest in this connection have been made by ERGIN (1952). Therefore a_2/v_2 was computed both with $v_2 = 5.57$ km/sec for P_g and with $v_2 = 3.36$ km/sec for S_g (see BULLEN, 1947, p. 193). The arrival times computed in this way are given in Table 2, where the phases have been denoted in the same way as in Table 1 (i_1, i_2, etc) in order to facilitate comparison. The differences between observed and calculated times $(O-C)$ are also given in Table 2.

Table 2. Comparison between observed (O) and calculated (C) arrival times of T.

Earthquake No.	Calculated arrival times of T			$O-C$ sec
1	i_1	07.04.48	(P_g)	— 4
		07.05.16	(S_g)	
2	i_1	06.16.56	(P_g)	— 9
	(i_2)	06.17.25	(S_g)	(— 18)
3	i_1	01.22.06	(P_g)	+ 7
	i_2	01.22.35	(S_g)	+ 11
4	e_1	06.08.39	(P_g)	— 14
	i_2	06.09.09	(S_g)	+ 9
5	e_1	02.19.59	(P_g)	+ 9
	i_2	02.20.27	(S_g)	+ 12

In the computation of the arrival times of T the time it takes for a P or an S wave to travel from the focus to the ocean bottom (approximately 5 and 8 sec resp.) has been neglected as such a correction is completely within the limits of error.

The agreement between observed and computed arrival times is as good as can ever be required, regarding the following uncertainties:

1. Uncertainty of observed arrival times. This may amount to several seconds, as the phases are usually not as sharp as the direct body waves.

2. Uncertainty of the position of the assumed transition point water to land.

3. Local deviations from the assumed velocities of P_g and S_g. A computation, using a value of 6.0 km/sec for the P_g velocity, however, showed that this change is of no importance in this connection.

The good agreement is even more obvious from a calculation, following up point 2 above. It has been calculated how much the assumed transition point must be displaced along the great circle arc between station and epicentre in order to give perfect agreement between observed and calculated arrival times with the assumed velocities. If t is the observed travel time, it is easily shown that the water path constitutes a fraction x of the total path a given by

$$x = \frac{t - \frac{a}{v_2}}{a\left(\frac{1}{v_1} - \frac{1}{v_2}\right)}$$

The results are given in Table 3.

Table 3. Comparison between calculated and measured water and land paths.

Earthquake No.	Phase	Calculated paths km		Measured paths km	
		Water	Land	Water	Land
1	P_g	824	246	830	240
2	P_g	515	265	530	250
3	P_g	546	234	530	250
	S_g	562	218	530	250
4	S_g	877	233	850	260
5	P_g	845	225	830	240
	S_g	813	257	830	240

It is obvious that with a maximum displacement of not more than about 30 km, the differences are completely within the limits of error. The coast is actually not very well defined as it consists of a large archipelago.

If, on the other hand, with the measured values of a_1, a_2, and t and assumed value of v_2 we calculate v_1, we obtain the velocities given in Table 4.

The agreement with Table 5 below is perfect. The agreement between the velocities of T and of sound through the ocean in our case taken together with the same agreement found

Table 4. Computation of sound velocity in sea water.

Earthquake No.	Sound velocity (km/sec) calculated from	
	P_g	S_g
1	1.46	
2	1.48	1.52
3	1.42	1.41
4	1.49	1.43
5	1.43	1.42
Mean ($n = 9$) and standard error.....	1.45 ± 0.01	

by EWING, PRESS, and WORZEL (1952) in conditions where both velocities were higher than here, is of decisive importance.

Thus, there seems to be no better explanation of the observed *T* phases than that according to which they propagate as sound waves through the water (either as a SOFAR channel wave or by multiple internal reflections) and as body waves over the land. We have found clear indications of *T* phases travelling as P_g over the land (observed in all cases 1 – 5); of *T* phases travelling as S_g over the land (observed in cases (2), 3 – 5);and of *T* phases travelling as a third wave with a velocity of 2.7 km/sec over the land (observed in cases 1(i_2), 2(i_3), [4(i_3)], 5(i_3) with land velocities 2.73, 2.66, [2.41], 2.70 km/sec resp.). The third wave may be an *S* wave in layers shallower than the granite. It will be denoted S_x in what follows. An explanation of the successive *T* phases as all being P_g but having different points of transition is excluded because that would require an inland transition point for the later phases which is not possible. A longer path than along the great circle in combination with lateral refraction may account for some of the later motion, but only in cases 2 and 3, and cannot be taken as an explanation of the later phases.

When the computed arrival times had been obtained (Table 2) they were compared with the records with the following results. In case 1 the computed S_g at 07.05.16 is confirmed by a phase, observed at 07.05.12. In case 2 the computed S_g at 06.17.25 corresponds to no marked phase at just this time, but there is an increase of the amplitudes at that time. The same is true at the computed time 01.22.35 of S_g in case 3. In case 4 a phase at 06.09.11 was on the point of being measured already in the first measurement, agreeing well with the computed S_g at 06.09.09. As the times, measured when the computed arrival times were known, cannot be attached the same weight as the originally measured times, they have been used in no calculations in this paper.

In addition to the clear cases reported in Table 1 also a somewhat doubtful *T* phase has been observed, where the possible *T* phase was disturbed by other short-period movements. This earthquake occurred on October 19, 1951, at 00.54,3 SW of Spitzbergen (about the same epicentre as 1 and 5) at an epicentral distance of 1,050 km from Kiruna (water path 810 km; land path 240 km). Kiruna recorded *P* at 00.56.38. A *T* phase of very small amplitude and short duration was observed at 01.04.22, which agrees well with the computed arrival time of 01.04.20 for $T(P_g)$.

The observations of *T* phases have particular interest in view of the recent investigations of long-range sound transmission by SOFAR channels by EWING and WORZEL (1948). Calculations of the depth of the SOFAR channel is not easy for our region, because data on water temperatures and salinities at greater depth usually seem to be limited to the summer months and because the conditions (temperatures and salinities) along the path through the water are rather variable. Every path crosses the Gulf Stream but passes also to a large extent through the drift-ice region. The vertical distribution of sound velocity has been computed, using three soundings by HELLAND-HANSEN and NANSEN (1912) in the sea west of Spitzbergen. The results are compiled in Table 5. New measurements in the Polar Sea have been given by WORTHINGTON (1953).

During winter the water temperature is probably not far from 0° C in this region with very little vertical variation. In these circumstances the minimum sound velocity is to be found in the surface layers of the ocean. With the indicated depths of the sound channel it is obvious that the sound travels right up to the steep coast before being transformed into body waves in the crust.

Table 5. Sound-channel transmission.

Date of sounding 1910	Location	Sound velocity at surface km/sec	Minimum sound velocity km/sec	Depth of SOFAR channel m	Remarks
July 18.....	78° 08′ N, 0° 35′ W	1.456	1.453	400—500	Location at the ice-edge
July 19.....	77° 41′ N, 0° 22′ W	1.463	1.452	200—500	Location at the ice-edge
July 19.....	77° 15′ N, 0° 35′ W	1.462	1.445	150	

3. Use of T in epicentre location

Due to the large difference in velocity of propagation of the direct P wave and the T wave, the difference in arrival times of P and T is very sensitive to changes in the epicentre location. Assuming only a water path for the T wave it is easily shown that within 15° from the epicentre the variation of the travel time difference between T and P with epicentral distance, $\frac{d\ (\delta t)}{d\ \Delta}$, is not less than 0.56 sec/km or 62 sec/1°. For greater epicentral distances this effect is still more pronounced due to the curvature of the travel time curve for P.

The use of T in epicentre location will be illustrated by case 2 above. In this case (but not in the others) a discrepancy was found between the epicentre location by BCIS and USCGS and the distance computed from the Kiruna record alone. BCIS gave $O = 06.10.03$ and epicentre at about 73° N, 0° long; USCGS gave $O = 06.10.05$ and epicentre at 72° 1/2 N, 2° E. These epicentres correspond to the distances 940 km = 8°.5 and 870 km = 7°.8 resp. from Kiruna. The S—P difference for Kiruna (both S and P are very well defined in the records) is 1 min. 19 s, i.e. a distance of only 780 km = 7°.0. The travel time of P to Kiruna (assuming $O = 06.10.05$) is 1 min. 47 s, also giving an epicentral distance of only 780 km = 7°.0. The epicentre given by BCIS was corrected by means of a method introduced by GUTENBERG and RICHTER (1937). There was no change of origin time, but the epicentre had to be displaced somewhat eastwards (to approx. 73° 1/4 N, 3° 1/2 E). But even this new epicentre, which gives the best fit to all station observations, does not agree with the observations at Kiruna alone; the distance to Kiruna from this point is 860 km = 7°.7. The arrival times of T computed for an epicentral distance of 860 km are 06.17.49 (P_g) and 06.18.18 (S_g), thus deviating by far too much from the observed times, whereas the agreement is good if an epicentral distance of 780 km = 7°.0 is assumed (see Table 2). This case clearly illustrates the efficient use which can be made of the T phase in epicentre locations and it also shows how records of sensitive instruments at relatively near stations may in cases give more trustworthy results than a value based on a large number of observations, many of which may be less certain. The most probable location of the epicentre is 72° 1/2 N, 5° E (determined from the distance 7°.0 to Kiruna and the distance 13°.6 to Uppsala, obtained from the travel time of P to Uppsala).

4. Periods, amplitudes, and duration of the T phase

The periods of the observed T waves are 0.5 sec in all cases with only a few periods slightly lower (0.4 sec). Only in case 5 a couple of waves had a period of 0.7 sec. The period is also remarkably constant through the whole T phase in every case. The extent to which the observed periods depend on the response of the seismograph cannot be decided as that would require several instruments with different response. The short-period vertical seismograph (Grenet-Coulomb) at Kiruna had a maximum magnification of 8,500 at 0.3 sec period in cases 1—3 and a maximum magnification of 9,615 at 0.6 sec in cases 4—5. The fact that no change occurred in observed periods of T between the two instrumental set-ups indicates that the period 0.5 sec for T is of real importance.

Table 6. Amplitudes (A) and periods (τ) of P, surface waves, and T.

Earthquake No.	P		Surface waves						$T(Z)$						Duration of observable T phase min
	Z		E		N		Z		P_g		S_g		S_x		
	A μ	τ sec	A μ	τ sec	A μ	τ sec	A μ	τ sec	A μ	τ sec	A μ	τ sec	A μ	τ sec	
1	0.6	1	3.8	15	8.3	18	7.7	19	0.05	0.5	—	—	0.07	0.5	2.7
2	0.4	0.5	9.3	19	4.8	18	13	18	0.07	0.5	0.3	0.5	0.5	0.5	4.7
3	0.1	0.7	not recorded						0.07	0.5	0.1	0.5	—	—	3.8
4	2.7	1.0	56	17	40	17	—	—	0.03	0.5	0.07	0.5	0.08	0.5	5.0
5	0.4	1.0	8.8	17	7.0	17	—	—	very small ampl.		0.03	0.5	0.04	0.5	3.2

On one hand, the amplitudes of T may in some cases be larger than that of P at Kiruna (see case 2 in Table 6 below; this has also been found in some cases for other stations by other investigators). On the other hand, we observe that in the same case the T phase has disappeared before Uppsala is reached, whereas P is clearly recorded there. These circumstances, which at first sight may seem surprising, are easily explained by a consideration of the geometry of the energy distribution. The energy of the sound wave through the water diminishes essentially as the inverse first power of the distance, whereas for the body waves the energy decreases as the inverse second power of the distance. As a first approximation we assume homogeneous media and neglect extinction. The energy of the P wave at a station at a hypocentral distance r is then

$$(E_r)_P = \frac{c' E_0}{r^2},$$

where c' is a constant, equal to 1 if E_0 is the energy for $r=1$. The corresponding energy at the epicentre (h = depth of hypocentre) is

$$(E_h)_P = \frac{c' E_0}{h^2}$$

A certain fraction α of this energy passes into the water as a sound wave. The energy of the T wave at a station (assumed coastal) is then

$$(E_r)_T = \frac{c\alpha\,(E_h)_P}{r} = \frac{c\alpha r}{h^2}(E_r)_P \qquad (1)$$

where the constant c depends on the energy transmission at the coast. From eq. (1) it is obvious that $(E_r)_T > (E_r)_P$, if $r > \frac{h^2}{c\alpha}$, which may easily happen. We then consider another station at distance R from the epicentre ($R > r$) and with a land path $= R - r$. The energy of the direct P wave is at that point

$$(E_R)_P = \frac{c' E_0}{R^2}$$

and the energy of the T wave, considering only the direct wave, is

$$(E_R)_T = \frac{c'\,(E_r)_T}{(R-r)^2} = \frac{cc'\alpha}{h^2} \frac{1}{r\left(1-\frac{r}{R}\right)^2} (E_R)_P \qquad (2)$$

From eq. (2) we find that $(E_R)_T < (E_R)_P$ at all points with epicentral distances

$$R > \frac{r}{1 - \sqrt{\frac{cc'\alpha}{r\,h^2}}}$$

From eq. (2) we further find that

$$\lim_{R \to r} \frac{(E_R)_T}{(E_R)_P} = \frac{c\alpha r}{h^2}$$

in agreement with eq. (1). These simple considerations help to explain why the amplitudes of T may be larger than those of P at Kiruna, and in the same case there is no T phase but a clear P phase recorded at Uppsala.

The amplitudes of $P(Z)$, the seismic surface waves, and the various T phases as well as the duration of the observable T motion are given in Table 6. The amplitudes of the surface waves were obtained from the records of the Galitzin instruments, the others from the Grenet-Coulomb seismograph.

We find that the amplitudes of S_x are larger than those of S_g, and these in turn are larger

than those of P_g. The largest amplitudes during the whole T phase belong to S_x. Comparing earthquakes at the same place (2 and 3; 1 and 5) we find that the amplitude of T increases with increasing earthquake magnitude; larger amplitudes of P are accompanied by T phases which are larger in approximately the same proportion. This is, however, not valid in comparison of earthquakes with different foci, even if the epicentral distance is the same. On the other hand, there is no obvious correlation between amplitudes of T and of the surface waves in 1 and 5. The duration (which is difficult to determine exactly) increases with increasing T amplitude in 2—3, but not in 1 and 5. If we compare earthquakes with different foci, we find that those NE of Jan Mayen (2, 3) are favourable for a large T phase; the ratio of the amplitudes of T to those of P as well as the surface waves are much larger than for the other earthquakes. The earthquake 4 at Jan Mayen is least effective in producing a T phase, whereas the Spitzbergen earthquakes (1, 5) are intermediate. The amplitudes of both P and the surface waves are about seven times as large in 4 as in 5 (same epicentral distance), whereas the amplitude of T is only twice as large in 4 as in 5. The same fact is clear from a comparison of 1 and 4.

The ratio of amplitude and period (A/τ) for T divided by the same ratio for P is given in Table 7.

Table 7. Ratios of A/τ for various T phases and P on the vertical component.

Earthquake No.	$\left(\frac{A}{\tau}\right)_T : \left(\frac{A}{\tau}\right)_P$		
	P_g	S_g	S_x
1	0.16	—	0.23
2	0.18	0.75	1.25
3	1.00	1.43	—
4	0.02	0.05	0.06
5	—	0.15	0.20

It does not seem excluded that a certain ratio of A/τ for T and P is characteristic for a certain epicentre location and a given station; this ratio is about 0.2 for 1 and 5; 1.3—1.4 for 2 and 3; 0.06 for 4. However, these numbers depend not only on the energy conditions but also on the lengths of the different water and land paths. From eq. (2) above we easily find that

$$\left(1-\frac{r}{R}\right)\sqrt{r}\,\frac{\left(\frac{A}{\tau}\right)_T}{\left(\frac{A}{\tau}\right)_P}=\sqrt{\frac{cc'\alpha}{h^2}}$$

where r = the lengh of the water path, R = the total path-length, h = the depth of the hypocentre, and c, c', α are constants depending on the energy transmission. The ratio of the factor $\left(1-\frac{r}{R}\right)\sqrt{r}$ for cases 2 and 3 to its value in cases 1, 4, and 5 is 0.7. Therefore comparative figures of $(A/\tau)_T : (A/\tau)_P$ for maximum amplitudes of T, when the influence of different path-lengths has been eliminated, are 0.23 for case 1, 0.88 for case 2, 1.00 for case 3, 0.06 for case 4, and 0.20 for case 5. These figures depend only on the efficiency of the different earthquakes in producing T phases. Still, cases 2 and 3 are the most efficient in producing a T phase. However, a much larger material than is now available is necessary in order to study these phenomena in detail.

By the way, the formula above indicates that the amplitude ratio of T and P is inversely proportional to focal depth. This is confirmed by observations of Leet, Linehan, and Berger (1951, p. 136, fig. 4, showing ratios of amplitudes of T and S plotted against focal depth or actually against pP—P).

There are several reasons for obtaining different amplitudes of T phases even from earthquakes of the same magnitude and at the same epicentral distance. The reasons may be summarized as follows:

1. The conditions for the energy transmission to the water at the epicentre (flat or sloping bottom).

2. The ocean depth at the epicentre in relation to the depth of the sound channel. For 1 and 5 the ocean depth at the epicentre is about 2,600 m, for 2 and 3 about 2,500 m, and for 4 about 1,500 m.

3. The conditions along the water path and the incidence on the shelf or coast. Part of the path for 1 and 5 is almost tangential to the continental slope, causing partial loss of energy due to refractions. The incidence upon the coast itself is practically normal in all cases. Especially for 2 and 3 the incidence is also normal to the continental slope. As the con-

Table 8. Earthquakes in the Norwegian Sea and the Atlantic which have given no *T* phases at Kiruna.

Date	Origin time G.M.T.	Epicentre	Distance to Kiruna km	*P*(*Z*)		Surface waves					
						E		*N*		*Z*	
				A μ	τ sec	*A* μ	τ sec	*A* μ	τ sec	*A* μ	τ sec
1951, Dec. 4	08.50.50	54° ½ N, 36° W	3,220	0.1	1.0	not recorded					
1952, Feb. 21	16.06.05	NE of Greenland	—	0.1	0.7	not recorded					
1952, Mar. 8	11.33.05	70° ½ N, 15° W	1,400	—	—	4.9	17	2.3	15	5.2	16
1952, Mar. 8	11.36.57	70° ½ N, 15° W	1,400	0.05	0.5	not recorded					
1952, Mar. 9	05.44.29	70° ½ N, 15° W	1,400	—	—	6.8	13	4.6	15	—	—
1952, Mar. 12	12.13.10	64° N, 22° W	1,950	0.1	1.0	3.1	15	2.2	13	2.8	15
1952, May 16	14.32.3	63° ½ N, 22° ½ W	1,980	—	—	1.7	14	0.9	11	1.3	14

tinental edge is here concave towards the sea we may expect convergence on the land side, which may in part explain the large *T* amplitudes observed in these two cases.

No correlation between the occurrence of *T* phases and tsunami has so far been definitely proved (Ewing, Tolstoy, and Press, 1950; Leet, 1951; Wadati and Inouye, 1953). If this is proved or disproved it may give further information on the mechanism for production of *T* phases, as the mechanism producing a tsunami is known.

The station at Scoresby-Sund would have a favourable location for recording *T* phases from earthquakes in the Norwegian Sea, having in general an unbroken water path. The records of the short-period vertical seismograph (Grenet-Coulomb) were investigated for the cases available (1—4), but I found no trace of a *T* phase. This is probably due to low magnification of the instrument. The reason is most probably the same why Reykjavik has recorded no *T* phase in the cases 1—5; the Reykjavik Sprengnether records were examined. An examination of the Uppsala records of a short-period vertical Grenet-Coulomb instrument for the cases 2—5 (the only available for comparison) also showed that no trace of a *T* phase had been recorded. The reason cannot here be low sensitivity, as this is practically the same as at Kiruna, but the reason is instead the much longer land paths. Table 8 gives a list of earthquakes in the Norwegian Sea which have been recorded at Kiruna but without *T* phase, probably due to low magnitudes and to large epicentral distances and possibly to other unfavourable conditions for production of a *T* phase.

No earthquakes in other parts of the Atlantic Ocean have so far given *T* phases at Kiruna. Not even the strong earthquake on March 19, 1953, in the Antilles (14° N, 61° W, depth = 150—200 km, magnitude = 7¾, distance 74° to Kiruna) gave a *T* phase at Kiruna, although almost the entire path was oceanic. The path had to cross the Mid-Atlantic Ridge under a small angle and this may possibly prevent the transmission.

REFERENCES

Bullen, K. E., 1947: *An Introduction to the Theory of Seismology*. Cambridge, 276 pp.

Coulomb, J., et P. Molard, 1949: Ondes séismiques au fond de la Mer des Antilles. *Ann de Géophys.*, **5**, pp. 212 – 214.

Ergin, K., 1952: Energy Ratio of the Seismic Waves Reflected and Refracted at a Rock-Water Boundary. *Bull. Seism. Soc. Am.*, **42**, 4, pp. 349 – 372.

Ewing, M., and J. L. Worzel, 1948: Long-Range Sound Transmission. *Geol. Soc. Am. Mem.*, **27**, pp. 1 – 35.

Ewing, M., I. Tolstoy, and F. Press, 1950: Proposed Use of the *T* Phase in Tsunami Warning Systems. *Bull. Seism. Soc. Am.*, **40**, 1, pp. 53 – 58.

Ewing, M., F. Press, and J. L. Worzel, 1952: Further Study of the *T* Phase. *Bull. Seism. Soc. Am.*, **42**, 1, pp. 37 – 51.

Gutenberg, B., and C. F. Richter, 1937: Materials for the Study of Deep-Focus Earthquakes (Second Paper). *Bull. Seism. Soc. Am.*, **27**, 3, pp. 157 – 183.

Helland-Hansen, B., and F. Nansen, 1912: *The Sea West of Spitsbergen. The Oceanographic Observations of the Isachsen Spitsbergen Expedition in 1910.* Christiania (Oslo), 89 pp.

Leet, L. D., D. Linehan, S. J., and Ph. R. Berger, 1951: Investigation of the *T* Phase. *Bull. Seism. Soc. Am.*, **41**, 2, pp. 123 – 141.

Leet, L. D., 1951: Discussion of "Proposed Use of the *T* Phase in Tsunami Warning Systems". *Bull. Seism. Soc. Am.*, **41**, 2, pp. 165 – 167.

Tolstoy, J., and M. Ewing, 1950: The *T* Phase of Shallow-Focus Earthquakes. *Bull. Seism. Soc. Am.*, **40**, 1, pp. 25 – 51.

Wadati, K., and W. Inouye, 1953: On the *T* Phase of Seismic Waves Observed in Japan. *Proc. Japan Acad.*, **29**, 2, pp. 47 – 54.

Worthington, L. V., 1953: Oceanographic Results of Project Skijump I and Skijump II in the Polar Sea 1951—1952. *Trans. Am. Geophys. Un.*, **34**, 4, pp. 543—551.

On the Interpretation of the Diurnal Variation of Cosmic Rays

By E. Å. BRUNBERG and A. DATTNER. The Royal Institute of Technology, Stockholm

(Manuscript received Dec. 19, 1953)

Abstract

The recorded data of diurnal variation of the cosmic ray intensity are analysed. By using the known deflection of the cosmic ray particles in the geomagnetic field (BRUNBERG and DATTNER 1953) and under an assumption of an anisotropy in the primary cosmic radiation, it is shown that the momentum of the primary radiation and the direction of the anisotropy can be determined.

The anisotropy is explained as an effect due to the distribution of cosmic ray particles rotating with the solar magnetic field as suggested by H. Alfvén.

The diurnal variation is ascribed to the earth's rotation in the anisotropic distribution of cosmic ray particles. The theoretical amplitude of this variation is calculated.

Measurements of the intensity of cosmic radiation have demonstrated that there is a solar time diurnal variation with an amplitude of about 0.2 % ("Progress of Cosmic Ray Physics" 1952). Whether a siderial variation exists or not is still an open question. In any case the siderial variation is much smaller than the solar time variation, probably less than one tenth. The diurnal variation is in part an atmospheric effect. The cosmic radiation is absorbed during its passage through the atmosphere and changes in barometric pressure and temperature affect the intensity of cosmic radiation. As the meteorological elements show a diurnal variation the result will be a diurnal variation in cosmic ray intensity. In principle it is possible to correct for this influence. Even if such a correction is applied, however, a residual diurnal variation remains. It might be suspected that this is due to some atmospheric influence for which the correction is unknown, but this possibility can be ruled out, by directional measurements with Geiger-Müller counters. If we measure the cosmic radiation coming from the north and compare this with the radiation from the south, a difference in phase of the diurnal variation is observed, which can not be due to the atmospheric conditions because the rays coming from the north and from the south have passed almost identical atmospheric layer. Such measurements made in Berlin (KOLHÖRSTER 1941), Stockholm (ALFVÉN 1938, ALFVÉN and MALMFORS 1943, MALMFORS 1949), and Manchester (ELLIOT and DOLBEAR 1950, 1951) demonstrate beyond any doubt that the phases of diurnal variation measured from the north and from the south are different. This shows that there is diurnal variation in the primary cosmic radiation.

The next problem is to decide which part of the primary radiation is responsible for the variation. We know that practically all the primary cosmic rays consist of positively charged particles. It is not ruled out, however, that there may also be a small neutral component. The assumption of a neutral anisotropic component is supported by the fact that usually the maximum occurs not very far from noon. The neutral component, which should exhibit a solar time variation would then derive from the sun or its close vicinity. If we measure cosmic radiation by ionization chambers or

by counters directed to zenith we must find a maximum of the neutral component occurring exactly at noon because the neutral particles are not deflected by the geomagnetic field.

Although it cannot be ruled out that there is a variation caused by neutral particles there is no positive indication that this is the case. We shall in the following assume that the whole variation is due to the charged particle component of the cosmic radiation. The atmospheric variation and a possible neutral particle component may introduce considerable corrections in the empirical material. But as these are unknown as yet we shall neglect them.

In order to study the charged particle component it is necessary to correct for the deflection of the particles in the geomagnetic field. This correction has been studied thoroughly by BRUNBERG and DATTNER (1953) and the result published in a series of diagrams. It is, however, necessary to know which part of the primary momentum spectrum is responsible for the observed variation, but unfortunately it seems to be unknown. The secondary processes in the atmosphere are not yet quantitatively known and furthermore the different types of apparatus, the different shielding employed, and different altitudes make it likely that all observers do not measure in the same momentum range. It would therefore be advantageous to have a method for analyzing the observed variations in such a way that conclusions could be drawn about which part of the momentum spectrum is responsible for the variation. One way of doing this is shown in the following discussion, which is based on a detailed knowledge of particle orbits in the geomagnetic field, together with the assumption that the diurnal variation is caused by an excess in the primary radiation coming in from one fairly definite direction.

Determination of the momentum of the variable component

Two different ways could be used and both of them require an assumption that there is only one direction of anisotropy in the primary cosmic radiation responsible for the diurnal variation.

1) Measurements in different directions at one particular station could be analysed and the difference in phase and amplitude in the different directions could be used to find the momentum of the variable component.

2) Comparisons of measurements at different latitudes.

As an application of the first method we will consider some measurements made in Stockholm by MALMFORS in 1948. Three sets of telescopes were directed, the first towards a point 30° to the north of zenith, the second one to a point 30° to the south of zenith and the third to the zenith. The local time for maximum amplitude in the three directions was determined. In fig. 1 the point of observation P is situated in latitude λ. We consider two coordinate systems, one system X', which is defined by the x'-axis pointing to the sun and the z'-axis coinciding with the earth's axis of rotation, and another system X with the x-axis defined by the intersection of the meridional plan through the point P and the equatorial plane of the earth.

In the X'-system the main direction of the anisotropy is defined by Ψ'_E and Φ'_N. In the X-system Ψ_E and Φ_N are angles which determine the direction of the measured cosmic particles far away from the earth. When the X-system rotates in relation to X' we measure at the point P a variation of the cosmic ray intensity with a maximum occurring when

$$\Psi'_E = \Psi_E + \Psi_t$$

where Ψ_t is the angular position of the sun as given by the local time.

For $\Phi_N = \Phi_N'$, the amplitude of variation is the largest possible because the telescope then points the direction of maximum anisotropy.

In fig. 2 Ψ'_E is plotted as a function of momentum in the range 15—40 GeV Z/c. The values of Ψ_t are given by Malmfors' telescope measurements in Stockholm 1948.

Assuming that there is only one direction of excess intensity we can determine its angle as well as the momentum of the important part of excess radiation by means of the points of intersection between the three curves in fig. 2. The momentum appears to be about 20 GeV Z/c.

The three curves should intersect in one point, but particles in the zenith direction have not passed the same atmospheric layer as particles in the north and south directions, and therefore they could have been influenced in an other way. Moreover the error in the deter-

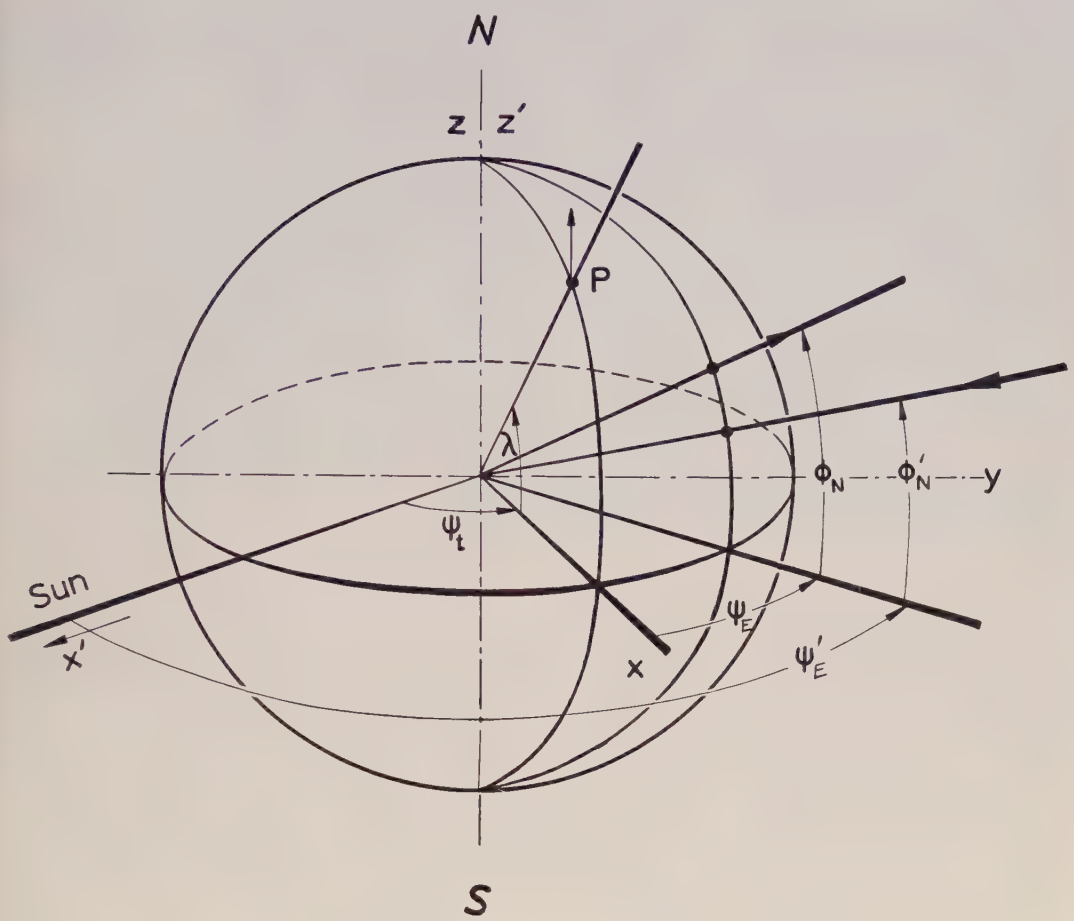

Fig. 1. The definition of the angles ψ_E, Φ_N, ψ'_E, Φ'_N and ψ_t.

mination of the time of maximum is about half an hour which means an error in the curves of $\pm 7°$. It must be pointed out that the curves do not intersect in any other point in the momentum range $10^{10} \rightarrow \infty$ eV Z/c.

A second method to determine the momentum is the following:

Consider two counter telescopes which measure the intensity in east and west directions respectively. Each of them registers a diurnal variation. Maxima of the cosmic ray intensity do not occur simultaneously for both telescopes but in general with a time interval of h hours due to the deflection in the magnetic field of the earth. For any particular momentum this interval can be plotted by the curves of Brunberg and Dattner as a function of zenith angle and latitude.

Fig. 3 shows 6 diagrams for different values of primary momenta. Each diagram gives $\Delta\Psi$ as a function of latitude, where $\Delta\Psi = h \cdot 15°$ (The earth rotates 15°/hour). The curves marked 8°, 16°.... etc. correspond to zenith angles of 8°, 16°.... etc. for the two telescopes, one directed east of zenith, the other west of zenith. The curves in fig. 3 are plotted from the diagrams by Brunberg and Dattner.

Concerning fig. 3 a few noteworthy properties should be pointed out. For the lowest momenta the curves begin at $\lambda = 30°$ and higher latitudes, because the corresponding particle orbits are either forbidden or so close to the forbidden cones that an experimental determination was impossible.

At the geomagnetic pole ($\lambda = 90°$) the limit of $\Delta\Psi$ for all zenith angles and all momenta is

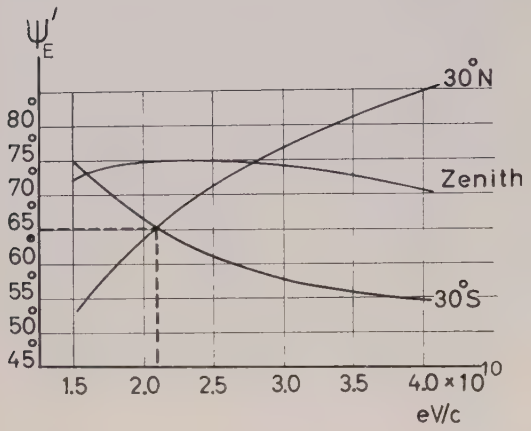

Fig. 2. The direction of anisotropy ψ'_E in the equatorial plane as a function of momentum. Particles arrive in the zenith direction and in directions which form an angle of 30° with the zenith. $\lambda = 58°$.

+ 180° or − 180° which is natural because the orbits arriving at the magnetic pole are symmetric in relation to the magnetic axis.

For low latitudes $\Delta\Psi$ is positive. That means that the maximum measured in east direction occurs before the maximum in west direction. This is typical for all momenta in this momentum range and can easily be seen in a simple model of two particle orbits arriving from east and west on the equator. However, a study of fig. 3 shows that the phase difference gets smaller for higher latitudes and $\lambda = 50°$ is a critical point for momenta below 30 GeV Z/c. On latitudes higher than 50°, $\Delta\Psi$ becomes negative for lower but not for higher momenta. This property gives a possibility to determine which part of the primary momentum spectrum gives the largest contribution to the measured intensity, and relevant observational data might give interesting results.

In other words for low primary momenta maximum in west direction should occur before maximum in the east direction for latitudes over 50° ($\Delta\Psi$ negative) and vice versa for latitudes between 0° – 50°. But on the other hand maximum should occur in east before west at all latitudes for momenta above 30 GeV Z/c.

Measurements of the diurnal variation in east-west directions in Manchester (Elliot and Dolbear 1951) indicate that maximum in the east direction comes before maximum in the west direction. Thus maximum in east direction occurs at 14*h* and in west direction at 16*h*. According to the analysis of fig. 3. the momentum appears to be more than 30 GeV Z/c.

These results, viz. the analysis of fig. 2 and fig. 3 seem to indicate that the main contribution to the variation considered comes from momenta in the region 20—40 GeV Z/c. In the following we shall assume that the whole variation is caused by particles in this momentum range and make a computation both for 20 and 40 GeV Z/c. It is possible that the maximum of the momentum distribution is rather flat so that we have to integrate over the measuring cone of the telescope for different momenta in order to find out the direction of anisotropy.

The phase angle of the diurnal variation

The analysis of the recorded data of the radiation gathered during the last 20 years gives a possibility to determine the phase angle and amplitude of the diurnal variation.

The apparatus used were Geiger-Müller telescopes and ionization chambers.

Values taken from recording stations with Geiger-Müller telescopes are rather easy to correct and the trajectories can be followed back to infinity by the curves of Brunberg and Dattner, because the telescopes measure in a cone well defined by the geometric arrangement. Ionization chambers, however, are not directional to the same extent, but owing to atmospheric absorption particles arriving in the zenith direction contribute more to the total intensity registered than particles arriving from other directions.

A fairly good correction for the influence of the geomagnetic field can be obtained also for an ionization chamber if the trajectories of particles hitting the chamber are followed backwards to infinity. The atmospheric absorption must then be included, for instance by the approximation that the intensity is reduced as $\cos^2 z$ where z is the zenith angle. (Cf. Montgomery, Cosmic Physics, p. 169.)

This has been done in the following way. The sky at the place of observation is divided into 36 regions bordered by the circles with zenith distance $z_n = n \times 10°$ ($n = 0,1, \ldots 9$) and azimuth $a = 45°, 135°, 225°, 315°$. Each of these regions is given a weight proportional

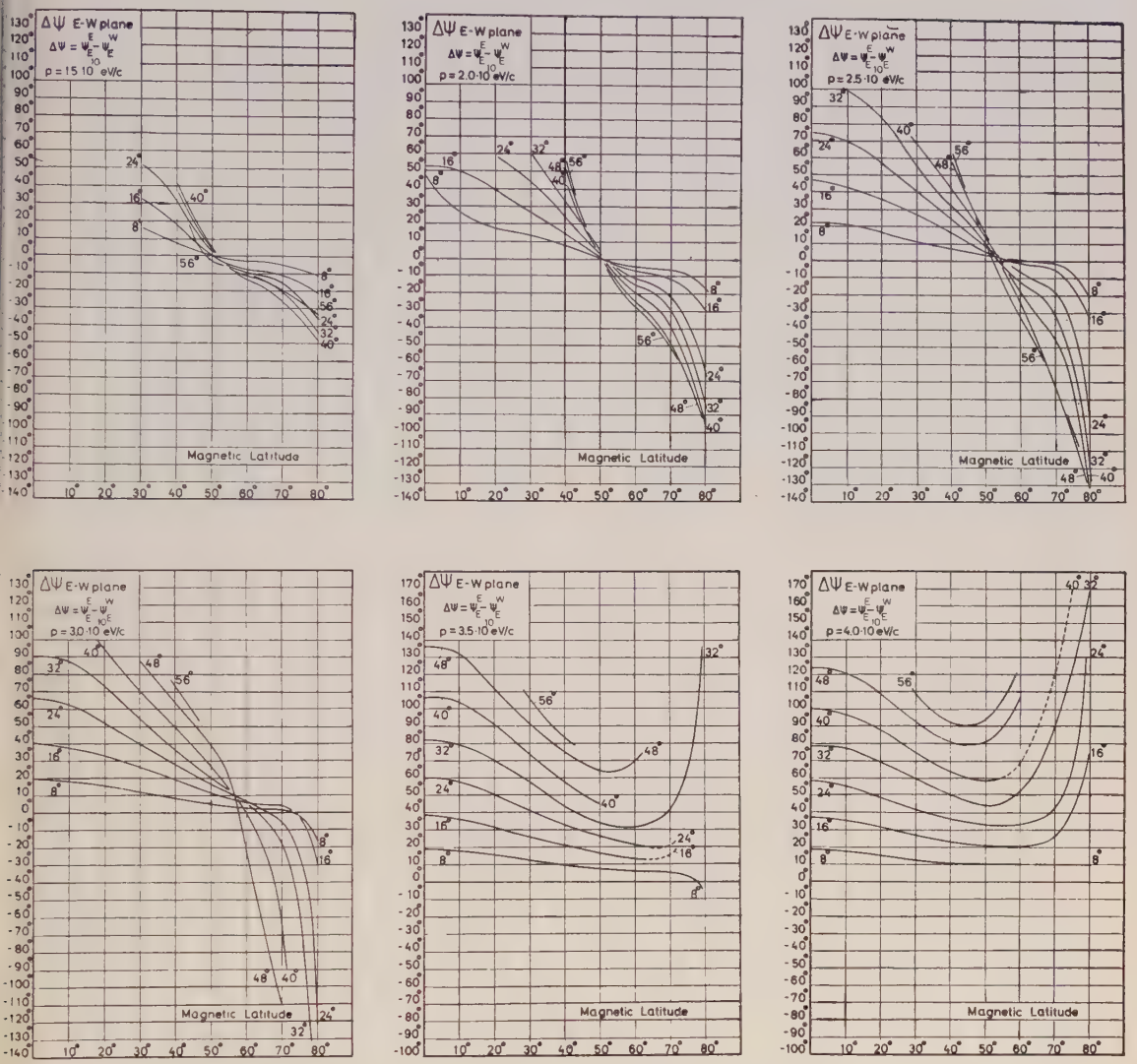

Fig. 3. $\Delta\psi$ as a function of magnetic latitude.

to $\cos^2 z_m \cdot \sin z_m$, where $z_m = (n+\frac{1}{2})\ 10°$. The first factor $\cos^2 z_m$ takes into account the diminishing sensitivity of the ionization chamber with increasing zenith distance, the second factor $\sin z_m$ the variation of the size of the regions with zenith distance.

A histogram is then prepared for the regions in each of the four main directions N, E, S, W. Let us take an example. Mark along the abscissa axis of the histogram for the north direction the deflections Ψ_E corresponding to $z_n = n \cdot 10°$ along the northern meridian. Above each interval between these marks we then draw a rectangle with area equal to the weight $\cos^2 z_m \cdot \sin z_m$ of the corresponding region in the sky. We finally add the four curves obtained in this way for the directions N, E, S, and W, and the position of the maximum in this final curve gives a definite direction of maximum sensitivity in the equatorial plane outside the earth's magnetic field. A complete correction should have included a

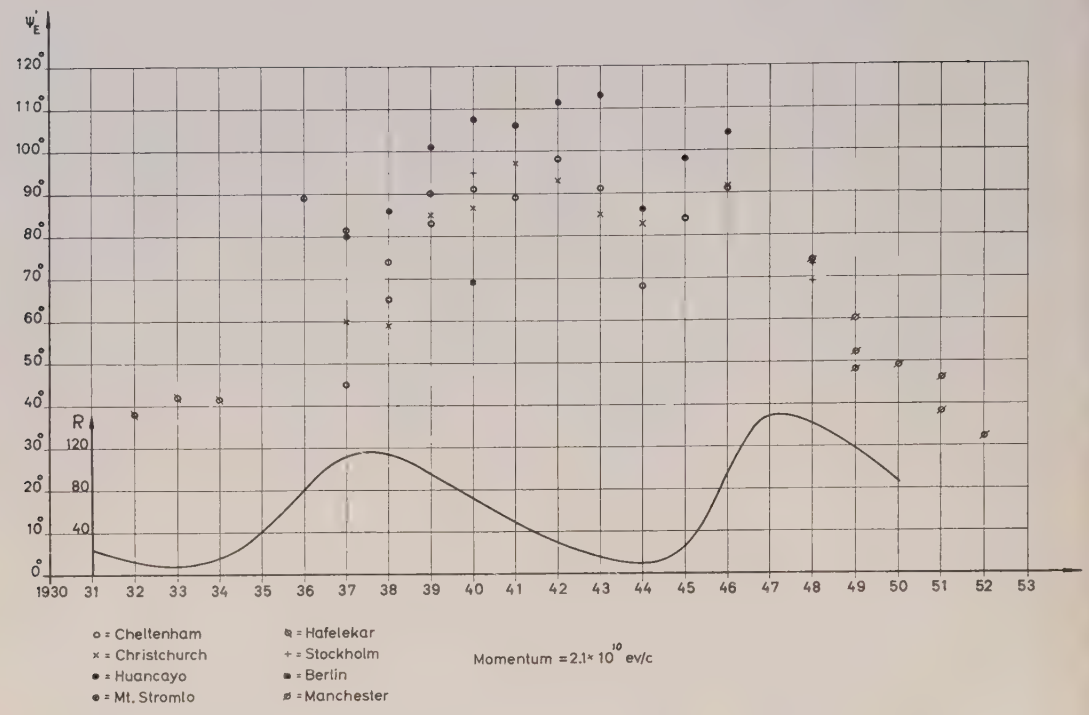

Fig. 4. The direction of anisotropy as a function of time. R is the Zürich sunspot number.

similar study of Φ_N, but as for the moment we are only interested in Ψ_E, it has not yet been done. This may include an error, but an inspection of the appearance of the Φ_N-diagrams in the chosen momentum range (Brunberg-Dattner, 1953) shows that the error is of no importance in this case.

Elliot and Thambyahpillai (1953) have published a diagram of the phase of the diurnal variation as a function of time over a period of 20 years, and it is very interesting that there appears to be a systematic change in phase over the years.

Fig. 4 shows Elliot's and Thambyahpillai's diagram when the correction has been app ied for the deflection in the geomagnetic field. Momentum is supposed to be 21 GeV Z/c. a value taken from fig. 2.

The most interesting result is that the diurnal variation seems to be due to an excess of particles arriving from the 18 *h* direction, although there are some fluctuations about this direction.

An example of these fluctuations is given in another form by Sarabhai and Kane (1953), who point out a correlation between the phase and amplitude of the diurnal variation and the sunspot activity, during the period 1938 – 45.

It may be physically significant to divide the diurnal variation into two components, one tangential component, arriving from the 18 *h* direction and another radial component, arriving from the 12 *h* direction. In the following we shall explain the tangential component by means of the rotation of the solar magnetic field.

Theory of the diurnal variation

Jánossy (1937) suggested that the solar magnetic field which he supposed to be a dipole field, cuts off the low energy part of the cosmic ray spectrum. This theory, which has been developed by Vallarta (1937) and Epstein (1938), indicated that a diurnal variation might possibly be produced by this effect, and the maximum should occur at 18 *h*. In spite of the fact that the corrected experimental results indicate that the maximum occurs at this time, the theory is not acceptable in its original form. It has been shown by Alfvén (1950) that already the scattering by the terrestrial mag-

netic field is enough to fill up the forbidden orbits in the solar magnetic field in such a way that no diurnal variation is produced. This has been confirmed by investigations by KANE, SHANLEY, and WHEELER (1949).

Diurnal variation produced by the solar rotation

Suppose that near the solar surface we have a magnetic field of such a shape that charged particles are trapped in it. Due to the inhomogenity of the solar field $\left(\frac{\partial B}{\partial r} \neq 0\right)$ charged particles even at cosmic ray energies move in trochoids around the sun.

After some time the distribution of these particles will be isotropic in a coordinate system which is at rest in relation to the sun.

In a fixed coordinate system which does not take part in the solar rotation, the isotropic distribution will be anisotropic due to the solar rotation. This obviously holds close to the solar surface, for example in the magnetic field produced by a sunspot. It is also likely that it holds good high up in the corona but far from the sun it does not. Charged particles which are trapped for example near the orbit of Neptune will certainly tend to be isotropic in a coordinate system fixed in the galaxy. The question is where the limit goes between the regions where charged particles are isotropic in relation to a fixed coordinate system and the region in which they are isotropic in relation to a system which takes part in the solar rotation.

Before we discuss the problem it is of interest to point out that the anisotropy of particles close to the sun could be explained as an effect of the solar electric field. Seen from a fixed coordinate system, the rotating sun is strongly polarized so that the voltage difference between the poles and the equator is of the order of 10^9 volts. In the equatorial plane the electric field is radial and determined by

$$E_r = \omega \cdot r \cdot B \quad \ldots\ldots\ldots\ldots\ldots \quad (1)$$

where ω = angular velocity of the sun
r = distance to the sun
B = magnetic field strength at the distance r.

When a charged particle moves in a homogeneous magnetic field, its path is a circle. If an electric field E is introduced perpendicular to the magnetic field, the circle drifts with the velocity

$$v = \frac{E}{B} \quad \ldots\ldots\ldots\ldots \quad (2)$$

and the path of the particle is a trochoid. Inserting $E_r = \omega r B$ from eq. (1), the drift velocity seen from a fixed coordinate system is found to be

$$v = \frac{E_r}{B} = \omega \cdot r \quad \ldots\ldots\ldots \quad (3)$$

i. e. particles follow the sun in its rotation. This is not valid for too large values of r, as discussed below.

Thus the combined action of the electric field from this polarization and the solar magnetic field will cause an anisotropy in relation to a fixed coordinate system.

Seen in this way our question is, how far out from the sun the solar electric field is strong enough to affect the cosmic radiation. In order that cosmic rays at a certain distance take part in the solar rotation the following two conditions must be satisfied.

1) There must be magnetic lines of force running from the volume element in question directly to the sun. If this is the case Ferraro's theorem shows that in average the ionized matter in this element must rotate with the same angular velocity as the sun.

2) The radius of curvature of the cosmic ray in the magnetic field must not be too large. If a cosmic particle has a very high momentum so that it passes almost rectilinearly through the magnetic field the effect of an electric field will be small. On the other hand if the radius of curvature is so small that the particles move in trochoids, the solar rotation is transferred to the cosmic radiation via the electric field E_r. Without an elaborate calculation it is difficult to decide exactly at what momentum this transition takes place, but it is likely that it occurs at a momentum which is of the order of magnitude of the momentum of a particle which moves in a circle around the sun. The momentum of this particle depends on the strength of the solar magnetic field. For this effect the value of the solar magnetic field at the earth's orbit is of decisive importance. Although the value is still not definite it seems reasonable that the strength of the solar

magnetic field is of the order of 10 gauss (Alfvén 1950, 1952). If no disturbance occurs outside the sun, this field should decrease as a dipole field. At the orbit of the earth the value of the field would the be 10^{-6} gauss. In this field a particle moves in a circle with a radius of curvature equal to the earth's orbit, if its momentum is 5 GeV Z/c.

Usually the solar magnetic field is disturbed very much. There is no doubt that solar activity especially solar flares and the presence of big sunspots, causes emission of streams from the sun which produce magnetic storms and auroras when they reach the earth. There are good reasons to believe that these streams consist of neutral ionized gas. The conductivity is certainly very high so we should expect that the magnetic lines of force are "frozen into" the volume of the gas which is sent out in the beam. This means that the conductivity of the gas in the beam is so large that any motion of the matter relative to the magnetic field lines would be retarded due to strong induced electric currents in the gas. We confine ourselves to a discussion of the phenomena near the equatorial plane.

Consider a volume element near the sun (fig. 5). The surface of this element parallel to the equatorial plane is

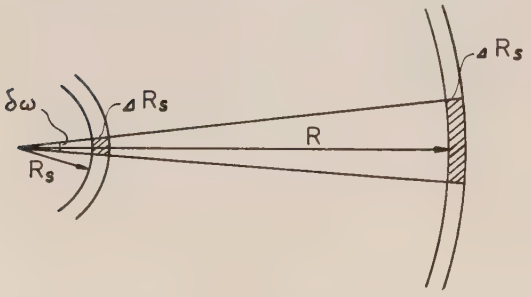

Fig. 5. A volyme element of matter is transported outwards from the sun.

$$\Delta R_S \cdot \delta\omega \cdot R_S \ldots\ldots\ldots\ldots \quad (4)$$

and the magnetic field strength

$$H_S = \frac{\Phi}{\Delta R_S \cdot R_S \cdot \delta_\omega} \quad \ldots\ldots\ldots \quad (5)$$

where Φ is the flux through the element. If the element is emitted radially, it will expand and its area is

$$\Delta R_S \cdot \delta\omega \cdot R \ldots\ldots\ldots\ldots \quad (6)$$

at a distance R from the sun. The magnetic field strength in it is now

$$H = \frac{\Phi}{\Delta R_S \cdot R \cdot \delta_\omega} = H_S \cdot \frac{R_S}{R} \ldots\ldots \quad (7)$$

or less.

Hence in a beam H is proportional to $1/R$. Even if several beams are active at the same time, we could not expect the solar magnetic field in average to decrease as slowly as $1/R$. However, in order to discuss two extreme cases we shall discuss this case and the dipole case. In order to treat the case when H decreases as $1/R$ we must put an outer limit to the field. We tentatively put this to twice the earth's orbit. Thus

1)

$$H = \text{const} \cdot \frac{1}{R^3}$$

$$H_E = \frac{10}{200^3} \approx 10^{-6} \text{ gauss (At the orbital radius of the earth)}$$

$$H_E \cdot \delta = H_E \cdot 1.5 \cdot 10^{13} = 1.5 \cdot 10^7$$

$$p = 300 \cdot 1.5 \cdot 10^7 \approx 5 \text{ GeV Z/c}$$

where p is the momentum of a particle, moving in a circle around the sun at the orbital radius.

2)

$$H = \text{const} \cdot \frac{R_S}{R}$$

$$\varphi = \int_{R_S}^{2R_{S-E}} \text{const.} \cdot \frac{R_S}{R} \cdot 2\pi R \cdot dR \approx 10 \cdot \pi R^2$$

where R_S radius of the sun

R_{S-E} = orbital radius of the earth

This gives

$$\text{const} \ \frac{10}{4} \cdot \frac{R_S}{R} = \frac{2.5}{200}$$

$$H_E = \frac{2.5}{200} \cdot \frac{7 \cdot 10^{10}}{1.5 \cdot 10^{13}} = 5.8 \cdot 10^{-5} \text{ gauss}$$

$$H_E \cdot \delta = H_E \cdot 1.5 \cdot 10^{13} = 0.89 \cdot 10^9$$

$$p = 300 \cdot 0.87 \cdot 10^9 = 260 \text{ GeV Z/c}$$

As the momentum which gives the diurnal variation is of the order of 30 GeV Z/c we find that this is intermediate between the two cases which we have discussed. Hence in some cases, especially when there is a strong solar activity so that the solar magnetic field is much disturbed, we should expect the cosmic radiation we measure to take part in the solar rotation. In other cases when the disturbances are small we should expect only a fraction of the radiation spectrum to take part in the rotation. If cosmic radiation takes part in the solar rotation completely, we should expect an anisotropy of the radiation so that we receive more radiation at 18*h*. Further the energy of the particles which reach the earth at the afternoonside will be higher and this also causes an increase in the measured intensity. Actually the whole phenomenon is of the same type as the Compton-Getting effect.

Compton and Getting (1935) showed that if cosmic radiation originates outside our galaxy we should expect a diurnal variation with sidereal time. This is due to the fact that the solar system is moving with a velocity of 300 km/sec toward declination 47° N and right ascension 20 h 40 min. owing to the rotation of the galaxy. If cosmic radiation is isotropic in inter-galactic space we should measure a greater intensity on that side of the earth facing the direction of motion.

The application of this effect discussed in the present paper was suggested to the authors by H. Alfvén.

Suppose the cosmic radiation in the neighbourhood of the earth takes part in the solar rotation with the same angular velocity as the sun, the velocity relative to the earth is

$$v = \frac{2\pi \cdot R_E}{T} = 4.0 \cdot 10^7 \text{ cm/sec} = 0.13 \cdot 10^{-2} \cdot c$$

where T = synodic rotation period of the sun = 27 days
R_E = orbital radius of the earth
c = velocity of light.

This gives us a possibility to calculate the expected excess of particles on the afternoonside of the earth.

According to Compton and Getting (1935) the number of particles, n', impinging on a surface moving with velocity $\beta \cdot c$, is given by the ratio

$$n'/n = 1/(1-\beta \cos \omega')^3 \quad \ldots\ldots \quad (8)$$

where c = velocity of light
$\beta \ll 1$
n = number of particles impinging on the surface at rest
ω' = angle between the velocity vector of the moving surface and the direction of a moving particle, with a speed almost equal to that of light.

Vallarta, Graef, and Kusaka (1939) have improved the calculations of Compton and Getting by taking into an account the deflection of cosmic particles in the magnetic field of the earth under the assumption of the primary energy distribution functions

$$f(E) = \text{const. } E^{-3} \text{ or } f(E) = e^{-KE}$$

In order to show the expected amplitude of diurnal variation due to a solar rotation a similar computation has been carried out below. However, although the primary spectrum is fairly well known, we do not know how the yield function varies with energy for the secondaries observed at sea level. In order to find an upper and a lower limit for this expected amplitude we shall deal with three cases:

1) Primaries having only one momentum and a velocity almost equal to that of light.
From equation (8) we get

$$n'/n \approx (1+\beta \cos \omega')^3 = 1 + 0.39 \cdot 10^{-2} \ldots \quad (9)$$

for $\omega' = 0$ and $\beta = 0.13 \cdot 10^{-2}$

Thus the amplitude of the diurnal variation, measured within a narrow solid angle with a counter telescope on the equator above the atmosphere, should be 0.39 %.

2) Primaries having an energy distribution function

$$f(E) = \text{const. } E^{-3}$$

Vallarta, Graef and Kusaka show that the fractional variation in intensity is

$$\frac{n'-n}{n} = 12\beta \cdot r_0^4 \int \cos \omega' \cdot \frac{dr}{r^5} \ldots \quad (10)$$

where r is in Störmer units

$$r_{\text{Störmer}} = 4.1 \cdot 10^{-6} \sqrt{V}$$

In fig. 6 the earth is seen from the north pole. Equation (10) is solved graphically for a few values of ω with $r_0 = 0.5$ Störmer, corresponding to the lowest particle momentum in the zenith direction. The maximum amplitude should be about 0.27 % and the maximum occurs at 12.30 *h*.

From this it appears that with a distributed spectrum the effect is smoothed out to some extent.

3) Primaries which have the same energy distribution but the integral is now taken from $r = 0.6$ Störmer up to $r = 0.8$ Störmer.

This gives a maximum of 0.36 % at 13.30 *h*.

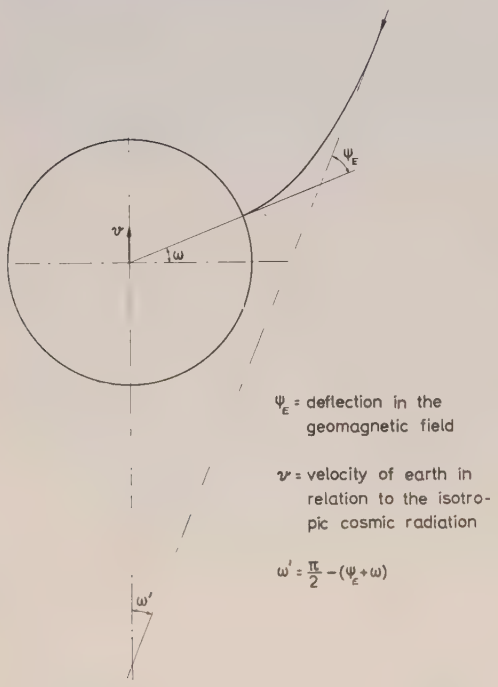
ψ_E
v
ω
ψ_E = deflection in the geomagnetic field
v = velocity of earth in relation to the isotropic cosmic radiation
$\omega' = \frac{\pi}{2} - (\psi_E + \omega)$
ω'

Fig. 6. The orbit of a cosmic ray particle in the equatorial plane of the earth.

All these values were calculated without taking into account the fact that a motion of the earth in relation to the isotropic cosmic radiation alters not only the number but also the energy of the particles observed. This may even increase the amplitude calculated above.

From this follows that if the radiation takes part in the solar rotation completely, we should expect a diurnal variation at the equator with an amplitude between 0.4 % – 0.3 % when measuring with a narrow counter telescope.

Some observers measure an amplitude of the diurnal variation of about 0.2 %. The difference between the calculated and measured values may be due to three causes.

The first of them is the possibility that the cosmic radiation only to some extent takes part in the solar rotation.

Secondly the angular resolution of cosmic ray instrument is limited. Counter telescopes have solid angles of $0.1\pi - 0.5\pi$ and ionization chambers 2π.

Finally, as shown in the comments to fig. 1, p. 75 the amplitude is a function of $\Phi_N - \Phi'_N$ and thus will be smaller than the calculated value if $\Phi_N \neq \Phi'_N$.

The secular variation of the phase, as shown by Elliot and Thambyahpillai's curves, indicates that there are also other factors influencing the diurnal variation. As will be discussed in a coming paper by Alfvén (Tellus 1954. In course of publication), changes in the solar magnetic field influence cosmic radiation inside the earth's orbit in such a way that when cosmic ray generation is strong, more cosmic radiation will diffuse outwards from the sun and thus alter the phase of diurnal variation.

We whish to point out that a computation of the expected amplitude of the diurnal variation can now be carried out in other latitudes than the equator by means of the curves of Brunberg and Dattner. Perhaps the discrepances between registrations of diurnal variation measured in different latitudes can at least to some extent be explained in this way.

The authors wish to express their gratitude to Prof. H. Alfvén for his valuable and stimulating ideas, and Dr. N. Herlofson for many helpful discussions.

The investigation has been supported by a grant from Knut and Alice Wallenberg's Foundation which is gratefully acknowledged.

REFERENCES

Alfvén, H., 1938: Registration of the Cosmic Radiation by means of Coincidence Counters. *Arkiv f. Matematik, Astronomi och Fysik*, 26B, No. 14.

— 1950: Cosmical Electrodynamics. *Oxford.*

— 1952: On the Zeeman effect measurements of the sun's general magnetic field. *Arkiv f. Fysik*, 4B, No. 14.

— and Malmfors, K. G., 1943: Directional Measurements of Cosmic Radiation. *Arkiv. f. Matematik, Astronomi och Fysik*, 29A, No. 24.

Brunberg, E. Å., and Dattner, A., 1953: Electron orbits in the field of a magnetic dipole. *Tellus.* Vol. 5, No, 2, 3.

Compton, A. H. and Getting, I. A., 1935: An Apparent Effect of Galactic Rotation on the Intensity of Cosmic Rays. *Phys. Rev.* **47**, o. 817.

Elliot, H. and Dolbear, D. W. N., 1950: Directional measurements of the diurnal variation of cosmic ray intensity. Proceedings of the *Physical Soc.* A. Vol. LXIII.

— 1951: Directional measurements of the diurnal variation of cosmic ray intensity. *Journ. of Atmospheric and Terrestrial Physics* Vol. 1.

— and Thambyahpillai, T., 1953: World-wide changes in the phase of the cosmic-ray solar daily variation. *Nature.* May 23.

Epstein, P. S., 1938: Influence of the solar magnetic field upon cosmic rays. *Phys. Rev.* 53

Ferraro, V. C. A., 1937: The Non-uniform Rotation of the Sun and its Magnetic Field. *Mont. Not. R. Astr. Soc.* **97**. p. 458.

Jánossy, L., 1937: Über einen möglichen Einfluss des Magnetfeldes der Sonne auf die in Erdnähe beobachtete Höhenstrahlung. *Zs. f. Physik*, **104**. 430.

Kane, E. O., Shanley, T. J. B., and Wheeler, J. A., 1949: Cosmic Rays and heavenly bodies. *Rev. Mod. Phys.* Vol. 21.

Kolhörster, W. 1941: Der Tagesgang der Höhenstrahlung. *Phys. Zs.* 42. 55

Lange I. and Forbush, S., 1948: *Carnegie Institution of Washington.* Publ. 175, 14.

Malmfors, K. G., 1949: Recordings of Cosmic Radiation. *Tellus.* Vol. 1, 2.

Montgomery, D. J. X., 1949: Cosmic Ray Physics. *Princeton University Press.*

Sarabhai, V. and Kane, R. P., 1953: World-Wide Effects of Continuous Emission of Cosmic Rays from the Sun. *Phys. Rev.* 90, No 2, p. 204.

Sekido, Y. and Kodama, M., 1952: Diurnal variation of vertical cosmic rays. *Rep. of Ionosph. Research in Japan.* Vol. VI nr 2.

Vallarta, M. S., 1937: Cosmic Rays and the Magnetic Moment of the Sun. *Nature*, May 17.

— Graef, C., and Kusaka, S., 1939: Galactic Rotation and the Intensity of Cosmic Radiation at the Geomagnetic Equator. *Phys. Rev.* **55**, p. 1.

The Gravimetric Method for Determination of the Form of the Geoid

By R. A. Hirvonen, Institute of Technology, Helsinki

(Manuscript received October 5, 1953)

The gravimetric method for the investigation of geoid is based on a theorem of Stokes (1849): If a surface is given, which encloses all attracting masses and at which the potential of the gravity —i.e. the sum of attracting and centrifugal forces—is constant, the gravity at this surface and everywhere outside it is given too. Here we are interested in the gravity at the geoid only; this surface will be compared with a regularized surface of reference, preferably with the ellipsoid that has been used for the trigonometric measurements. The deviations of the ellipsoid from a sphere are of order 10 km = 1/600 = p, those of the geoid from the ellipsoid, according to the comprehensive investigation of Tanni (1948), of order 60 m = = 1/100,000 = q. The differences between geoid and ellipsoid can be expressed by infinite sums of spherical harmonics:

$$\triangle r = R\sum_2^\infty u_n$$

$$\triangle g = G\sum_2^\infty v_n$$

and Stokes' theorem by the formula

$$v_n = (n-1)u_n$$

In this original direct form the theorem has no practical significance, owing to the fact, that the local disturbances are represented by terms with great values of n, wherefore the computation from u to v, i.e. from the form of geoid to the gravity looses in accuracy. But it is more advantageous when applied to the inverse problem: given the gravity at the geoid, to be computed the form of the latter. For this purpose Stokes eliminated the spherical harmonics from the formulas above, obtaining that famous integral formula known by his name. Nevertheless, this formula requires, that the gravity is known everywhere around the world, before the deviation of the geoid from the ellipsoid can be computed at a single point.

Hence even this formula had no practical significance before Vening Meinesz (1927, 1932) had developped the device for measuring the gravity at deep sea. Vening Meinesz accomplished a valuable improvement to the theory too: performing an horizontal differentiation of the Stokes' formula he obtained another integral formula for the computation of the tilt of the geoid, or the deflection of the vertical, immediately from the anomalies of gravity.

Before entering the practical applications of these formulae, there are some points in the theory that must be discussed. After Stokes his formula has been developped also without using the spherical harmonics, but one particularity remains: the development of the gravity anomalies must not contain any terms of first order. In other words: if the anomalies are represented by a mass coating, the gravity center of this coating must coincide with the centre of the Earth. This balance of anomalies prescribes three equations of condition which should be taken into consideration by a proper adjustment of the gravity field observed. This adjustment has always been neglected in the applications hitherto performed. No error in the computations, however, has been caused, because the integral formulae of Stokes and Vening Meinesz con-

tain the adequate correcting terms, which were unnecessary for an adjusted gravity field.

The original treatise of Stokes neglected all terms of order p^2 or smaller, but, q being of the order p^2, this was not satisfactory. Later it has been shown, that the theoretical errors of Stokes' formula anyway are of order $pq = 10$ cm. Moreover, as ZAGREBIN (1944) has shown, the spherical harmonics can be replaced by Lamé's functions and the Stokes' formula duly corrected, in which case a considerable—at present quite unnecessary—improvement can be ascertained.

As mentioned above, the theory presumes, that there are no masses outside the geoid, which requirement by no means is met in the practice. Nowadays it has been shown by MALKIN (1933) and others, that the masses protruding outside the geoid can be allowed for by applying corrections to both sides of the Stokes' formula. Stokes' own idea was, that these masses should—in imagination—be condensed to the geoid, in which case slight corrections both to the anomalies and to the resulting elevations of geoid must be computed. In practice both these methods thus are qualitatively similar. But there are many other methods of reduction, and a closer comparison of them deserves now our attention.

The purpose of the reductions is threefold. At first the theory demands, that the values of gravity which have been observed at different altitudes, refer to the same surface of equilibrium. Then the original formula of Stokes presumes, that no masses are left outside the geoid. Finally the reduced anomalies must vary so smoothly, that the gravity field can be completed by interpolation using as small a number of original observations as possible.

The two last mentioned requirements mean, that the gravity field used is not the actual one. The actual anomalies could be obtained by Prey's method of reduction, in which case the Stokes' formula should be replaced by the corrected formula of Malkin. But these Prey's anomalies vary very irregularly requiring a great number of observations and an intricate integration. Therefore Malkin's formula or the other similar modifications hardly have any practical advantages.

The most simple method of reduction is that of Faye, usually known by the name free-air reduction. The value of the observed gravity is transferred to sea level as through empty air. If the terrain is level, this reduction comprises the entire Stokes' condensation, because an even infinite layer can be moved or condensed in a vertical direction without any changes in the gravity outside it. Only for a rough terrain a topographic correction of gravity is necessary. This correction can be evaluated with the aid of topographical maps, and it is not necessary to consider very wide surroundings of the station.

The transfer of the attracting masses causes, that the potential of gravity changes too, and thus Stokes' formula does not give the actual geoid but a deformed cogeoid, which in general lies slightly above the actual one. The difference has been estimated to be at most 2 m; and its indirect effect back to the gravity can be neglected. The only drawback of the method is, that these free-air anomalies even with terrain corrections still show too rough variations.

If the masses are transferred still further downwards below the sea level, the potential, which was increased by the condensation, begins to decrease again, and when the masses have reached the mirror points of their original positions, the potential has its true value again. This is Rudzki's method of reduction, which leaves the geoid unaltered; the gravity, however, needs almost a double topographic correction. The labour involved by the reduction is augmented, and the resulting anomalies still show rough variations.

The isostatic hypotheses upon the structure of earth's crust suggest, that the topographic irregularities are compensated by opposite irregularities deep below the sea level. Consequently, if we continue the transfer of the masses past the mirror points of Rudzki down to the proper depth of isostatic compensation, we have a possibility to get rid of the rough and irregular variations of anomalies. The experience shows, that in most cases this is true enough. Considering the third of our requirements the isostatic reduction seems to be ideal. But this method has its drawbacks too: the transfer of masses is so great, that the labour involved by the computations reaches its maximum. Not only the topographical maps of the nearest surroundings must be consulted, but this reduction must be extended

around the entire globe. The contribution of the remotest zones, which varies very slowly from point to point, has once for all been computed by the Isostatic Institute in Helsinki, and that of the inner zones surely in the future will be computed by the aid of electronic machines. The drawback, however, remains that the deformation of the geoid and the indirect effect of the isostatic reductions are great.

Now de Graaff Hunter (1935) has suggested a new kind of reduction that combines the advantage of smooth anomalies with the minimal transfer of masses. It can be called regional Stokes' condensation: the protruding topographic features will be condensed to sea level, only not just vertically downwards, but spreading them around on an adequate region. This method being rather new, nobody has tried it in actual studies of the geoid, but I believe it will prove to be very useful.

The reduction methods that give smooth anomalies imply transfer of masses and require a special computation of the deformation of the true geoid. If different reductions, or even different depths of isostatic compensation have been used in different regions of the earth, this computation can be as intricate as the integration of Stokes' formula with unsmoothened anomalies. Therefore it is advisable to use only the free air anomalies as a standard. It will be quite satisfactory in most regions where the terrain is not too rough. In mountainous or otherwise disturbed areas the isostatic or the regional Stokes' condensation can be used as a device for interpolation. The topographic reduction will be applied at first to all observed gravity stations, rendering a smooth field of gravity anomalies. These anomalies can be interpolated for any desidered number of intermediary stations,and the topographic reductions for these stations applied backwards, so that very reliable free air anomalies can be obtained with a minimum amount of actual observations.

There is another point concerning the free-air reduction that may deserve consideration. The coefficient implied by this reduction consists of the curvature of the geoid, which in unfavourable cases can differ by 10 % from that of the ellipsoid. For the first determinations of the geoid only the latter can be used, and the results may need a correction, when the true form of the geoid is approximately known. No experimental information about the magnitude of this correction is so far available.

With the field of anomalies provided, the integration by the aid of Stokes' or Vening Meinesz' function can begin. There are now two alternative ways to be chosen:

1) If the number of points, where the elevation of the geoid or the deflection of the vertical is wanted, is not very great, a special template can be prepared, dividing the surface of the earth into concentric zones and compartments. This template will be attached to each point to be computed, and the mean anomalies in the compartments evaluated separately in each case. Because the outer zones can be very broad, the actual integration, i.e. the multiplication by a factor tabulated and the summing up of the products, can be performed very easily in the usual simple way.

2) If the number of points to be computed is great, or if the computation must be renewed often on the ground of additional observations, it is better to divide the earth once for all into fixed compartments, square degrees or $10° \times 10°$ squares. For each compartment a punch card will be prepared, and the integration can be performed by electronic machines. It is always possible to use smaller squares for the nearest surroundings and larger ones for the more distant zones.

The second method has not yet been experimented, but it will be applied to the investigations that at present are going on in Columbus, Ohio, under the direction of W. A. Heiskanen.

Now we shall consider the question, which accuracy can be obtained in computing undulations of the geoid and deflections of the vertical from gravity anomalies.

At first we must estimate the *probable error of representation*, the uncertainty arising from the fact that it is impossible to measure the gravity at each point on the earth. An observed anomaly in general must be taken as representative of the mean anomaly on a greater area, extending halfways towards the neighbouring stations. The error of representation is the difference of the observed and the real mean value, and taken statistically, it increases, when the size of the area to be represented increases. For very small areas, where an in-

terpolation between the observed stations is reliable, the error of representation can be taken as equal to the mean error of the observation itself, for modern observations practically speaking zero.

The mean anomaly for a square or compartment, on the other hand, begins with a maximal value for smallest squares and decreases, statistically taken, towards zero, when the squares increase. The maximal value of error of representation for the largest squares is equal to the maximal mean anomaly for smallest squares. The curve expressing the increasing of error of representation with the size of square leaves slowly its minimal value (zero), then rises more rapidly, and at last tends again slowly towards its maximal value. But no mathematical function can properly be prescribed for this curve; it can be established only empirically on the basis of numerous different samples. I have made an attempt to determine this curve, in order to get a basis for the investigation of the accuracy of the gravimetric computations of the geoid. My results concerning the precision obtainable for the elevations of geoid and for the deflections of vertical can be stated as follows.

The height of the geoid above the ellipsoid can be computed with a probable error of $\pm$ 7 m, if there are 1,728 observed stations properly distributed around the earth. The distribution used consists of 248 stations up to 40° from the point to be computed with a decreasing density; and of a general world survey with a constant spacing of 5° for distances from 40° to 180°. This is almost the same result which was obtained by de Graaff Hunter.

The deflection of the vertical can be computed with a probable error of $\pm$ 0″.8 ($\pm$ 0″.56 for either component), if there are 1975 stations in all. The distribution consists of 100 stations up to 0°.5, 137 stations from 0.5 to 5°, 258 stations from 5° to 40° and 1,580 stations from 40° to 180° with a constant spacing of 5°. This result differs unfavourably from that of de Graaff Hunter, who obtained $\pm$0″.5 with 1,654 stations. As shown elsewhere, the disagreement is due to a questionable detail in the discussions of de Graaff Hunter.

These results are based on the prerequisite of a complete gravimetric survey over the entire world that by no means has been accomplished at present. The most urgent questions right now are: 1) which is the precision obtainable on the basis of the present observations for the points where the gravimetric elevations of geoid or the deflections of the vertical are desirable, and 2) where are the most harmful gaps of the gravimetric survey that in the first place should be filled up. The second question is one of the main concerns of the Columbus-program, namely to give suggestions to observers, where additional observations are wanted. Here in Scandinavia we know, that submarine observations in the Baltic Sea, North Sea and Northern Atlantic are our first goals.

As a summary about the present situation can be stated: There are about 12,000 gravity observations with pendulum apparatus of Sterneck, Lejay or Vening Meinesz. Most of these have been used by Tanni in 1949 for his extensive studies on the continental undulations of the geoid. The additional stations are situated in Europe, South Africa, on the Pacific and around the American continents. Then there are the new observations with Worden-gravimeter at the national reference stations and at about 50,000 field stations around the earth. The main bulk of gravimeter observations with millions of stations has been furnished by the oil companies. These stations are concentrated with an extraordinary density on the areas where oil or ore is to be expected, but, unfortunately, they cover extensive and conherent regions only in Canada, United States and around the Gulf of Mexico.

It is obvious, that the best results for the gravimetric deflections of the vertical can be obtained in the central parts of regions that have a general gravimetric survey. The immediate surroundings of the points to be computed need a detailled survey with a density of stations which makes the interpolation between the observed points possible. In addition to this it must be pointed out that there should be no exceptional disturbed anomalies within these regions. The mountainous regions are not favourable, even though the triangulations often preferably follow the mountain chains. Considering the moderate accuracy of the deflections of the vertical, it is not necessary, that the astronomi-

cal points should be first order trigonometric points. They can be choosen from the most favourable parts of the anomaly map and connected by triangulations of lower order or by traverses to the main net. The number of these super control points, which render the absolute orientation of triangulations possible, is just a few for each continent, and therefore it is probable, that the adequate completion of the present gravity survey can be accomplished in a very near future.

REFERENCES

de Graaff-Hunter, J., 1935: The Figure of the Earth from Gravity Observations and the Precision Obtainable. *Phil. Trans. R. S.* London.

Heiskanen, W., 1953: Isostatic Reductions of Gravity Anomalies by the Aid of High-speed Computing Machines, *Ann. Ac. Sci. Fennicae.*

Malkin, N., 1933, Lambert, W. D., 1937: *Gerlands Betiräge zur Geophysik.*

Stokes, G. G., 1849: On the Variation of the Gravity at the Surface of the Earth. *Transact, Cambridge Phil. Soc.*

Tanni, L., 1948: On the Continental Undulations of the Geoid as Determined from the Present Gravity Material. *Annales Ac. Sci. Fennicae.*

Vening Meinesz, F. A., 1927: A formula expressing the deflection of the plum-line in the gravity anomalies and some formulae for the gravity field and the gravity potential outside the geoid. *Koninkl. Akad. van Wetensch. te Amsterdam.*

— —, 1932: Gravity Expeditions at Sea. *Netherl. Geod. Comm.*

Zagrebin, D. V., 1944: Stokes Formula for the Case of an Ellipsoidal Level Surface (in russian). *Bull. Inst. Astr. Ac. Sci. URSS.*

LETTERS TO THE EDITOR

To the Editor of Tellus

My dear Colleague,

Herewith a letter from Dr. Herman of the Department of Agriculture, Canada, on the question of nitrogen in precipitation. I have got the permission of Dr. Herman to ask you to be kind to publish the letter.

Yours sincerely
Anders Ångström

Dr. Anders Ångström
Swedish Meteorological &
Hydrological Institute

Dear Sir,

On reading the contribution by yourself and Dr. Högberg, On the Content of Nitrogen (NH_4-N and NO_3-N) in Atmospheric Precipitation which appeared in Tellus, 4, 1; 1952, on page 42 you make a hypothesis, "does the concentration approach zero or a negligible value?" From our study now in progress we conclude that the concentration may reach zero.

In a one year's study of soil fertility furnished by the precipitation we have found that 2.004 pounds of NH_4-N and 0.907 pounds of NO_3-N, or 2.92 pounds of total nitrogen was supplied per acre for the twelve-month period, as well as 6.07 pounds of sulphur (S) per acre by the total precipitation experienced here. Now last year was somewhat abnormal for we experienced little snowfall and a continuation of our study may reveal an entirely different picture from year to year.

What we consider of interest is the following occurrence.

On August 15 we experienced one of our customarily yearly cyclonic rainstorms. When the storm struck Kentville, N.S. a rainfall of 2.19 inches was recorded for the day rain. Analysis of the rainfall for NH_4-N and NO_3-N gave zero readings. As we never had experienced negative readings previously, I wrote to Dr. Hornstein, Meteorologist-in-Charge, Dominion Public Weather Office, Halifax to find out if records of precipitation were on file from United States cities in the path of the storm. I received the following information. "The storm was of tropical origin; the air within the storm had been hovering over the subtropical regions for several weeks and was reasonably homogeneous, having taken on all the characteristics of a tropical air mass. Reporting stations along the eastern seaboard of North America indicated that rain was falling throughout the period of the storm's northward advance and in many cases the records indicated exceptionally large rainfall amounts, both in the United States and Canada, as shown by the following statistics."

	inches
Norfolk, Va.	5.80
Atlantic City, N.J.	7.29
Nantucket, R.I.	2.54
Block Island	4.86
Providence, R.I.	3.03
New York City	1.59
Bridgeport, Conn.	0.91
Philadelphia, Pa.	0.64
Eastport, Me.	2.73
Yarmouth, N.S.	2.99
Kentville, N.S.	[1]2.90

[1] Total for 24 hour period

The above record of precipitation reveals a picture of the abnormal rainfall of tropical origin. The storm proceeded on to Labrador, then turned and petered out in Quebec Province on its way back.

From our negative findings for NH_4-N and NO_3-N on examination of the heavy day rain we can only assume that the nitrogen forms being investigated were "washed out" of the atmospheric precipitation.

Kentville, October 30, 1953.

Yours very truly,
F. A. Herman
Chemist, In Charge.

Amino Acids in Rainwater

Organic nitrogen compounds in rainwater have been known to exist and have also been determined by Kjeldahl digestion in a few cases. They are referred to in literature as albuminoid nitrogen (see Eriksson 1952). No attempt, however, has been made to determine their nature.

In order to investigate whether this organic nitrogen fraction contained amino acids or not, large samples of water and of snow were collected and evaporated to dryness in vacuum. The residues, after removal of inorganic salts and some interferring organic substances were subjected to paper chromatography. The spots appearing on the papers in some preliminary runs were identified as most probably due to glycine and α-alanine present in the residues. Amino acids seems, thus, definitely to be present in rainwater, although in small quantities.

Miller (1953) synthesized amino acids in a closed system containing methane, ammonia, water vapor, and nitrogen by electric discharges. He found aspartic acid, glycine, α-alanine, β-alanine, and α-amino-n-buturic acid to be synthesized under these conditions. Whether such a synthesis can occur in presence of oxygen is not known but it is interesting to note that glycine and α-alanine which seemed to be most abundant in Miller's experiment also seems to occur in rainwater.

The work will be continued and a full account given later.

REFERENCES:

Eriksson, E., 1952: *Tellus* **4**, p. 225.
Miller,s S., 1953: *Science* **117**, p. 528.

Stockholm, March 17, 1954

S. Fonselius
Institute of Meteorology and Institute of Organic Chemistry and Biochemistry
University of Stockholm

NOTE

Note on the Symposium on the Use of Models in Geophysical Fluid Dynamics[1]

A symposium was held September 1—4, 1953 at The Johns Hopkins University, Baltimore, Maryland to discuss the problems and potentialities of models in investigations of geophysical phenomena. About 25 research workers in the fields of oceanography, meteorology, aeronautics, geo-magnetism, civil engineering, and applied mathematics attended the conference. Fifteen papers were presented followed by discussions.

The first session was devoted to a paper by Professor Stanley Corrsin, The Johns Hopkins University, on general problems of modeling and dimensional analysis. One of the important parts of Corrsin's paper was the suggestion that a fluid system is not sensitive to changes in a non-dimensional number, characteristic of the system, if the number is very small or very large. This was supported by several examples.

Next Professor G. W. Morgan of Brown University presented an historical summary of theoretical and experimental work with rotating, homogeneous liquids, together with an account of his own research in this field. Most of the theoretical work was inspired by Taylor's experiments which showed a definite tendency for the relative motion of a rotating fluid to become two-dimensional when the relative motion becomes very small (highly geostrophic). Most theoretical solutions, assuming small motions, involve singularities in the velocity field and it is not apparent whether this is due to neglect of viscosity or of the non-linear convective acceleration terms. Morgan discussed a publication by R. R. Long on the motion of an obstacle along the axis of a rotating fluid in which the relative motions need not be small. Questions were raised regarding the existence and uniqueness of such flows.

The discussion of basic problems of rotating fluids was completed by a paper by Professor Dave Fultz of Chicago which included a number of experiments with obstacles towed in rotating vessels of water. Many of these were similar to the basic experiments of Taylor.

The next session was concerned with realistic models of large-scale atmospheric phenomena and was devoted largely to a description by Professor Fultz of the "dish-pan" experiment, and some theoretical work on this experiment by Drs H. L. Kuo and Edward Lorenz of Massachusetts Institute of Technology. This experiment involves a cylinder of rotating water heated at the bottom perimeter in an effort to simulate the rotating atmosphere heated at the equator. Fultz described in detail the two regimes of motion that occur. They are called the Hadley and Rossby regimes. The former is characteristic of low rotations and strong heating and resembles the classical trade-wind cell. The motions on the free surface are zonal without sensible disturbances. The Rossby regime occurs for higher rotations at a given heating and is characterized by zonal winds at the free surface, but with regular or irregular, long wave patterns resembling the flow at high levels in the atmosphere.

Kuo and Lorenz presented two separate approaches to the problem of explaining the breakdown of the low-rotation regime. Although some of the assumptions and boundary conditions of the theory were questioned by several of the participants, both approaches seemed very promising for this very important and very difficult problem.

[1] The symposium was supported by the Office of Naval Research with the cooperation of the U. S. Weather Bureau and the Geophysics Research Directorate, U. S. Air Force. A complete report of the proceedings, including papers and discussions, will be published at a later date.

Morton Rubin, U.S. Weather Bureau, discussed the general circulation of the southern hemisphere. Rubin pointed out that the simplicity of the topography of this hemisphere and the apparent stabilizing effect of the huge cold source of the antarctic continent might make the southern hemisphere a more suitable prototype for the dish-pan experiment.

Professor Paul Raethjen of Hamburg gave a discussion of cyclogenesis in the atmosphere together with some considerations of the problems of constructing models of developing highs and lows. Raethjen discussed the role of the "adaptation number" in this process. This is the ratio of Rossby and Froude numbers.

The use of rotating models in other geophysical problems was discussed by William von Arx of Woods Hole and Raymond Hide of Cambridge. Von Arx gave an account of a model of the effect of wind stress on the motion of water in the oceans. He showed how it was possible to reproduce the effect of the latitudinal variation of Coriolis parameter by an appropriate variation of the basic depth of the fluid shell measured parallel to the axis of rotation. This is extremely important for large-scale models of oceans and atmosphere. Hide gave a summary of the very careful experimental observations of the jet stream and wave patterns in his experiment with a rotating, heated fluid. This resembles the dish-pan experiment of Fultz except that it incorporates a carefully controlled heat and cold source. Hide's work was inspired by the problem of explaining the earth's magnetic field, which is believed to be caused by slight motions in the molten core of the earth. The remarkable feature of Hide's experiment is the regularity of the wave patterns. His empirical investigation should inspire a theoretical attack on this model.

The remainder of the conference was devoted to a discussion of smaller scale geophysical phenomena in which the rotation of the earth is not a major factor. First, Dr C. S. Yih of Iowa State gave a paper on a theoretical and experimental investigation of convection above a heat source. Yih included a discussion of possible applications to convective phenomena in the lower atmosphere.

Professor R. R. Long of Johns Hopkins discussed a model of air flow over mountain barriers, together with a demonstration of this experiment in the hydrodynamics laboratory. In the demonstration a fluid with continuous density gradient was moved over a barrier. The motion resembled very closely the violent type of flow frequently encountered in the vicinity of the Sierra Nevada mountains in California. In particular, motion resembling that in the rotor cloud of the atmosphere was also observed in the experiment.

Professor George S. Benton, The Johns Hopkins University, discussed the concepts of critical flow in a stratified fluid. Supercritical and subcritical regimes were examined from the viewpoint of energy and momentum transfer. A general equation was derived for finding the lower limit of the absolutely supercritical regime for any velocity and density distributions. The equation was solved for a rather general class of flows. Benton gave a brief account of the connection between these regimes and the occurrence of shock waves.

Harlow Farmer gave a discussion of model experiments being conducted at Woods Hole Oceanographic Institute. The problems in this work involve mainly the flow of fresh water over salt water in estuaries.

Dr M. G. Wurtele of Massachusetts Institute of Technology gave an example of a technique that permits the calculation of the development of lee waves downstream of a source of disturbance in a homogeneous fluid with free surface. The indeterminacy that arises from a steady-state assumption is avoided by this approach. Unfortunately, this method cannot be applied to stratified fluids.

The final discussion of the symposium was presented by Professor Robert T. Knapp of California Institute of Technology. Knapp showed a number of motion pictures of models of density current. The discussion included suggestions for applications of these models to various phenomena in oceans and reservoirs.

Considerable time was available for informal discussion of the papers. These comments contributed significantly to the overall success of the symposium.

Robert R. Long
The Johns Hopkins University

BOOK REVIEW

P. Raethjen: Dynamik der Zyklonen, Leipzig 1953, 384 pp., 92 figures. Akademische Verlagsgesellschaft, Geest & Portig K.-G.

A large number of books covering various fields within meteorology have been published since the war. However, at least within the field of dynamic meteorology most of these have merely aimed at developing the very basic relations and tools in the field and have only given very brief introductions to more advanced ideas. This state of affairs is very understandable. In the first place there was a real lack of elementary text-books when the big training programs were started during the war and this need had to be met first. In the second place, our knowledge of the behaviour of the atmosphere as well as of the laws that govern its behaviour has been increasing very rapidly during this same time. However, as time goes on it will be felt more and more important to try to summarize into one consistent picture what has been accomplished up to the present time. As yet any such attempt necessarily must be fairly incomplete and the interpretation arrived at would also to a large extent depend upon the "school of thought" from which the author stemmed. Still such attempts would be very valuable and stimulating. The present book by Professor Raethjen from the University of Hamburg represents such an attempt. It is not a text-book but a research report.

The book covers a much wider scope within the field of dynamic meteorology than the title at first seems to indicate. Since the problem of the formation and behaviour of cyclones never can be treated as an isolated phenomenon, many problems concerning the general circulation of the atmosphere are taken up for detailed discussion.

It is quite apparent to anyone reading this book that the differences in approach between the german and the anglo-saxon groups of meteorologists that developed during the war, have not yet been fully eliminated. This may not stand out so clearly when looking through the bibliography where a large number of, for example, american investigations of later years are listed. However, it is quite clear, as is also pointed out in the preface, that these investigations have not always been fully considered. At some places the results thus obtained are in disagreement with recent findings elsewhere and sometimes one would like to have had a more detailed comparison between the different results. Such a comparison would also have been useful to eleminate certain misunderstandings because of terminology that now may arise. Examples of this will be given below.

The book is divided into two parts: one non-mathematical and one mathematical part. This procedure is especially good as done here. The non-mathematical part is not merely a description of observed facts but an attempt to explain the main physical ideas which are used as the basis for the theoretical treatment in the latter part of the book. A synoptic meteorologist without any advanced training in mathematics will thus be able to grasp the general ideas of the book and certainly dynamic meteorology should be written not only for those meteorologists that have a certain skill in mathematics.

In the preface the author points out that the mathematical treatment has not been made more accurate than seems justified from a meteorological point of view. This is certainly an important principle when working in theoretical meteorology. It seems to the reviewer, however, that some of the assumptions made are too restrictive and that thus certain important *physical* relations may have been left out of the picture. Furthermore meteorology seems now to have reached the stage when it is not always sufficient any longer merely to make sure that the orders of magnitude are correct but, if possible, one wants quantitative forecasts. Some cases will be given below where this criticism seems to be justified.

The two first chapters of the book are devoted to a critical discussion of previous ideas of cyclogenesis and certain simple but sometimes overlooked facts are pointed out. The author is very sceptical about any attempt to deal with cyclones as small perturbations superimposed upon a certain type of basic current. The reviewer agrees by and large but wants to point out that certain quantitative agreements have been obtained from such investigations in recent years.

In the third chapter the author reviews and interprets some of the most important aerological observations made lately. The interaction between the mean field of motion and the cyclones is very clearly described as well as the structure and behaviour of the jet-stream but few details are given. Furthermore, the slope between the boundary between the cold and warm air in fig. 17, where the former is advancing seems hardly to be synoptically confirmed. In the

light of the later discussion of the approximate geostrophic balance of atmospheric motion the discussion of the maintenance of a difluence field ("Delta") does not seem conclusive.

The general circulation of the atmosphere is discussed in some detail in the following chapter. It would have been desirable if some of the quantitative data that have been obtained at MIT, Cambridge and University of California had been discussed in comparison with the development presented by the author. With regard to the proposed tropopause circulation the reviewer would like to ask if we really know that the tropospheric air mainly enters the stratosphere in tropical latitudes?

In chapter five the different possibilities for cyclogenesis are clearly discussed starting from the vorticity considerations. The establishment of the corresponding pressure field is assumed to take place through a process very similar to the one proposed by Rossby some 15 years ago. In the following two chapters certain models for cyclone formation are presented: The well-known model for the generation of a heat-low as well as a simplified picture of the air flow in an extra-tropical cyclone based upon the work by Kleinschmidt Jr. and the author himself. The main reason for a cyclone to deepen and show its typical asymmetry should according to this idea be the irreversibility of the condensation processes because of the release of rain. This may be an important factor, but recent computations at Princeton seem clearly to indicate that a development of a (surface) cyclone may also take place in a (hypothetically) dry atmosphere. Furthermore the reviewer has difficulties in seeing that the reasoning presented to explain cyclone formation in a "Delta"-region is anything but the description of the changes of the vorticity field that have to exist for keeping the field itself stationary (p. 141 ff.).

The mathematical part of the book starts with the development of the vorticity equation and a detailed discussion of its various terms. In the following chapter the importance of the horizontal divergence and vertical velocity for vorticity changes are developed. This presentation is clearly written and easy to follow but might have been supplemented by at least some comments on the main assumptions and simplifications that are involved in the various models for numerical forecasting and the capability of these models of forecasting cyclogenesis.

Following the physical ideas presented before chapter ten and eleven are devoted to the pressure changes induced by the vorticity changes. This line of thinking seems very important to the reviewer. The whole approach to the problem of the pressure changes as mainly being the reactions of the mass-field because of changes in the wind field has not been stated so explicitly in any of the more well-known books in dynamic meteorology. This principle has earlier been advocated by Rossby but it is quite apparent that the idea as well as the development by professor Raethjen has been done quite independently. However, a more accurate treatment would have been instructive. For example the dissipation of some energy by inertia-gravity waves is automatically excluded in the way the problem is formulated. The very reason that such oscillations never (or seldom) are observed in reality does not depend on surface friction, since the friction would damp the basic current as fast as the oscillations. It depends rather upon the dispersion and interference between a large number of waves originating from different portions of the atmosphere and being of different frequencies and phases.

Chapter twelve gives a discussion of large scale turbulence in relation to cyclone theory. The idea that the maintenance of the permanent centers of action is the result of such a turbulent process along the polar front is a novel and interesting idea but is certainly not prooved by the author. The mathematical treatment in this section is again slightly restricted and excludes for example the possibility of mixing with conservation of absolute vorticity.

In the following chapters the idea of long waves is presented. The author also develops an interesting variation of the principle of constant potential vorticity. At the tropopause level two isentropic surfaces are usually at a small vertical distance to the north of the jet stream (in the polar stratosphere). Further south (in the tropical troposphere) these same isentropes spred out in the vertical. Assuming that the wave motion takes place between such fixed isentropic surfaces, the divergence term in the vorticity equation provides the stabilizing factor that is necessary for wave formation. On the other hand it is not obvious to the reviewer in which sence surface friction influences the speed of propagation of the waves as stated on page 288.

The last chapter is devoted to a treatment of the convection cyclone. In particular the application to tropical hurricanes as originally developed by Kleinschmidt Jr. gives a very enlightening picture of some necessary relations that must exist within such a field of motion.

Professor Raethjen's book is interesting to read. Even if one does not always agree with the author

it certainly is useful to follow a presentation of the point of view of an experienced research worker of professor Raethjen's standing. The reviewer believes that some of the theoretical developments need a more detailed treatment which in some cases also has been carried through by other investigations. On the other hand the theories presented are based upon physical models obtained from a study of current weather maps, a procedure which not always has been followed in meteorology. Finally the book has a very personal touch and it is easy to see that "the Lady of Meteorology" is the great devotion of professor Raethjen.

Bert Bolin